Loading, modelling and costing of concrete and steel support structure designs: large wind turbines in South Africa

by

Conrad Jeanne de Kock

A thesis presented in partial fulfilment of the requirements for the degree of Master of Science in Civil Engineering at the Stellenbosch University

Supervisor: Mr. Etienne van der Klashorst

December 2015

Declaration of Authorship

By submitting this thesis electronically, I declare that the entirety of the work contained therein is my own, original work, that I am the authorship owner thereof (unless to the extent explicitly otherwise stated) and that I have not previously in its entirety or in part submitted it for obtaining any qualification.

Signed:

Date:

Summary

Wind energy has the potential to be a strong contributor to a more sustainable future. Globally it is a major player in the market and is expected to become more influential in the future. In South Africa the potential exists and major development is under way. A modern wind turbine has a horizontal axis orientation, three rotor blades, active pitch and face into the wind using yaw control. It has a steel monopole tower between 60 m and 80 m high with a reinforced concrete foundation. However, this design presents various problems for structural integrity, manufacturing and viability at heights above 80 m. These constraints has led to a movement towards steel-concrete hybrid and full concrete towers. Such designs present an alternative and possibly more optimal solution for tower heights over 100 m.

This hypothesis was tested for South African conditions. Steel and prestressed concrete tower designs were acquired for a 3 MW reference wind turbine with 100 m hub height. Towers were loaded according to local conditions and the structural soundness thereof was tested and proved. Structural parameters were optimized and material mass and volume were determined for each. A cost estimation and sensitivity analysis was performed for the following life-cycle phases: manufacture, construction and installation; transport; and disposal and recycling.

Margins of cost between the tower designs were low enough for all three to be considered competitive alternatives at 100 m in height. The cast-in-place prestressed concrete design was estimated to be the most affordable solution. However, its high sensitivity to variation in erection cost causes uncertainty and a higher financial risk. Furthermore, the steel tower was the most viable for low steel prices and high erection costs. For a larger foundation size it still remained a competitive alternative to the concrete towers. Overall the prestressed precast design was the most expensive. However, for high erection costs it was more affordable than the cast-in-place tower. For disposal and recycling the steel solution was a much more favourable financial alternative to the concrete design. However, salvage income does not contribute a significant gain compared to overall cost.

Opsomming

Wind energie het die potensiaal om 'n sterk bydra te lewer tot 'n meer volhoubare toekoms. Wêreldwyd beklee dit 'n belangrike posisie in die mark en sal na verwagting meer invloedryk word in die toekoms. Suid-Afrika het baie potensiaal en grootskaalse ontwikkeling is aan die gang. 'n Moderne windturbine het 'n horisontale asoriëntasie, drie rotorlemme met aktiewe draai-aksie en word in die wind in gerig met behulp van beheersisteme. Dit het 'n silindriese staaltoring met 'n hoogte tussen 60 m and 80 m en 'n bewapende beton fondasie. Hierdie ontwerp bied egter verskeie probleme rakende strukturele integriteit, vervaardiging en lewensvatbaarheid vir hoogtes bo 80 m. Bogenoemde beperkinge het gelei tot 'n industriële beweging na staal-beton hibriedontwerpe en volle betontorings. Sulke ontwerpe bied 'n alternatief en moontlik meer optimale oplossing vir toringhoogtes bo 100 m.

Hierdie hipotese is getoets vir Suid-Afrikaanse toestande. Staal en spanbeton toringontwerpe is verkry vir 'n 3 MW verwysingswindturbine met 100 m ashoogte. Die torings is belas vir plaaslike toestande en die bouvorm daarvan is getoets en bewys. Struktuurparameters is gebruik om geoptimeerde materiaalmassa en volumes vir elk te bepaal. 'n Kosteberaming en sensitiwiteitsanalise is vir die volgende lewensiklusfases uitgevoer: vervaardiging, konstruksie en installering; vervoer; en beskikking en herwinning.

Kosteverskille was laag genoeg vir al drie ontwerpe om as medidingend beskou te word teen 'n hoogte van 100 m. Die insitu spanbetonontwerp is as die goedkoopste oplossing beraam, maar die toring se hoë sensitiwiteit vir variasie in oprigtingskostes veroorsaak onsekerheid en 'n oënskynlike finansiële risiko. Verder was die staaltoring die mees lewensvatbaar vir lae staalpryse en hoë oprigtingskostes. Dit was steeds mededingend met die beton torings ten spyte van 'n groter fondament. Die voorafvervaardigde spanbetonontwerp was oor die algemeen die duurste. Dit was egter goedkoper as die insitu toring vir hoë oprigtingskostes. Vir beskikking en herwinning was die staalontwerp 'n meer gunstige finansiële alternatief as die beton. In vergeleke met die totale koste van 'n toring het herwinning egter nie 'n beduidende wins bygedra nie.

Acknowledgements

With all my heart I want to thank God the Father, Jesus Christ and the Holy Spirit for giving me the ability and privilege to perform this master study. Furthermore, I thank my parents, family and friends for all their prayer and support.

I sincerely thank my supervisor, Mr. Etienne van der Klashorst, for support and guidance.

I thank Mr. Greg Mitchell from the Finite Element Analysis Services (FEAS) team for assisting me with queries regarding FEM modelling in Abaqus.

I want to sincerely thank Me. Daleen Filbey and Mr. Jaco Maré for giving me access to use Merkel's live and Mr. James Olawuyi for assisting me with high strength concrete mix design. Furthermore, I thank Dr. Peter Day for providing costing information about surveying and geotechnical design.

Contents

Declaration of Authorship i

Summary ii

Opsomming iii

Acknowledgements iv

List of Figures ix

List of Tables xi

Abbreviations xii

1 Introduction 1
- 1.1 Background . . . 1
- 1.2 Problem statement . . . 2
- 1.3 Objectives . . . 3
- 1.4 Scope . . . 3
- 1.5 Limitations . . . 4
- 1.6 Chapter overview . . . 5

2 Literature Review 6
- 2.1 Introduction . . . 6
- 2.2 Overview of wind energy . . . 7
- 2.3 Overview of wind turbine design . . . 9
  - 2.3.1 Historical background . . . 9
  - 2.3.2 Design classification . . . 10
  - 2.3.3 Control systems . . . 14
  - 2.3.4 Wind power parameters . . . 15
  - 2.3.5 Turbine configuration . . . 18
  - 2.3.6 Development trends . . . 18
- 2.4 Wind turbine support structure design . . . 19
  - 2.4.1 Modern industry trends . . . 19
  - 2.4.2 Steel monopole tower . . . 19
  - 2.4.3 Concrete monopole tower . . . 20
  - 2.4.4 Other tower designs . . . 22
  - 2.4.5 Foundation design . . . 23

2.5 External conditions . . . 23
2.5.1 Wind turbine classes . . . 24
2.5.2 Wind conditions . . . 24
2.5.3 Other conditions . . . 25
2.6 Wind data considerations for South Africa . . . 25
2.6.1 Wind Atlas for South Africa . . . 26
2.6.2 South African wind loading code . . . 26
2.7 Structural loading of wind turbines . . . 27
2.7.1 Design loads . . . 27
2.7.2 Fatigue loading . . . 29
2.7.3 Ultimate loading . . . 30
2.7.4 Situations and design load cases for ultimate loading . . . 30
2.7.5 Extreme tower load cases . . . 32
2.7.6 Typical tower loading . . . 33
2.7.7 Aero-elastic load calculations . . . 35
2.7.8 Simplified load calculations . . . 35
2.7.9 Blade lift and drag coefficients . . . 40
2.8 Considerations for structural analysis of wind turbine towers . . . 41
2.8.1 Partial safety factors . . . 41
2.8.2 Analysis of ultimate strength . . . 43
2.8.3 Analysis of fatigue failure . . . 44
2.8.4 Stability analysis . . . 44
2.8.5 Critical deflection analysis . . . 46
2.8.6 Dynamic considerations . . . 47
2.8.7 Prestressing of a tubular concrete tower . . . 49
2.8.8 Modelling of a tubular tower . . . 53
2.9 Cost analysis of wind turbine towers . . . 55
2.9.1 Overview of engineering economics . . . 55
2.9.2 Life-cycle costing of a wind turbine . . . 57
2.9.3 Cost breakdown of a wind turbine . . . 57
2.9.4 Cost estimation of a wind turbine tower . . . 59
2.9.5 Sensitivity analysis . . . 62
2.10 Conclusion . . . 63

3 Methodology for Comparative Study 64
3.1 Introduction . . . 64
3.2 Reference wind turbine and site . . . 65
3.2.1 Finding a suitable reference wind turbine . . . 65
3.2.2 Suitable site and location . . . 68
3.2.3 Properties of the reference wind turbine . . . 69
3.3 Support structure designs . . . 69
3.3.1 Steel monopole . . . 69
3.3.2 Prestressed concrete monopole . . . 70
3.4 Considerations for wind conditions . . . 74
3.5 Wind turbine tower loading . . . 74
3.5.1 Critical design load case . . . 74
3.5.2 Critical tower loading . . . 75

3.5.3 Tower loading calculations . . . 75
3.6 Structural analysis and modelling . . . 80
3.6.1 Critical deflection analysis . . . 80
3.6.2 Fatigue failure analysis . . . 81
3.6.3 Dynamic considerations . . . 81
3.6.4 General modelling methodology . . . 81
3.6.5 Steel monopole . . . 84
3.6.6 Prestressed concrete monopole . . . 85
3.6.7 Optimisation and material mass . . . 90
3.7 Life-cycle cost analysis . . . 91
3.7.1 Cost estimation of life-cycle phases . . . 91
3.7.2 Comparison with actual costs . . . 94
3.7.3 Sensitivity analysis . . . 94
3.8 Conclusion . . . 97

4 Results for Structural Analysis 98
4.1 Introduction . . . 98
4.2 Results for steel monopole . . . 98
4.2.1 Loading . . . 98
4.2.2 Ultimate strength analysis . . . 99
4.2.3 Global buckling analysis . . . 100
4.2.4 Local buckling analysis . . . 102
4.2.5 Optimal design and material mass . . . 103
4.3 Results for concrete monopole . . . 104
4.3.1 Loading . . . 104
4.3.2 Prestressing . . . 105
4.3.3 Ultimate strength analysis . . . 106
4.3.4 Global buckling analysis . . . 108
4.3.5 Optimal design and material mass . . . 110
4.4 Conclusion . . . 110

5 Findings for Life-cycle Costing Analysis 111
5.1 Introduction . . . 111
5.2 Manufacture, construction and installation . . . 111
5.2.1 Estimated costs . . . 111
5.2.2 Comparison with actual costs . . . 113
5.2.3 Foundation cost variation . . . 114
5.2.4 Material cost variation . . . 115
5.2.5 Fabrication and field erection cost variation . . . 116
5.2.6 Transport cost variation . . . 117
5.2.7 Labour cost variation . . . 118
5.3 Disposal and recycling . . . 119
5.4 Conclusion . . . 122

6 Conclusion 123
6.1 Summary of findings . . . 123
6.2 Main conclusions . . . 124

6.3 Recommendations for future research 125

Bibliography **127**

Appendix A: Mast Information for the Wind Atlas of South Africa **135**

Appendix B: Reference Wind Turbine and Site **136**

Appendix C: Geometry of Support Tower Designs for Study **137**

Appendix D: Blade Profile and Scaling **140**

Appendix E: Stress-Strain Curves **141**

Appendix F: Distributed Load Over Tower Height **142**

Appendix G: Cost Estimation of Life-cycle Phases **144**

List of Figures

2.1 Growth of total installed global wind power capacity. 8
2.2 Growth of total installed wind power capacity in South Africa. 9
2.3 A horizontal-axis wind turbine at Gordonbush Wind Farm in Sutherland. 11
2.4 Vertical-axis wind turbine concepts: Sivonius, Darrieus and 'H' rotor. . . 12
2.5 Stream tube for a wind turbine. 15
2.6 Typical power curve for a modern wind turbine. 16
2.7 The configuration of a modern wind turbine. 18
2.8 Typical loading for a tubular tower. 33
2.9 (a) The typical global buckling mode of an axially compressed beam-column. (b) The diamond shaped local buckling pattern of a cylindrical shell. 46
2.10 Static clearance of a wind turbine blade. 46
2.11 Typical Campbell diagram for a wind turbine. 48
2.12 Stress block for a tubular tower section. 52
2.13 Installed capital costs for a 1.5 MW reference wind turbine with 82.5 m rotor diameter and 80 m hub height. 59
2.14 Specific investment costs for a 3 MW reference wind turbine with differing tower types. 60
2.15 Installed costs of various tower designs for a 3.6 MW reference wind turbine. 62

3.1 Distribution of rated power for commercial wind turbines. 66
3.2 Distribution of hub heights for capacity range of 1.5 MW to 3 MW. 67
3.3 Distribution of rotor diameters for capacity ranges of 1.5 MW to 3 MW. . 68
3.4 Placement of nominal and prestressing reinforcement in the tower wall (N.T.S). 71
3.5 Prestressing tendon anchorage detail. 72
3.6 Assumed critical loads acting on the tower. 76
3.7 Values of C and m for integral length scale of Kaimal spectrum. 78
3.8 Lift forces on rotor blades inducing M_{yT} and M_{zT} (N.T.S). 79
3.9 Representation of tower models used for structural analysis. 82
3.10 Kinematic coupling and load application. 83
3.11 Material orientation of tower shell sections and reinforcement layers. . . . 86
3.12 Representation of a segment. 89

4.1 Stress distribution for the ultimate strength analysis of the steel tower. . . 99
4.2 Stress path results for ultimate strength analysis of the steel tower (above 65 m height). 100
4.3 Global buckling failure of the original steel tower design. 101
4.4 Increase in LPF for global buckling analysis of the steel tower. 101

4.5 Stress results for global buckling analysis of the adjusted steel tower. . . . 102
4.6 Stress distribution for the local buckling analysis of the steel tower. 103
4.7 Stress results for local buckling analysis of the adjusted steel tower. 103
4.8 Flexural stress for SLS loading in the concrete tower prior to prestressing. 105
4.9 Flexural stress for SLS loading in concrete after prestressing. 106
4.10 Flexural stress in the concrete for the ultimate strength analysis of the prestressed tower. 108
4.11 Increase in LPF for the global buckling analysis of the prestressed concrete tower. 109
4.12 Flexural stress in concrete for global buckling analysis of the prestressed tower. 109

5.1 Influence of foundation cost variation on MCI cost. 115
5.2 Influence of material price variation on MCI cost. 116
5.3 Influence of fabrication and field erection cost variation on MCI cost. . . . 117
5.4 Influence of transport on MCI cost. 118
5.5 Influence of variation of labour cost on MCI cost. 119
5.6 Estimated salvage values for the concrete and steel towers. 120
5.7 Estimated transport costs for disposal of recyclable materials for the concrete and steel towers. 121
5.8 Estimated disposal and recycling costs for the concrete and steel towers. . 122

List of Tables

2.1 Wind turbine size classification. 13
2.2 Basic parameters for wind turbine classes. 24
2.3 Air velocities at wind turbine blade cross-section. 28
2.4 Load specification parameters for the Quasi-Static method. 36
2.5 Equivalent surface roughness for wind turbine tower surfaces. 39
2.6 Comparison of γ_f for ultimate strength analysis. 43
2.7 Material factors for ultimate strength analysis. 44
2.8 ICC percentages of a 1.5 MW baseline wind turbine. 58
2.9 Component percentages of ICC for 1.5 MW, 3 MW and 4.5 MW wind turbines. 58

3.1 Statistical properties and hub height ranges for significant capacities. . . . 67
3.2 Statistical properties and rotor diameter ranges for significant capacities. . 68
3.3 Technical information for the reference wind turbine. 69
3.4 Material properties of structural steel. 70
3.5 Material properties for the prestressed concrete tower design. 73
3.6 Assumed critical loads acting on the tower. 76
3.7 Assumed values of critical parameters for the Quasi-static method. 77

4.1 Loading and partial factors for steel tower design. 99
4.2 Optimum wall thickness change (in mm) of steel tower. 104
4.3 Material volume and mass of original and adjusted steel tower design. . . 104
4.4 Loading and partial factors for the prestressed concrete tower design. . . . 105
4.5 Ultimate applied moment for the prestressed concrete tower. 106
4.6 Significant parameter values for ultimate strength analysis of the prestressed concrete tower. 107
4.7 Strain in tension reinforcement for Abaqus ultimate strength analysis of the prestressed concrete tower. 108
4.8 Strain in tension reinforcement for Abaqus global buckling analysis of the prestressed concrete tower. 110
4.9 Material volume and mass of the prestressed concrete tower. 110

5.1 Estimated manufacturing, construction and installation costs for towers. . 112
5.2 Manufacturing, construction and installation costs for local wind farms. . 114

Abbreviations

ULS	Ultimate Limit State
SLS	Serviceability Limit State
HAWT	Horizontal-Axis Wind Turbine
VAWT	Vertical-Axis Wind Turbine
IEC	International Electrotechnical Commission
WASA	Wind Atlas for South Africa
SANS	South African National Standard
CSIR	Council for Scientific and Industrial Research
DLC	Design Load Case
EWM	Extreme Wind speed Model
ETM	Extreme Turbulence Model
FEM	Finite Element Method
DS	Danish Standard
SABS	South African Bureau of Standards
LPF	Load Proportionality Factor
DOF	Degree Of Freedom
FW	Future Worth
PW	Present Worth
PWA	Present Worth Analysis
LCC	Life-Cycle Cost
ICC	Initial Capital Costs
BOS	Balance Of Station
TCC	Turbine Capital Costs
NREL	National Renewable Energy Laboratory
GRP	Glass Reinforced Plastic

N.T.S	Not To Scale
FEAS	Finite Element Analysis Services
REIPPPP	Renewable Energy Independent Power Project Procurement Program
MCI	Manufacture, Construction and Installation
CISCO	Cape Town Iron and Steel Works
AMSA	ArcelorMittal South Africa

Chapter 1

Introduction

1.1 Background

Wind energy is a renewable source and can contribute to the solution for global environmental concerns. During operation wind power generation does not produce waste. Therefore, wind energy production is clean and environmentally friendly. Energy payback time for initial manufacture and installation emissions is approximately 5 months [1][2]. The resource is freely available, well distributed [3], inexhaustible and plentiful. Wind power is also a significant player in the global energy market and Gsanger and Pitteloud [4] reports that the installed capacity at the end of 2012 contributed to 3 % of the global demand. Financially the wind sector had a turnover of 60 billion Euro at the end of 2012.

South Africa has a promising supply of wind resources. The Western Cape has 3100 MW and 1500 MW worth of on-shore and off-shore potential. There are also significant resources in the Northern Cape, Eastern Cape and KwaZulu Natal. Furthermore, a national study assumed that 1 % of the land in the five regions with the highest wind resources could be allocated for wind farms amounting to 50 GW resource potential [5]. Local wind power development has remained negligibly small up to 2013. However, from 2014 onwards major development and capacity increases are expected. Eberhard [6] reports that the South African government has initiated a competitive tendering program to utilize private sector expertise and investment in grid-connected renewable

energy. Up to date a total capacity of 1984 MW (over three bidding stages) has been awarded for wind energy.

In the modern industry wind is primarily harvested by 3-bladed horizontal-axis wind turbines [7][8]. Since the 1980s commercial sizes have grown from small capacities of 55 kW [8] to large multi-megawatt giants ranging from 1 MW to 6 MW [9]. Currently 2 MW to 3 MW machines are being installed on most on-shore sites [10][9]. According to Thresher et al. [7] the most popular support structure configuration used today is a free standing steel monopole (or tubular) tower on a concrete foundation. Generally tower heights range from 60 m to 80 m, but 100 m towers are becoming more prevalent. However, the steel design does present various problems regarding structural integrity [11][12], manufacture [13] and viability [14] for heights over 80 m. This has led to a movement towards steel-concrete hybrid and full concrete tower solutions. Such designs present an alternative and possibly more optimal solution for heights over 100 m [15][10].

1.2 Problem statement

It is apparent that wind energy has the potential to be a strong contributor to a more sustainable future for global and local (South African) energy demand. Globally it is a major player in the market and is expected to become more influential in the future. Locally the potential exists, and an effort is being made to utilize it with major developments under way. This study aims to contribute to the effort by increasing the information and knowledge base of design, analysis and costing of wind energy technology in a South African context. The focus shall be on wind turbine towers.

This study shall investigate whether prestressed concrete tower solutions are financially viable alternatives to the conventional steel design, or perhaps even more viable at higher heights for local conditions. Realistic and comparable support structure designs shall be obtained. The structural soundness thereof shall be tested and proved for loading conditions in South Africa. A cost study shall be performed to determine and compare its local viability.

1.3 Objectives

The main aim of the study is to increase the information and knowledge base of design, analysis and costing of wind turbines in South Africa. To achieve this the following objectives need to be met:

- to define a reference wind turbine of which the most significant parameters (such as size indicators) are realistic,
- to find realistic and comparable support structure designs for the reference wind turbine from literature,
- to determine realistic structural loading for South African conditions according to recognized methods,
- to perform a structural analysis on each tower design in order to prove its soundness for the required loading, and
- to use the final geometric and material properties of the towers to perform a comparative costing analysis according to local economic trends.

1.4 Scope

The variation of parameters for the reference wind turbine shall not be investigated. For example, the study does not consider the influence of the variation in the height of a tower, capacity or blade radius on its structural performance or cost. In other words, all significant parameters for the reference turbine remain constant.

This study shall investigate two separate tubular tower designs: one for prestressed concrete and one for steel. The focus shall be on the overall geometric dimensions of the tower. However, for the former two construction methods shall be considered for costing: precast and in-situ.

Ultimate limit state (ULS) design shall be the main focus for structural analysis. Loading shall be determined for the most unfavourable design situation and load case using simplified calculation methods.

The main focus of the life-cycle cost analysis shall be on the following phases:

- manufacture, construction and installation,
- transport, and
- disposal and recycling.

1.5 Limitations

Steel lattice and concrete-steel hybrid tower designs shall not be considered due to time constraints and modelling challenges. These designs can also be considered to be viable alternatives to the steel solution at 100 m in height and would make the study more comprehensive.

Fatigue design shall not be considered due to lack of time and suitable information regarding stress ranges for wind turbines. Dynamic design shall only be considered in part due to lack of time and information. Foundation design shall also not be considered due to time limitations. Furthermore, the identified site for this study is in a region with seismic activity. However, seismic design is also not considered. Furthermore, connection design is not considered for this study. Any of the above verifications can affect or govern the tower designs. Therefore the resulting geometric values for the towers of this study might be structurally and economically non-conservative.

There are no sufficient public information on costing of wind turbines or its support structures for South Africa. The Merkel's service provides local values for general construction cost items, but does not contain sufficient data regarding special structural operations. Consequently values for the use of large cranes, prestressing operations, field welding and in-situ jump-forming are based on cost studies for other countries. If the values from those studies are inaccurate for local conditions it can significantly affect the results for this study.

Financial investigation of the following life-cycle phases are not performed: operation and maintenance, and decommissioning and dismantling. No information was found for the former regarding wind turbine support structures. For decommissioning and dismantling, costing information is available, but is not comprehensive enough for this study. However costs for both phases should be low relative to those included in this study and would not impact costs significantly if included.

1.6 Chapter overview

The list below presents a brief overview of the topics that shall be discussed in this document.

- Chapter 2: Literature Review. A general overview is given of wind energy. Furthermore, the design, structural loading, analysis, modelling and costing of wind turbines are discussed in depth.
- Chapter 3: Methodology for Comparative Study. Methods for finding a suitable reference wind turbine and site are discussed and the steel and concrete support tower designs are presented. The procedures for performing structural loading, analysis and modelling on the designs are described. Lastly the model for the tower costing analysis are presented.
- Chapter 4: Results for Structural Analysis. The results for loading and structural analysis are presented and discussed.
- Chapter 5: Findings for Life-cycle Costing Analysis. The results of the costing analysis are presented and discussed.
- Chapter 6: Conclusion. The main findings of the study are summarized, a final conclusion is drawn and recommendations are made for future research.

Chapter 2

Literature Review

2.1 Introduction

This chapter presents and interprets the literature on which this study is based. The main aim is to increase the information and knowledge base of design, analysis and costing of wind turbines in South Africa. General overviews are given of wind energy as a renewable source, and the design of wind turbines. More in-depth discussions are presented for the design of wind turbine support structures and the structural loading and analysis thereof. Furthermore, cost analysis of wind turbines and its tower structures are also investigated. The chapter follows the outline below:

- overview of wind energy,
- overview of wind turbine design,
- wind turbine support structure design,
- external conditions,
- wind data considerations for South Africa,
- structural loading of wind turbines,
- structural analysis of wind turbine towers, and
- cost analysis of wind turbine towers.

2.2 Overview of wind energy

According to Tong [9] rising concerns regarding global warming, climate change, environmental pollution and energy security have increased interest in developing renewable energy sources to replace fossil fuels and nuclear power. During operation, these sources produce harmful wastes. Burning of fossil fuel releases green house gasses (CO_2, SO_2 and NO_x) into the atmosphere, while nuclear plants produce toxic waste that is extremely detrimental to the environment. Furthermore, these sources are exhaustible.

Wind energy is a renewable source and can contribute to the solution for the current energy crisis. During operation wind power generation does not produce any waste. However, during manufacture and installation of wind turbines wastes such as CO_2 emissions are still produced. This is very small when considering the whole life-cycle [14], and energy payback time of a multi-megawatt machine is approximately 5 months [1][2]. Therefore, wind energy production is clean and environmentally friendly. The resource is also freely available, well distributed across the continents [3], inexhaustible and plentiful. The available wind power is approximately 1.26×10^9 MW and represents twenty times the rate of current global consumption. Therefore, theoretically wind energy could easily meet the entire demand of the world [9].

Wind power has risen to become a significant player in the global energy market. Over the past two decades it has become the world's fastest growing energy source [3]. Figure 2.1 shows the total installed production capacity for wind energy on a global scale [4]. Here we see that exponential growth has taken place between 1997 and 2012. Gsanger and Pitteloud [4] reports that the installed capacity at the end of 2012 contributed to 3 % of the global electricity demand. Forecasts show that total global capacity should reach 500 000 MW by 2016 and 1 000 000 MW by 2020. Financially the wind sector had a turnover of 60 billion Euro at the end of 2012.

South Africa has a promising supply of wind resources. A mapping exercise in the Western Cape concluded that sufficient land is available in areas with medium to high wind resource potential to conservatively house installation of 3100 MW worth of on-shore capacity. Off-shore potential was estimated to be 1500 MW. There are also significant resources in the Northern Cape, Eastern Cape and KwaZulu Natal. Furthermore, a national study assumed that 1 % of the land in the five regions with the highest wind

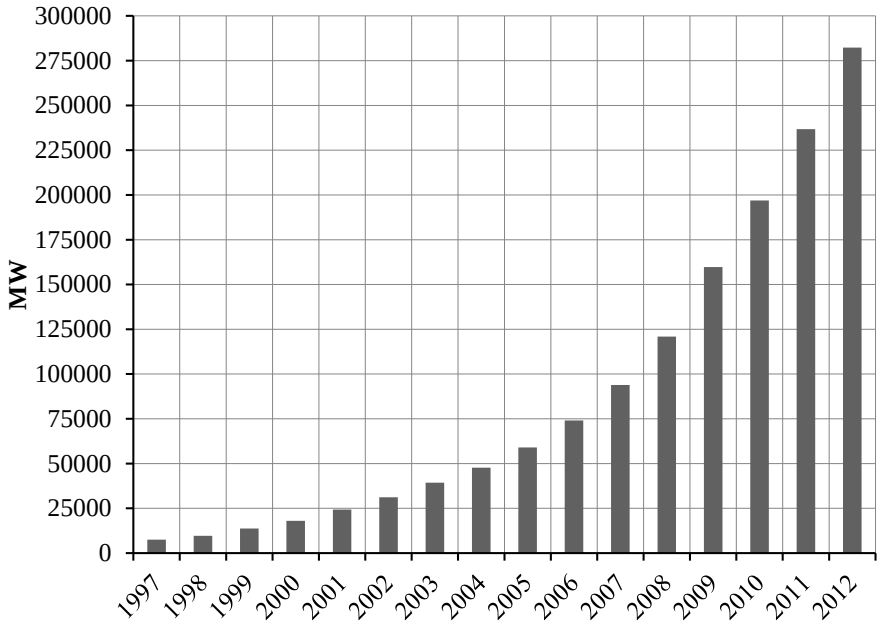

FIGURE 2.1: Growth of total installed global wind power capacity [4].

resources could be allocated for wind farms. This amounts to an area of 4100 km^2 and resource potential of 50 GW [5].

South Africa has seen little wind power development over the past decade. Figure 2.2 shows that total installed capacity remained negligibly small until 2013. However, from 2014 onwards major development and capacity increases are expected. Eberhard [6] reports that the South African government has initiated a competitive tendering program to utilize private sector expertise and investment in grid-connected renewable energy. Up to date a total capacity of 1984 MW (over three bidding stages) has been awarded for wind energy. Some of the major projects are: Amakhala Emoyeni with a potential 750 MW capacity [16], Cookhouse at 138.6 MW and the up and running Jeffreys Bay at 138 MW [6].

It is apparent that wind energy has the potential to be a strong contributor to a more sustainable future for global and local (South African) energy demand. Globally it is a major player in the market and is expected to become more influential in the future. Locally the potential exists, and an effort is being made to utilize it with major developments under way. This study aims to contribute to the effort by increasing the information and knowledge base of design, analysis and costing of wind energy technology in a South African context. The focus shall be on wind turbine towers.

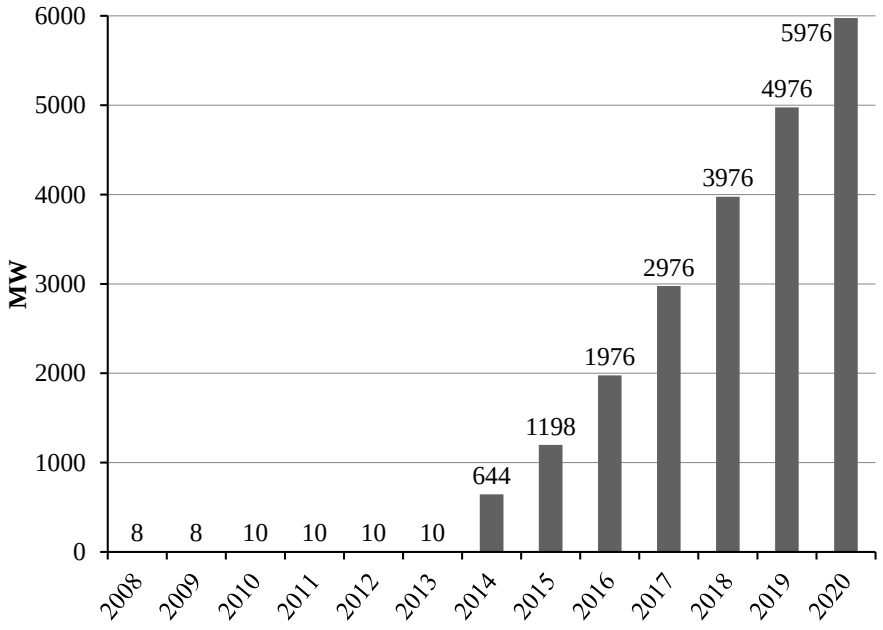

FIGURE 2.2: Growth of total installed wind power capacity in South Africa [17].

2.3 Overview of wind turbine design

2.3.1 Historical background

Application of wind energy is an ancient endeavour and as early as 4000 B.C. Chinese attached sails to their primitive rafts. Around 300 B.C. the Sinhalese civilisation used strong monsoon winds to provide furnaces with sufficient air for raising temperatures in excess of 1100 °C during iron smelting processes. Paintings from the late eastern Han Dynasty (25 to 220 A.D.) shows images of windmills [9]. In the ninth century the first practical vertical-axis mills were built in Sistan (Eastern Persia) for grain grinding and water pumping. Horizontal-axis designs were invented for the same purpose in Europe in the twelfth century. Early concepts featured four blades with yawing and were mounted on a central post (Post mills) [9][18]. By the thirteenth century horizontal-axis mills were an integral part of the rural economy. Windmills eventually fell into disuse with the advent of cheap fossil-fuelled engines and rural electrification [14].

In 1888 the first automatically operated wind turbine was designed by Charles Brush, which was an ordinary windmill modified to produce electricity. The design featured 144 cedar blades with a rotor diameter of 17 m and charged batteries at a peak output of 12 kW [9][14]. In the twentieth century early innovative designs were driven by three

philosophies for handling loads: Withstanding, avoiding (or shedding), and mechanical or electrical managing. Two fundamental design paths developed. The first was horizontal-axis wind turbines (HAWT's) and the second, vertical-axis wind turbines (VAWT's) [8]. These concepts developed in parallel for most of the century, but HAWT's gained more interest and financial support [18]. Smith and Putnam developed a 1250 kW HAWT in 1941, which remained the largest for 40 years. In 1956 the pioneering Gedser machine was built in Denmark [14][9]. For VAWT's the Savonius design was found in 1922 by a Finnish engineer and in 1931 the Darrieus concept was invented [18].

Despite these developments there was still little interest in the technology up until 1973. The price of oil rose drastically, creating awareness of the limited fossil fuel resources. This resulted in substantial government-funded research in North America and Europe during the 1970's and 1980's. Various innovative concepts were fully investigated from small (100 MW) to large (4 MW) scale in order to find the most economical design philosophy. These programmes produced significant scientific and engineering information which is still being used in the modern industry [14]. Furthermore, VAWT's fell victim to the poor wind energy market in North America [18]. This and various disadvantages led to its lag behind HAWT's in development, size and production in recent years [9].

In the modern industry wind is primarily harvested by 3-bladed horizontal-axis wind turbines [7][8]. Today, the main driver for using wind turbines is low CO_2 emissions over its life-cycle and therefore it has the ability to help limit climate change [14]. These drivers have caused the technology to evolve rapidly over the past few decades. Since the 1980s the sizes of commercial turbines have grown from small capacities of 55 kW [8] to large multi-megawatt giants ranging from 1 MW to 6 MW [9]. Currently 2 MW to 3 MW machines are being installed on most on-shore sites [10][9].

2.3.2 Design classification

2.3.2.1 Axis orientation

The most fundamental classification criteria for a modern wind turbine is axis orientation. According to Tong [9] two types exist: Horizontal-axis wind turbines (HAWT's) and vertical-axis wind turbines (VAWT's). The rotor of the former rotates around an

axis pointing in a horizontal direction parallel to the ground. For the latter it rotates around the vertical axis perpendicular to the ground.

HAWT's are the most common machines in use in the modern industry. It has a propeller-type rotor mounted on top of a vertical tower as shown in Figure 2.3. Significant advantages are high efficiency, high power density, low cut-in wind speeds and low cost per unit power output [9].

FIGURE 2.3: A horizontal-axis wind turbine at Gordonbush Wind Farm in Sutherland [19].

VAWT's are classified according to the Sivonius, Darrieus and 'H' rotor designs as shown in Figure 2.4 [18]. These designs can accept wind from any direction, the gearbox and generator are located on the ground for easy access and lower cost. However, general power efficiency is much lower, the axis is supported only on one end and an external energy source is needed to rotate the blades during initialization. Consequently VAWT's only contribute to a small percentage of today's wind energy industry [9][8].

It should be noted that further discussions regarding wind turbines shall be based on the HAWT concept.

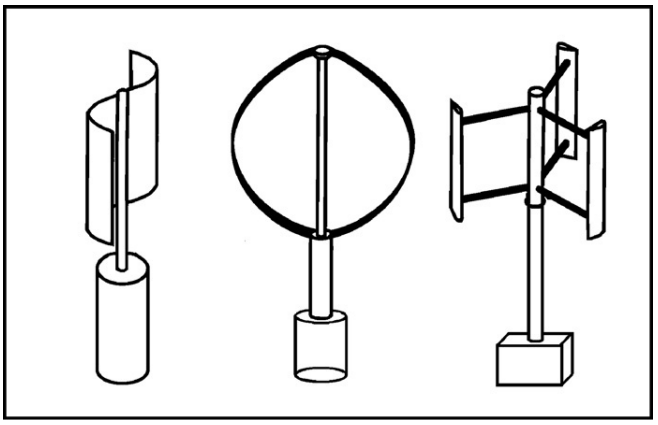

FIGURE 2.4: Vertical-axis wind turbine concepts: Sivonius, Darrieus and 'H' rotor [18].

2.3.2.2 Rotor position

The rotor of a wind turbine must be aligned with the wind direction to promote flow parallel to the rotational axis. Accordingly designs are categorized for upwind and downwind positions. The vast majority of industry turbines follow the upwind configuration, which uses yaw control to keep the rotor facing into the wind in front of the tower. The design avoids wind shade effects, but accurate prediction of blade deflection is required to avoid blade-tower strikes. For downwind turbines the wind flows by the nacelle and tower before reaching the rotor. When blades pass the unstable wake it induces great fluctuations in power output, significant fatigue and thumping noises. However, no yaw mechanism is needed and more flexible blades can be used [8][9][14].

2.3.2.3 Number of rotor blades

The number of rotor blades used for wind turbines are categorized according to one, two or three bladed designs. The three bladed concept is the most common in the modern industry [8]. This is the most efficient design for meeting commercial, economic and environmental restrictions [20]. The major advantage of the designs with fewer blades are reductions in rotor and nacelle weights for more affordable design [8][20]. However, the two and one bladed concepts are 3 % and 7 % to 13 % less efficient than the 3-bladed concept. Furthermore, the marginally improved efficiency of a four bladed design does not justify its increase in manufacturing cost. Further drawbacks for the one and two bladed designs are visual impact and increased dynamic and fatigue loading [20].

2.3.2.4 Size

The most common size indicator of a modern wind turbine is its capacity to generate energy. Typical output ratings are listed in Table 2.1. Micro turbines are most suitable in remote areas with no grid access and can be installed in most locations around the world. Small turbine application has been extensive in rural areas, mainly for water pumping and telecommunication sites. Medium size turbines are the most common. These have both on and off grid application for wind farms or villages. Large turbines have become mainstream in the global wind power market and are installed on most wind farms. Ultra-large turbines are still in early stages of research and development [9].

TABLE 2.1: Wind turbine size classification [9].

Category	Rated power (kW)
Micro	Not available
Small	< 100
Medium	100 to 1000
Large	1000 to 10 000
Ultra-large	$> 10\,000$

2.3.2.5 Grid application

According to Tong [9] wind turbines can either be connected to the electricity infrastructure (utility grid) or not. Most medium sized and all large machines are designed for on-grid application. No energy storage devices are needed for these turbines. However, for off-grid application intermittency necessitates some form of storage. Batteries, generators or small photovoltaic devices can ensure a more stable output.

2.3.2.6 Location

The criteria for the location of a wind turbine is based on whether it is situated on-shore or off-shore. For the on-shore design, access and grid integration is easy, and tower and foundation costs are lower [9][10]. The advantage of off-shore technology is resource quality. Wind speeds over the sea level are generally 20 % higher than on nearby land and the wind shear profile is less steep. This leads to favourable wind conditions at lower heights and therefore off-shore towers tend to be lower. Furthermore, better continuity of wind causes off-shore turbines to operate more hours per annum [7] [9].

2.3.3 Control systems

2.3.3.1 Power control

Veritas [8] states that wind turbines are generally designed to yield a maximum power output at lower wind speeds of around $15\,\mathrm{m\,s^{-1}}$. The rarity of extreme winds render the maximization of output at high speeds infeasible. However, in these conditions the maximum output can be exceeded and might damage the turbine. Power control systems are used to safely manage the rotor speed of the turbine. The most common systems are passive stall, active pitch and active stall [9][14][8].

Passive stall is the simplest and most reliable control method. Rotor blades are bolted to the hub at a fixed angle, causing power regulation to be dependent on blade aerodynamics. A fixed pitch ensures maximum power output at the design wind speed. At excessive speeds stall limits the rotor speed and output by causing separation and lift reduction at the downwind side of the blade. However, the design has uncertainties in post-stall aerodynamics and low efficiency at low wind speeds [8][9][14].

In the modern industry active pitch control is favoured due to increased energy capture, aerodynamic braking and reduced aerodynamic loads at shut down [9] [14]. Active pitch manages power output by rotating blades in and out of the wind to change the angle of attack. Rotation out of the wind is called feathering and reduces the lift of the blade [14]. The required pitch range is usually from 0°(fine pitch) to 35°. At fine pitch the blade tip chord is in the plane of rotation. To apply aerodynamic braking the blades must be pitched to full feather at 90°. In this position the tip chord is parallel to the rotor shaft with the leading edge into the wind. Blade pitching is performed by either using a single actuator for all the blades or blade-independent pitch. Drawbacks of this design are extra complexity and high power fluctuations at high wind speeds [8].

According to Tong [9] active stall control was developed for large wind turbines. This method implements stalling blades and a pitching mechanism. At low wind speeds it performs similar to an active pitch design. However, at high speeds blades are pitched in the opposite direction to induce stall. This ensures accurate control and the ability to maintain rated power at high wind speeds [8]. The main disadvantages are: prediction of aerodynamic behaviour in stalled flow [14], reliability and cost [9].

2.3.3.2 Yaw control

Yaw control is used to orient the rotor of a wind turbine into the wind. This maximizes power output and minimizes asymmetric loading in the blades and tower. Modern turbines implement electric motors to drive the yaw system (See Figure 2.7). During operation a vane records the wind direction and signals a controller. An average yaw angle is then calculated over a time interval. If this angle exceeds the prescribed limit the yaw motor is activated to align the rotor into the wind. When the rotor is aligned the turbine is locked into position through a brake [9].

2.3.4 Wind power parameters

2.3.4.1 Power

According to Burton et al. [14] a wind turbine is a device used to extract kinetic energy from the wind. Theoretically this energy is extracted by a disc in the rotor plane and is represented by the swept area of the rotor. This is called the actuator disc concept. The air passing through the disk loses kinetic energy. Assuming the affected mass of air remains separate from the unaffected, a stream tube of circular cross-section is formed as shown in Figure 2.5. Momentum theory can be applied to the tube to derive the mechanical power captured by the disc. This derivation is expressed in equation 2.1 [8]. We see that wind speed has the most significant influence on the power production with a third order magnitude and the change in rotor diameter has a second order effect.

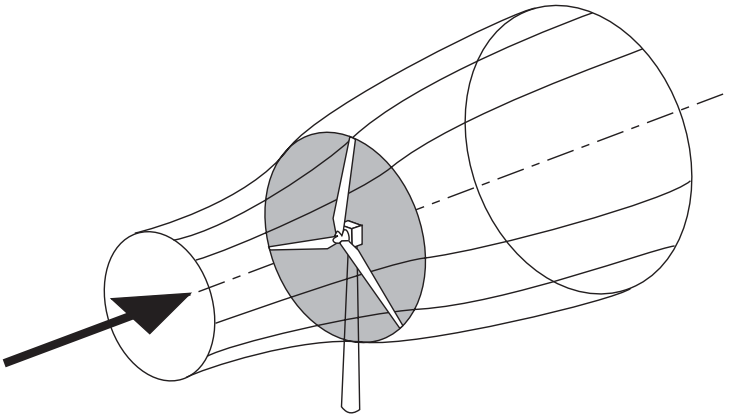

FIGURE 2.5: Stream tube for a wind turbine [14].

$$P = \frac{1}{2}\rho V^3 A C_p \tag{2.1}$$

Where:

P	=	mechanical power
ρ	=	air density
V	=	free wind speed
A	=	rotor swept area
C_p	=	power coefficient

The power coefficient represents the mechanical efficiency of a wind turbine and Lanchester and Betz derived its theoretical limit of 0.5926 [9][14][8]. This is due to the expansion of the stream-tube upstream of the actuator disc, causing its cross-section at free-stream velocity to be smaller than the disc itself [14]. Due to aerodynamic losses the practical value usually range from 30 % to 45 % [9]. Tong [9] states that mechanical energy (torque) captured by the rotor still needs to be converted to electrical energy via an oscillating generator. The effectiveness of the process is determined by the efficiency of the gearbox (η_{gear}), generator (η_{gen}) and electrical equipment (η_e). Therefore the effective power output (P_{eff}) for grid feed can be determined by multiplying equation 2.1 with the above three coefficients.

To determine the performance of a wind turbine the above relation can be used to plot its power output as a function of mean wind speed, as shown in Figure 2.6 [9].

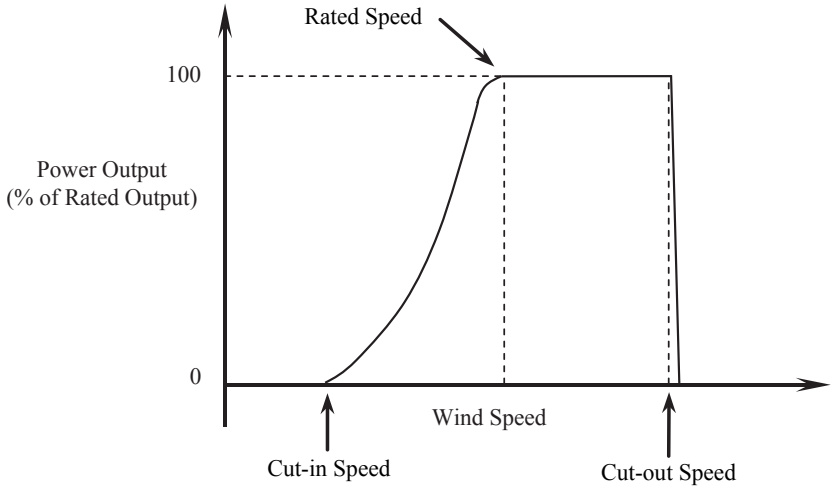

FIGURE 2.6: Typical power curve for a modern wind turbine [9].

When the cut-in speed is reached the turbine starts generating electricity. At the design wind speed (rated speed) power production is at 100 %. The control system activates and limits the output at this level in order for it to stay constant as wind speeds increase. At cut-out speed the machine shuts down to avoid damage, and output returns to zero.

2.3.4.2 Tip speed ratio

According to Tong [9] the tip speed ratio (λ) is an important factor for efficiency of wind turbines. It is the ratio of tangential speed at the tip of the rotor blade to the free wind speed, as shown in equation 2.2. If the blade angular velocity (ω) is too low, large amounts of wind will pass through the rotor area without doing work. However, if ω is above optimal the blades might block the wind. The optimum angular frequency (ω_{opt}) can then be approximated by equation 2.3. Next, equation 2.3 can be substituted into equation 2.2 to approximate the optimum tip speed ratio (λ_{opt}) as shown in equation 2.4. The bracketed ratio was empirically proven to be 2.0 and for a three-bladed machine λ_{opt} is then calculated as 4.2.

$$\lambda = \frac{(L_b + R_h)\omega}{V} \tag{2.2}$$

$$\omega_{opt} \approx \frac{2\pi V}{nL_a} \tag{2.3}$$

$$\lambda_{opt} \approx \frac{2\pi}{n}\left(\frac{L_b + R_h}{L_a}\right) \tag{2.4}$$

Where:

L_b	=	length of rotor blade
R_h	=	hub radius
n	=	number of blades
L_a	=	length of strongly distributed air stream up and downwind of rotor

2.3.4.3 Capacity factor

Wind turbines cannot always generate power, due to the intermittent nature of wind [9]. Therefore a capacity factor is typically used to measure the production efficiency. This factor is determined by the ratio of average actual power to the production at rated

power over a period of time [8]. A high factor is approximately 0.4 and reasonable values range from 0.25 to 0.3 [9].

2.3.5 Turbine configuration

Modern wind turbine designs typically follow the configuration shown in Figure 2.7. The rotor is fixed to a low-speed shaft, which transfers drive torque to the gearbox [14]. The gearbox links the low-speed shaft to the high-speed shaft and the latter drives the generator. This drive-train layout causes the generator to rotate much faster than the rotor, allowing more efficient torque transfer [9]. The gearbox is the main transfer mechanism and can be fixed-speed, two-speed or variable speed. For fixed-speed machines the rotor turns at a fixed tip-speed ratio, which only runs optimally at its corresponding wind speed. However, variable-speed machines can vary rotor speed to maintain the optimum ratio [14]. The nacelle is the cover housing all the main turbine components [21].

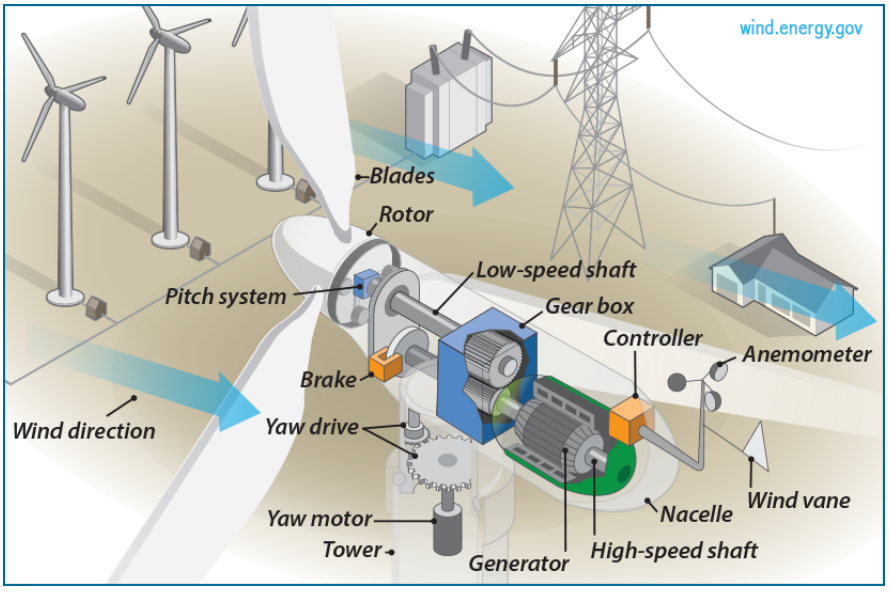

FIGURE 2.7: The configuration of a modern wind turbine [22].

2.3.6 Development trends

According to Tong [9] higher power and lower energy cost has driven increase in wind turbine size over recent years and currently 7 MW to 10 MW capacity machines are under development by some of the larger commercial manufacturers.

2.4 Wind turbine support structure design

The support structure of a wind turbine usually consists of a tower and a foundation. According to Tong [9] the tower supports the nacelle and rotor. The most common modern designs are the tubular monopole (steel and concrete), steel lattice and steel-concrete hybrid. Tower selection and design is based on characteristics such as site conditions, tower stiffness, mode of erection and manufacture, crane size, noise, avian population and aesthetics [9]. Furthermore, the foundation keeps the tower from overturning and is very important for structural dynamics.

2.4.1 Modern industry trends

According to Thresher et al. [7] the most popular modern support structure configuration is a free standing tubular steel tower on a concrete foundation [9][8]. Tower heights typically range from 60 m to 80 m, but 100 m heights are becoming more prevalent. However, the tubular steel design presents various problems regarding structural integrity, manufacture and viability for heights over 80 m. A study by Petcu and Marí-Bernat [11] established that steel towers should only be used up to 80 m in height, Harte and Van Zijl [12] stated that these towers can no longer balance vibration excitation at heights over 85 m and Hau and Von Renouard [13] highlights significant manufacturing problems for steel sections for heights above 90 m. Furthermore, the outer base diameter is limited to 4.2 m due to transport limitations [14]. These constraints have led to a movement towards steel-concrete hybrid and full concrete tower solutions. Such designs present an alternative and possibly more optimal solution for heights over 100 m [10][15].

2.4.2 Steel monopole tower

According to Burton et al. [14] modern steel monopole towers are manufactured from a series of structural grade [8] plate pairs rolled into half circles. These pairs are then welded together to form circular hollow sections of 2 m to 3 m in height [14]. Due to transport and lifting [23] requirements these sections are fabricated into larger parts ranging from 20 m to 30 m. Larger parts have flanges at either end and are bolted or welded on site for easy and fast erection [8][24]. The most popular bolted arrangement is the internal flanged joint. Flanges are butt welded to the ends of the matching parts

with its outer edge against the tower wall [14]. If field welding is required, an automated submerged-arc butt welder is used to achieve fatigue requirements [24]. However, this method tends to be avoided due to high cost [14].

It is common for tubular towers to have a slight taper [14], giving it a conical shape. It results in increased strength towards the base. This is significant, because wind induces increased load response from the top towards the base [8]. Therefore key design parameters are the base diameter and wall thickness. Furthermore, the top diameter is determined by the yaw bearing. The wall thickness for this section should be approximately 1 % of the local radius. Thickness for intermediate heights can be interpolated [14]. The mechanisms governing the dimensions at the base are: buckling of the shell wall in compression, fatigue strength and stiffness for natural frequency requirements [14].

2.4.3 Concrete monopole tower

In the modern industry the concrete monopole design is a practical alternative to its steel counterpart and is sometimes used for large wind turbines. Geometrically this solution is similar, except it has much thicker walls and a wider base. Concrete tower designs are versatile and key performance parameters such as strength and stiffness can be optimized through mixture design [23]. Furthermore, designs can be adapted for in-situ or precast construction methods [25][23]. Concrete construction of wind turbine towers have no height or size restrictions and are also able to successfully accommodate transport restrictions [23].

2.4.3.1 Strength considerations

Wind turbine towers are considered to be high performance structures. Therefore high grade concrete is advised for its construction [15][26]. Significant benefits are: increased compressive and tensile strength, increased modulus of elasticity and reduced creep. It is generally accepted that the characteristic strength for concrete towers should not be less than 25 MPa. Singh [25] further suggests strengths of as much as 34 MPa and 48 MPa. Marshall and Robberts [26] recommends that for pre-tensioned and post-tensioned structures minimum strengths of 30 MPa and 40 MPa should be used. Furthermore, Quilligan

et al. [15] specifies a grade of 60 MPa and higher. It should be noted that there is limited knowledge regarding the dynamic behaviour of high (above 41.4 MPa [27]) and ultra-high (150 MPa to 207 MPa [28]) strength grades [25].

2.4.3.2 Precast segmental construction

According to Singh [25] the prestressed (post-tensioned) precast concrete tower is emerging as the preferred construction method. This design consists of numerous ring units stacked on top of each other using large cranes [24]. The units are prestressed to act in a monolithic manner. Post-tensioned high strength steel tendons absorb tension stresses and keep the concrete in constant compression for service loads [29]. Ring units are prefabricated under controlled conditions in specialized factories. Embedded items, steel reinforcement, tensioning ducts and alignment features are meticulously placed into precise forms and the concrete is cast [24]. Due to transport limitations some units consist of two to three [30] arc segments that are combined in-situ [24][25][31]. Advantages of this design are: stiffness values matching steel for extreme loading, better fatigue resistance and no risk of buckling [25].

2.4.3.3 In-situ construction

In-situ (cast-in-place) slip forming and jump forming construction have proved to be successfully applied for chimneys in the past. Logistically these are easily implemented for pylons, because in-situ methods are performed on all wind turbine construction sites. These are entirely crane-independent using a hoist to lift materials, equipment and crew to the required level [24][23]. Tapered towers of any height can be constructed without joints [32]. However climbing or sliding form work raise additional costs and limit the geometry of the structure. Furthermore, construction is weather sensitive and time consuming [33]. The two methods shall be described below.

Slip forming is a continuous casting technique. Form work is slowly and consistently moved upwards using screw jacks. The rate of upward movement allows enough time for concrete poured at the top to set and gain sufficient strength before emerging at the bottom of the rising form. Sufficient strength is required to support its own weight and the weight of setting concrete above it [23]. The process is slow and must be

performed 24 hours per day until the tower is completed. External post-tensioning is usually applied for these structures. Steel tendons are then mounted and tensioned after sufficient curing is done [30][32][24].

According to LaNier [24] jump forming is not a continuous casting technique. An erection derrick with a specified daily height capacity is assembled on the site. Adjustable inside and outside form work is installed. Embedded items, steel reinforcement and tensioning ducts are placed and the concrete is cast. After casting the form work is raised and adjusted for taper. From a required construction level upward the derrick is raised using chain blocks and attached to embedded inserts in previously placed concrete. This procedure is repeated until the top level of the tower is reached.

2.4.4 Other tower designs

2.4.4.1 Steel lattice

Steel lattice towers are typically assembled from bolted angle sections and square in plan, with four braced legs. Loads in the legs result from tower bending moments, while the bracing carry a combination of shear and torsion. Friction grip bolts are used to avoid fatigue and therefore members are galvanized to acquire enough friction for slippage prevention. Its main failure mechanisms are: fatigue at joints and local buckling under extreme loading. This concept has no limitations for base size and therefore legs are spread wide without compromising stability. However, at a certain height the tip-clearance comes into play and therefore waisted designs are common. This design leads to less material use and cost savings [14]. According to Veritas [8] at equal stiffness a lattice tower uses half the amount of materials than its tubular counterpart. However, dynamic properties are hard to control and it contains a high amount of bolts needing periodic maintenance [30]. Furthermore, due to aesthetics the design is seldom used in the modern industry [8].

2.4.4.2 Steel-concrete hybrid

According to Tong [9] various steel-concrete hybrid tower designs exist. The fundamental principle is to mount a conventional steel monopole tower on a wider concrete base

section. Therefore the steel tower is not at risk for transport limits. Furthermore, stiffness design of the concrete section is easier to control [30].

2.4.5 Foundation design

According to Tong [9] foundations are a crucial part of multi-megawatt wind turbine design. The stiffness significantly affects the natural frequency of the support structure. This directly influences its dynamic behaviour, which is of particular concern for weak and loose soils [23]. Various foundation designs can be implemented depending on geotechnical conditions on site. These are divided between spread footings and piles, of which the former is most commonly used [8][25][34]. The spread footing is a simple and economic solution and is suitable for sites with strong and stiff soils, which give small amounts of settlement. If soil properties on site are not sufficient to support the foundation, piles can be installed. Piles transfer loads to better soil or bedrock at greater depth [34].

2.5 External conditions

IEC61400-1 [35] provides extensive requirements for safety and reliability regarding external conditions for wind turbine design. These are for: electrical, soil and environmental parameters. External conditions may affect loading, durability and operation and must be taken into account in design. Electrical parameters refer to power network conditions and soil properties are relevant for foundation design. Environmental conditions are subdivided into wind and other conditions.

External conditions are also divided into normal and extreme categories. Normal conditions refer to recurrent structural loading. Extreme conditions represent rare external design situations. Design load cases consist of potentially critical combinations of these conditions with operational modes and other situations. The focus of this discussion will be on extreme environmental conditions.

2.5.1 Wind turbine classes

External conditions are defined according to four classes in order to cover most applications. As shown in Table 2.2 each class is defined in terms of wind speed and turbulence, and all parameters apply at hub height. Class I, II and III are defined as standard and do not cover offshore design or tropical storms. Such conditions require class S (special) design for which designers or clients must specify basic parameters. The symbol V_{ref} represents the reference wind speed average over 10 min. Categories A, B and C define higher, medium and lower turbulence characteristics respectively. The expected value of turbulence intensity is denoted as I_{ref} at $15\,\mathrm{m\,s^{-1}}$.

TABLE 2.2: Basic parameters for wind turbine classes [35].

Class		I	II	III	S
V_{ref}		50	42.5	37.5	
I_{ref}	A		0.16		
	B		0.14		
	C		0.12		

2.5.2 Wind conditions

Wind is the primary external condition affecting structural integrity of a wind turbine. Extreme wind is defined as having a 1 year or 50 year recurrence period. This condition can be approximated as follows by a steady extreme wind speed model [35]:

- V_{e50}, with a 50 year return period (equation 2.5) and
- V_{e1}, with a 1 year return period (equation 2.6).

$$V_{e50} = 1.4V_{ref}\left(\frac{z}{z_{hub}}\right)^{0.11} \tag{2.5}$$

$$V_{e1} = 0.8V_{e50} \tag{2.6}$$

Where:

z = height above ground

z_{hub} = hub height

In equation 2.5 the wind speed increases with height to account for wind shear and from this a wind profile can be approximated over the height of a wind turbine. The value 1.4 is the gust factor, which accounts for the dynamic effects of resonance between wind turbulence and structural vibration [35]. Furthermore, constant yaw misalignment of $\pm 15^{\circ}$ is assumed to allow for short-term deviations from the mean wind direction.

2.5.3 Other conditions

Other environmental conditions also affect the safety and integrity of design features such as control system function, durability and corrosion. Combinations of these climatic conditions may increase its effect and an array of normal and extreme conditions must be taken into account for wind turbine design. For extreme conditions the following apply: temperature, lightning, ice and earthquakes.

2.6 Wind data considerations for South Africa

According to the IEC61400-1 code [35] wind is considered to be the most influential external condition for wind turbine design and therefore it is important to acquire accurate on site measurements. Site measurements should comply with the following criteria:

- it must range from $0.2\,V_{\text{ref}}$ to $0.4\,V_{\text{ref}}$ and be extrapolated, or
- be calculated from recordings at the site, long-term records from available local meteorological stations, or local codes and standards.

On-site measurements are usually done by the turbine designers and are not made available to the public. However, records for meteorological stations and local codes are available in South Africa. The Wind Atlas for South Africa (WASA) project has 10 meteorological stations situated at various locations throughout the country. These stations measure wind speeds at heights of up to 62 m [36]. Furthermore, the South African wind loading standard [37] gives local requirements for wind actions on buildings and industrial structures.

2.6.1 Wind Atlas for South Africa

South Africa seeks to develop capacity, skills and data that would enable investigation and planning for large-scale wind exploitation for electricity generation. In order to achieve this, methods for wind resource mapping on regional and national scale should be developed. Furthermore, reliable estimation procedures should be established for annual energy production of proposed wind farms. The numerical WASA is being developed for this purpose [36]. Ten wind measurement masts were installed at various locations throughout South Africa. The Council for Scientific and Industrial Research (CSIR) provides recorded data for these masts stored online in Microsoft Excel files [38]. The data sets contain maximum, minimum, mean and standard deviation of the wind speed for 10 min intervals and are recorded at five heights up to 62 m. Table 1 in Appendix A shows significant information about the ten masts. Information currently available are from start dates in 2010 until March 2014 [38], amounting to a reliable record of over 3 years for each of the sites. However, according to Winkler et al. [39] a long term record should be at least 10 years in length. Therefore the WASA data does not meet IEC [35] specifications and cannot be used for wind calculations in this study.

2.6.2 South African wind loading code

SANS 10160-3:2010 [37] is a loading code providing specifications for South African wind conditions. This code gives a static representation of wind actions. These actions are determined from basic values for wind speed and pressure, which have a mean return period of 50 years. Wind actions calculated from this code are equivalent to extreme effects of turbulent wind. However, it has some limitations that are significant for this study and does not cover:

- effects due to high intensity winds (tornadoes or micro-bursts),
- dynamic properties and response for structures, and
- tall and dynamically sensitive structures.

High intensity winds are rare in South Africa and have a very small probability of occurrence. However, forces caused by short duration gusts are usually significantly

larger than those considered for international standards. The main concerns for the last two points are along-wind response due to resonance between atmospheric wind turbulence and structural vibrations, and across-wind excitation due to vortex shedding. The latter is of particular concern for circular cylinders.

According to Kruger et al. [40] the last comprehensive strong wind analysis for South Africa was performed in 1985 and the current loading code [37] is still based on this data. Employment of automatic weather station technology has significantly increased available wind data for such an analysis. An updated assessment of strong winds in South Africa has been performed and based on this data. New wind maps were created showing the annual maximum gust and hourly mean wind speeds for various locations. The gust values are particularly important regarding the South African code, but does not influence this study.

2.7 Structural loading of wind turbines

A wind turbine is subject to various types of loads throughout its operational lifetime. To successfully perform structural analysis and modelling, accurate approximation and application of these loads are essential. Design loading, design situations and load cases for extreme conditions, and load calculation methods shall be discussed.

2.7.1 Design loads

Wind turbine design loads are classified according to four categories: gravitational and inertia loads, aerodynamic loads, actuation loads and other loads [8][14][35].

Gravitational and inertia loads are mass dependent [8]. These include static and dynamic actions that result from gravity, vibration, rotation and seismic activity [35]. Gravity loads apply for the rotor, tower and nacelle and can be calculated using equation 2.7 [8].

$$F_g = mg \tag{2.7}$$

Where:

F_g = gravity force

g	=	gravity acceleration
m	=	total mass of component

Gyroscopic loads tend to act on the rotor during yawing. In the rotor plane this will result in a yaw moment, M_K, around the vertical axis and a tilt moment, M_G, around the horizontal axis. For a three bladed rotor the net effect of M_K equals zero due to the gyroscopic effect, but M_G is non-zero and constant. Angular velocity of the yaw system is usually small and therefore gyroscopic effects are mostly neglected. However, these forces should be considered for megawatt size turbines [8].

For aerodynamic loading, static and dynamic actions are caused by airflow and its interaction with stationary and moving parts of the wind turbine [35]. These loads mainly act on the rotor blades, tower and nacelle [8]. Airflow is dependant upon average wind speed and turbulence across the rotor plane, rotor rotational speed, air density and aerodynamic shapes of turbine components. It also depends on the interactive or aero-elastic effects of these components [35].

The wind flow in the vicinity of the rotor is very complex. Velocities at a typical blade cross-section is shown in Figure 2.3. The inflow wind velocity (V_0) is perpendicular to the rotor plane. When wind passes through this plane, V_0 is reduced to the value aV_0 due to axial interference. A blade element at a distance (r) from the rotor axis, will move at speed ωr within the rotor plane. Interaction between the wind and moving rotor blade produces a tangential slipstream wind velocity, $a\omega r$ [8].

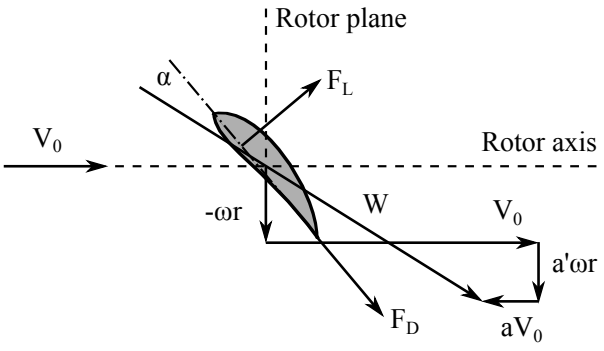

TABLE 2.3: Air velocities at wind turbine blade cross-section [8][20].

The resulting relative velocity at which air strikes the rotor blade (W) is a function of wind and blade velocity as shown in equation 2.8. This relative airflow reaches the blade at an angle (α) from the blade plane, which is called the angle of attack. The

relative velocity induces aerodynamic lift (F_L) and drag (F_D) forces, of which the former is responsible for power generation [20]. These forces are determined using equations 2.9 and 2.10 [8]. For the tower and nacelle the aerodynamic drag force, F_d, can be calculated using the projected area perpendicular to the flow. This is expressed in equation 2.11.

$$W^2 = \left[\frac{4\pi}{3} n_r R\right]^2 + V_0^2 \tag{2.8}$$

$$F_L = 0.5 C_l \rho c W^2 \tag{2.9}$$

$$F_D = 0.5 C_d \rho c W^2 \tag{2.10}$$

$$F_d = 0.5 C_d \rho A V_0^2 \tag{2.11}$$

Where:

R	=	rotor radius
n_r	=	rotor frequency
V_0	=	nominal stall wind speed at hub height
C_l	=	aerodynamic lift coefficient
C_d	=	aerodynamic drag coefficient
ρ	=	air density
c	=	blade chord length
A_p	=	projected area perpendicular to the flow

Actuation loads result from the operation and control of wind turbines and several exist: torque control from a generator or inverter, yaw, pitch or air brake, and mechanical braking. For calculation of response and loading it is important to consider the range of actuator forces available. Other loads include wake effects from nearby wind turbines, impact loads, ice loads, tower shadow and vortex shedding [8][35].

2.7.2 Fatigue loading

According to Burton et al. [14] a wind turbine is subject to severe loading throughout its lifetime. The rotor of a 600 kW turbine typically complete 2×10^8 cycles in a 20 year life. Each cycle induces design load effects such as gravity stress reversal, blade out-of-plane bending, yaw error, shaft tilt and tower shadow. Due to these effects fatigue

often governs the design of various turbine components. The load spectrum for fatigue should mainly represent loading cycles experienced during power production. These cycles should include the full operational wind speed range. Furthermore, the number of cycles should be weighted in accordance with the proportion of time spent operating at each wind speed. Load cycles for start-up and shut down should also be considered for completeness. It is generally assumed that extreme loading conditions will not have a significant effect on fatigue strength due to rarity of occurrence.

2.7.3 Ultimate loading

The worst values for design loads are used to determine ultimate loading. Various critical situations and design load cases (DLC's) must be chosen to cover a range of combinations of machine states and external wind conditions. The IEC code [35] provides 8 situations and 22 DLC's to verify structural integrity of wind turbines. For ultimate design it should be chosen from the following states [14][35]:

- normal wind conditions with normal machine states,
- normal wind conditions with machine fault states and
- extreme wind with normal machine states.

Normal and extreme wind conditions are usually defined as the worst cases occurring for 1 year and 50 year return periods. Normal machine state refers to a turbine that has no broken or faulty components and a fault state signals that equipment failure has occurred. The fault state is assumed to happen so rarely that it does not coincide with extreme wind and the load combination for these two is generally not considered [14].

2.7.4 Situations and design load cases for ultimate loading

The most significant IEC [35] situations and the relevant extreme DLC's specified for it shall now be discussed.

2.7.4.1 Non-operational with normal machine state

According to Burton et al. [14] a non-operational machine state occurs when a wind turbine is not generating power, not starting up or shutting down. It should be stationary, which means that it is either parked or idling. The 50 year gust is generally used as the design wind speed and the DLC's below should be investigated.

- DLC 6.1: Apply the steady extreme 50 year wind speed model (EWM) with yaw misalignment of up to $\pm 15^\circ$ for an active yaw system. Otherwise apply the turbulent extreme wind model (ETM) with mean yaw error of $\pm 8^\circ$. These cases apply where restraint against yaw slippage can be assured.
- DLC 6.2: Loss of electrical power network at an early stage of a storm with extreme 50 year wind conditions. If power backup is provided for the control and yaw system to ensure alignment for at least 6 hours, this case can be disregarded. Otherwise the effect of a wind direction change of up to $\pm 180^\circ$ should be investigated.
- DLC 6.3: Extreme wind with a 1 year recurrence period shall be combined with extreme yaw misalignment. Misalignment of up to $\pm 30^\circ$ should be considered when using the EWM and $\pm 30^\circ$ for the ETM.

Burton et al. [14] states that when grid loss occurs without power backup (DLC 6.2), the yaw system cannot track changes in wind direction. If the direction changes by 90° to 180°, the turbine becomes side or back winded. This situation should be investigated even with the low likelihood that winds will change by more than 90° and still remain at extreme speeds. However, for wind farms in general the level of grid security should be high enough to rule out this possibility, especially if the yaw drive is designed to stay operational in extreme wind [8].

2.7.4.2 Non-operational with machine fault state

Typical load cases for non-operational machine fault involve failure of pitch or yaw mechanisms and design wind speed is usually taken as the 1 year return period gust [14].

2.7.4.3 Operational with normal machine state

In this state a wind turbine is running and connected to the electrical grid, and DLC's should be investigated for atmospheric turbulence, extreme turbulence, and transient conditions [35].

2.7.4.4 Operational with machine fault state

In this event a machine fault occurs during operation and it can be located in the control or electrical system. When grid connection is lost the generator will no longer resist aerodynamic torque (loss of load) and the rotor will accelerate until braking is applied. This case may result in critical rotor loading [14][35], but designers generally assume that machine fault is uncorrelated with extreme winds and normal conditions are considered. In some cases the tip speed of an operational turbine is high relative to the design gust speed. For such an occurrence the extreme operational load cases sometimes govern instead of the static ones. However, for all other cases it is customary to base extreme loading on a static wind turbine [14].

2.7.5 Extreme tower load cases

According to Burton et al. [14] pitch regulated wind turbines apply full feathering at shut down. This significantly reduces non-operational rotor loading for stationary three bladed machines and is assumed for the two critical load cases below.

- Case 1: Maximum drag forces for tower base bending. Sideways wind loading with two blades inclined at 30° to the vertical.
- Case 2: Maximum lift forces for tower base bending. Wind from the front with a 15° to 20° yaw error. One blade faces vertically upwards with the other two inclined at 30° to the horizontal.

The rotor loading for both cases are similar in magnitude. However, for case 2 it is caused by blade lift. This induces forces at right angles to the wind direction and as a result the total moment at the tower base is significantly less than for case 1. Furthermore,

extreme design loads can only be determined using calculations, because it cannot be measured due to long recurrence periods between extreme wind events [8].

2.7.6 Typical tower loading

Veritas [8] gives guidelines for the design of tubular wind turbine towers. In order to calculate section loads, it can be viewed as a cantilever beam. The typical loading for such a tower is presented in Figure 2.8. External loads are denoted by index, T, and applied at the top flange of the tower located at a height, H, above the base. This height is not necessarily the hub height. The four external design loads are:

- horizontal axial force perpendicular to the rotor plane and parallel to its axis (F_{yT}),
- vertical downward axial force parallel to the rotor plane (F_{zT}),
- tilt moment around horizontal axis parallel to rotor plane (M_{xT}), and
- torsion moment around vertical axis (M_{zT}).

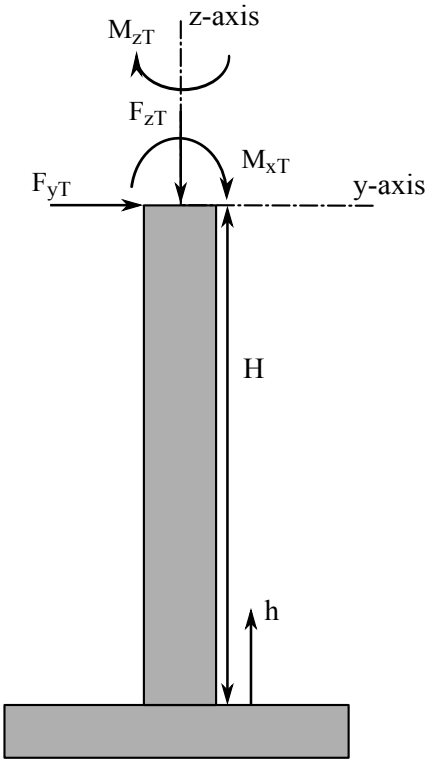

FIGURE 2.8: Typical loading for a tubular tower [8].

Section loads in the tower at a specific height, h, can be calculated from the external loads and own weight of the tower. Formulas for calculating these are expressed in equations 2.12 through 2.15:

$$F_z(h) = F_{zT} + \rho_t \sum_{h}^{H} A(z)dz \tag{2.12}$$

$$M_z(h) = M_{zT} \tag{2.13}$$

$$F_z(h) = F_{yT} + F_w(h) \tag{2.14}$$

$$M_x(h) = M_{xT} + F_{yT}(H-h) + M_w(h) + F_{zT}\big(\delta(H) - \delta(h)\big) \tag{2.15}$$

Where:

F_y	=	thrust from wind load
M_x	=	bending moment from wind load
F_z	=	gravity force
M_z	=	torsional moment
ρ_t	=	density of tower including appurtenances
$A(z)$	=	cross-sectional area as a function of height
δ	=	deflection of tower due to thrust from wind

It is particularly important to include the effect of eccentricity of the nacelle for M_{xT}. Furthermore, the second term in equation 2.12 calculates the own weight of the tower at h. The section force, $F_w(h)$, and moment, $M_w(h)$ model the loading on the tower due to wind speed pressure. These loads are calculated using equations 2.16 and 2.17. It should be noted that the form factor depends on the Reynold's number.

$$F_w(h) = 0.5\rho \sum_{h}^{H} V(z)^2 \varphi D(z) C(z) dz \tag{2.16}$$

$$M_w(h) = 0.5\rho \sum_{h}^{H} (H - h - z) V(z)^2 \varphi D(z) C(z) dz \tag{2.17}$$

Where:

ρ	=	air density
$V(z)$	=	wind speed

$D(z)$	=	outer tower diameter
$C(z)$	=	form factor
φ	=	gust factor

2.7.7 Aero-elastic load calculations

According to Veritas [8] load calculations for a wind turbine are generally performed by means of a computer program based on an aero-elastic calculation procedure. The procedure solves the equations of motion for an arbitrary set of forces that act on the structure and are generated by it. A geometrically nonlinear Finite Element Method (FEM) approach or modified modal analysis is typically applied. Loads that are derived from an aero-elastic model is then used for tower and other component design.

For extreme conditions the load combination producing the highest possibility of structural failure should be found. When using an aero-elastic computer program this can be a big task. The software simulates a large amount of load cases in 10 min time series. Different governing cases might even occur at different sections in the tower. Alternatively, loads can be combined by taking the maximum of each component from the load case where the dominant load is at a maximum. For a more conservative approach, maximum values of the various load components can be used regardless of the load case it applies to. Currently available computer resources are generally adequate to perform these computer-intensive calculations. Therefore, most load calculations for wind turbines are done using aero-elastic methods.

2.7.8 Simplified load calculations

When computer software is not available, the aero-elastic procedure becomes tedious. Therefore, various simplified methods exist to perform load calculations for a wind turbine [8]. The quasi-static method and South African code calculations were used for this study.

2.7.8.1 Quasi-static method

According to Veritas [8] the quasi-static method has four design loads which are calculated for a static wind turbine in extreme wind conditions (see subsubsection 3.5.3.1). External loads are assumed to include dynamic effects or a gust factor for this approach.

For rotor blade load calculation one blade is assumed to be positioned vertically above the hub. The root moment of this blade is assumed to be the design tilt moment. This moment is calculated using the force on the blade and a lever arm from its location to the hub. The axial force is determined by summing axial wind loads calculated for each blade. Furthermore, the yaw moment is assumed to be the root moment for a horizontally positioned blade. The load per unit length of a blade, $p(r)$, is calculated using equation 2.18:

$$p(r) = 0.5\Psi\rho U_{10}^2 D(r) C \tag{2.18}$$

Where:

Ψ	=	gust factor
U_{10}	=	10-minute mean wind speed with a recurrence period of 50 years at height, h
$D(r)$	=	blade chord length at a distance, r, from the hub
C	=	maximum value of C_l or C_d (see subsection 2.7.9)

The height is calculated according to formulas shown in Table 2.4.

TABLE 2.4: Load specification parameters for the Quasi-Static method [8].

Load	Eigen-frequency (f_0) corresponding to	Threshold (f^*)	C	Height (h)
Blade load	Blade flapwise bending	1.7	$C_{l,max}$	$z_{hub} + \frac{2}{3}L$
Axial force	Tower bending	0.45	$C_{d,max}$	z_{hub}
Tilt moment	Blade flapwise bending	1.7	$C_{l,max}$	$z_{hub} + \frac{2}{3}L$
Yaw moment	N/A	0	$C_{d,max}$	z_{hub}

The gust factor (Ψ) is calculated according to equation 2.19:

$$\Psi = \begin{cases} \left[\frac{ln\left(\frac{z_{hub}}{z_0}\right)+3.1}{ln\left(\frac{z_{hub}}{z_0}\right)}\right]^2 & \text{for} \quad \frac{f_0 R}{U_{10}} > f^* \\ 1 + 3.9\left[\frac{2\sqrt{k_b+k_r}}{ln\left(\frac{z_{hub}}{z_0}\right)}\right] & \text{for} \quad \frac{f_0 R}{U_{10}} \leq f^* \end{cases} \tag{2.19}$$

Where:

z_0	=	roughness length
R	=	rotor radius
f_*	=	given in Table 2.4
f_0	=	eigenfrequency of vibration mode associated with the design load under consideration

The background turbulence, k_b, and resonance effect, k_r, is estimated using equations 2.20 and 2.21:

$$k_b = \begin{cases} 0.9 - 2.5\frac{R}{\ell} & \text{for blade load} \\ 0.75 - 3\frac{R}{\ell} & \text{for axial force} \end{cases} \tag{2.20}$$

$$k_r = \frac{\frac{f_0 \ell}{U_{10}}}{\left[1 + 1.5\frac{f_0 \ell}{U_{10}}\right]^{\frac{5}{3}}} F(f_0)\frac{\pi^2}{2\delta} \tag{2.21}$$

Where:

ℓ	=	$6.8L_u$
δ	=	logarithmic increment of damping
$F(f)$	=	aerodynamic admittance function

The symbol, L_u, represents the integral length scale of the Kaimal spectrum. Furthermore, δ is calculated using equation 2.22:

$$\delta = 2\pi(\zeta_0 + \zeta_a) \tag{2.22}$$

Where:

ζ_0 = structural damping ratio

ζ_a = aerodynamic damping ratio

The value of $F(f)$ depends on which design load is considered and is calculated using equation 2.23:

$$F(f) = \begin{cases} \frac{1}{1+3\left(\frac{fR}{U_{10}}\right)} & \text{for blade load} \\ \frac{1}{1+12\left(\frac{fR}{U_{10}}\right)} & \text{for axial force} \\ \frac{2.7\left(\frac{fR}{U_{10}}\right)}{1+4.4\left(\frac{fR}{U_{10}}\right)+21.8\left(\frac{fR}{U_{10}}\right)^2} & \text{for rotor moments} \end{cases} \tag{2.23}$$

2.7.8.2 South African code calculations

The SANS code [37] gives various local requirements and procedures for wind loading on structures. Calculation of peak wind speed pressure, wind forces, force coefficients and end-effects will be discussed in this subsection.

The peak wind speed pressure, $q_p(z)$, represents the pressure exerted on a structure due to wind flow at a certain height. This value includes mean and short duration wind speed fluctuations. It is calculated using equation 2.24. Recommended values for ρ are determined according to site altitude above sea level at an assumed average temperature of 20 °C.

$$q_p(z) = 0.5 \times \rho \times v_p(z)^2 \tag{2.24}$$

Wind forces can either be determined by applying force coefficients to $q_p(z)$ or by integration of surface pressures. The former shall be the focus of this discussion. Therefore, the design wind force (F_w) can be determined using equation 2.25:

$$F_w = c_s \times c_d \times c_f \times q_p(z_e) \times A_{ref} \tag{2.25}$$

Where:

$c_s c_d$	=	structural factor equal to 1.0
c_f	=	force coefficient for a structure or structural element
A_{ref}	=	reference area for a structure or structural element

The structural factor takes into account the combined effects of:

- non-simultaneous occurrence of peak pressures over external surfaces of buildings and structures, and
- dynamic effects due to resonance between the turbulence of flow and vibrations of a structure.

For structures falling inside the scope of the SANS code [37], $c_s c_d$ shall be assumed to be 1.0. Annex B of the code [37] can be consulted for those falling outside.

Force coefficients are used to specify the magnitude of the pressure forces for a range of structures. It should be noted that these factors include the effects of friction. Coefficients for circular cylinders are of particular concern for tubular tower design. The force coefficient for a finite circular cylinder is calculated using equation 2.26:

$$c_f = c_{f,0} \times \Psi_\lambda \tag{2.26}$$

Where:

$c_{f,0}$	=	force coefficient of cylinders without free-end flow
Ψ_λ	=	end-effect factor

The value for $c_{f,0}$ is acquired from Figure 30 in the SANS code [37]. The values in this figure is dependent on the Reynolds number and $\frac{k}{b}$ ratio. The symbol k represents the equivalent surface roughness. Relevant k values are listed in Table 2.5. Furthermore, b is the diameter of the cylinder.

TABLE 2.5: Equivalent surface roughness for wind turbine tower surfaces [37].

Type of surface	Equivalent roughness, k (mm)
Fine paint	0.006
Galvanised steel	0.2
Smooth concrete	0.2

The reference area is obtained using equation 2.27. For a cylindrical tower L is its maximum height above ground.

$$A_{ref} = L \times b \tag{2.27}$$

Where:

L = length of structural element under consideration

The end-effect factor accounts for the reduced resistance of a structure due to wind flow around its loose end. This factor is acquired from Figure 38 in the SANS code [37]. It is a function of the slenderness and solidity ratio. The former is dependant on the dimensions and position of a structure. It is derived from Table 22 in the SANS code [37]. The latter is a measure of the amount of holes in the surface area facing the wind. For a monopole tower, this ratio is equal to 1.0.

2.7.9 Blade lift and drag coefficients

According to Burton et al. [14] maximum blade loading occurs for two cases where the wind direction is:

- approximately normal to the blade inducing maximum drag, and
- at an angle between 12° and 16° to the blade plane, inducing maximum lift.

In the past designers used an infinitely long flat plate to calculate a drag coefficient (C_d) of 2.0, which was adjusted towards the blade tip according to its aspect ratio. For the old CP3 British code this approach would produce a value of 1.68 for a typical wind turbine. However, recent studies reported values of 1.24 and 1.25. The Danish standard (DS) 472 requires a minimum value of 1.3. Aerofoil data for lift is more readily available, due to its need for assessing rotor performance. The maximum lift coefficient (C_l) rarely exceeds 1.6 and values of 1.1 can be obtained on the thicker inboard portion of the blade near the hub. The DS 472 code specifies a minimum lift coefficient of 1.5. Veritas [8] states that typical maximum values for C_d and C_l range from 1.3 to 1.5.

2.8 Considerations for structural analysis of wind turbine towers

According to the IEC code [35], ultimate and fatigue strength of members should be verified by calculations and/or tests to demonstrate the structural integrity of a wind turbine tower. Furthermore, evidence or references to verification studies should be included in design documentation to prove the validity of the calculation and test methods used. Any test for strength verification shall correspond with safety factors appropriate for the characteristic loads.

An ultimate limit state analysis is suggested. This method uses partial safety factors to account for uncertainties and variability in loads and materials, uncertainty in analysis methods and the consequence of failure of important structural components. It also suggests four analysis methods. Each type requires a different formulation of the limit state function and uses different partial material factors to account for uncertainties.

2.8.1 Partial safety factors

2.8.1.1 Loads and materials

For safe design, the variability of loads and materials are taken into account using equations 2.28 and 2.29:

$$F_d = \gamma_f F_k \tag{2.28}$$

$$f_d = \frac{1}{\gamma_m} f_k \tag{2.29}$$

Where:

F_d	=	design value for internal load or load response to various simultaneous load components for a given DLC
γ_f	=	partial safety factor for loads
F_k	=	characteristic value of the load
f_d	=	design value for material strength
γ_m	=	partial safety factor for materials

f_k = characteristic value for material strength

The factor γ_f takes the following into account: uncertainties in the loading model and unfavourable deviations of the load from F_k. For γ_m the following is considered:

- possible unfavourable deviations of material strength from the characteristic value,
- possible inaccurate assessment of the resistance of sections or load-carrying capacity of parts of the structure,
- uncertainty in geometrical parameters,
- uncertainties in the relation between material properties in the structure and those measured from tests on control specimens, and
- uncertainties in conversion factors.

2.8.1.2 Consequence of failure

The consequence of failure of important structural components is represented by the factor γ_n. It is used to distinguish between the component classes below.

- Class 1: "Fail-safe" structural components whose failure does not result in failure of a major part of a wind turbine.
- Class 2: "Non fail-safe" structural components for which failure may result in failure of a significant part of a wind turbine.
- Class 3: "Non fail-safe" mechanical components linking actuators and brakes to main structural components in order to implement non-redundant wind turbine protection functions.

It should be noted that wind turbine towers are defined as class 2 components.

2.8.2 Analysis of ultimate strength

Fundamentally, the limit state is separated into two functions for loading (S) and resistance (R) as shown in equation 2.30. For an ultimate strength analysis S is typically defined as the highest value of structural response, hence $S(F_d) = F_d$. The maximum design value for material resistance corresponds with R, leading to: $R(f_d) = f_d$. Equation 2.30 then takes the form of equation 2.31. The latter is used to verify the most critical limit state for all relevant DLC's for each wind turbine component. This state is determined as the case with the smallest margin.

$$\gamma_n S(F_d) \leq R(f_d) \tag{2.30}$$

$$\gamma_f F_k \leq \frac{1}{\gamma_m \gamma_n} f_k \tag{2.31}$$

Safety factors for loads are given in Table 2.6. These are compared for the following codes and guidelines: IEC61400-1 [35], GL rules [41] and Danish standard DS 472.

TABLE 2.6: Comparison of γ_f for ultimate strength analysis [14].

Source of loading	Unfavourable						Favourable		
	Normal			Extreme	Abnormal				
	IEC	GL	DS	GL	IEC	GL and DS	IEC	GL	DS
Aerodynamic	1.35	1.2	1.5	1.3	1.1	1.0	0.9	-	-
Operational	1.35	1.35	1.2	1.3	1.1	1.0	0.9	-	-
Gravity	1.1*	1.1*	1.1*	1.0	1.1	1.0	0.9	1.0	-
Inertia	1.25	1.1*	1.1*	1.0	1.1	1.0	0.9	1.0	-

*Factor increased to 1.35 if masses are not determined by weighing

The material factor is defined for ductile and non-ductile materials whose failure could lead to the failure of a major part. Tubular steel towers fall under the former and failure may occur through yielding or bolt rupture. The IEC code [35] specifies a general value of at least 1.1. For the latter, the following factor values apply:

- 1.2 for global buckling of curved shells (tubular steel towers and blades) and
- 1.3 for rupture from exceeding tensile or compression strength.

Table 2.7 list relevant material factors from local codes [42][29]. It should be noted that when considering the effects of excessive loads or localized damage, γ_m for concrete and

steel can be taken as 1.3 and 1.0 respectively. Furthermore, the consequence of failure factor of a wind turbine tower equals unity.

TABLE 2.7: Material factors for ultimate strength analysis [42][29].

Material	γ_m
Structural steel	1.11
Steel reinforcement	1.15
Concrete in flexure or axial load	1.5

2.8.3 Analysis of fatigue failure

Fatigue damage is usually calculated with Palmgren-Miner's rule [8][35]. The limit state for this method is reached when the accumulated damage exceeds 1.0. For a wind turbine accumulated damage occurs over its design lifetime. Calculations include the formation and effects of both cyclic range and mean strain or stress levels. Furthermore, partial safety factors are applied to both of the above when assessing the increment of damage associated with each fatigue cycle.

The partial safety factor for loading is unity and consequence of failure equals 1.15. The material factor is 1.5 for a material with a SN curve based on 50 % survival probability and coefficient of variation smaller than 15 %. However, for larger variation (15 % to 20 %) the factor increases to 1.7. The latter applies for composites such as reinforced concrete. A factor of 1.1 is suitable for structural steel [35].

2.8.4 Stability analysis

The IEC code [35] states that for a stability analysis load-carrying parts of "non fail-safe" components should not buckle under the design load. For other components, elastic buckling is acceptable, but no buckling of any component is allowed under characteristic load. Specified safety factors are the same as those for the ultimate strength analysis.

Given perfect geometry, the strength of a cylindrical steel tube in axial compression is dependant on either the yield strength or elastic critical buckling stress. The classic theory for the latter is expressed in equation 2.32. Yield strength governs for a $\frac{r}{t}$ ratio of less than $\frac{0.605E}{f_y}$, where f_y is the yield stress of steel. This equates to 340 for grade S355 structural steel. However, imperfections significantly reduce the compression resistance

of the tube. Although relatively low tower-wall radius to thickness ratios are usually adopted for wind turbine towers, buckling strength generally governs for design of wall thickness [8][14][43].

$$\sigma_{cr} = \frac{0.605Et}{r_t} \tag{2.32}$$

Where:

σ_{cr}	=	elastic critical buckling stress of a cylindrical shell
E	=	modulus of elasticity
t	=	wall thickness
r_t	=	radius

For wind turbine towers instability can either occur globally or locally. These structures are usually geometrically nonlinear due to variation in wall thickness and imperfections. Therefore global instability involves buckling or collapse behaviour, as shown in Figure 2.9(a). The load-displacement response should show negative stiffness and the structure must release strain energy to remain in equilibrium. If instability is localized (local buckling, surface wrinkling or material instability) local transfer of strain energy will occur from one part of the structure to neighbouring parts. Figure 2.9(b) shows the typical diamond shaped buckling pattern that should form [43].

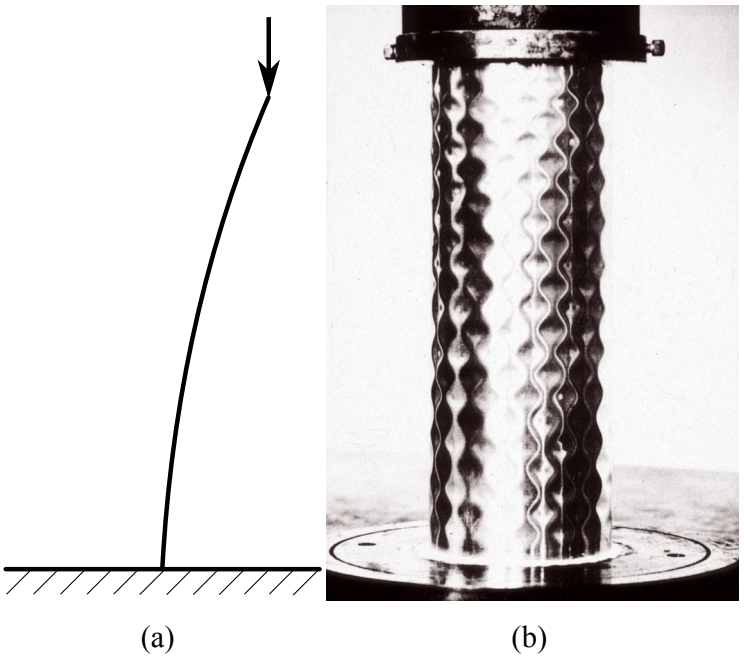

FIGURE 2.9: (a) The typical global buckling mode of an axially compressed beam-column. (b) The diamond shaped local buckling pattern of a cylindrical shell [44].

2.8.5 Critical deflection analysis

According to the IEC code [35] critical deflection should not affect structural integrity for any of the relevant DLC's. One of the most important considerations for such an analysis is to verify that no mechanical interference occurs between the blade and tower. This is done by determining the static clearance as shown in Figure 2.10. Static clearance is the baseline axial distance between the tip of the rotor blade and the wall of the support tower when fully unloaded and in the 6 o' clock position [9].

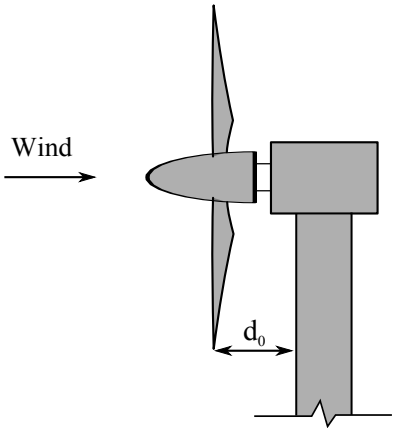

FIGURE 2.10: Static clearance of a wind turbine blade.

The IEC code [35] requires that the maximum elastic deflection in the unfavourable direction be determined for all relevant DLC's. Characteristic loads should be applied to the calculation. Furthermore, the resulting value should be multiplied with a combined partial safety factor for loads, materials and consequence of failure. The distance between the tower and blade tip should comply with equation 2.33 to ensure non-interference [8]. It should be noted that tip deflections of wind turbine blades can be up to 10 % of its radius for extreme wind conditions [14].

$$d_0 - \gamma u_{max} > F \tag{2.33}$$

Where:

d_0	=	distance between the tower and blade tip in the unloaded state
γ	=	combined partial safety factor for u_{max}, chosen according to relevant DLC's
u_{max}	=	maximum deflection of the blade for characteristic load and material values
F	=	requirement for the residual clearance between the tower and blade tip, usually 0.0

The partial safety factors for loads are the same as those used for the ultimate strength analysis, but the material factor is generally taken as 1.1 and γ_n equals unity.

2.8.6 Dynamic considerations

2.8.6.1 Stiffness

A wind turbine tower is typically classified according to the relationship between its first natural frequency (1 T) and exciting frequencies during operation [9][14]. Actions inducing the latter are: rotor imbalance, wind shear or tower shadow (1 P), and blade passing (3 P). To avoid resonance during operation 1 T should be kept outside ±10 % ranges of these [8].

The overall stiffness of a tower is the main design parameter affecting natural frequency. Therefore designs are defined according to three types: stiff, soft and soft-soft as shown

in the Campbell diagram in Figure 2.11. Structurally a stiff tower is preferred, because 1 T is then higher than 3 P and resonance is avoided altogether. However more material is required to attain the higher natural frequency, leading to increased cost. For this reason soft designs are generally used in practice. The natural frequency of such a tower lies between 1 P and 2 P and for the soft-soft design it is less than 1 P [9][14]. For the last two designs a proper analysis of the start-up and stopping sequences should be performed. The analysis should account for the increased dynamic loading that occurs when 1 P and 3 P is passing through 1 T [45].

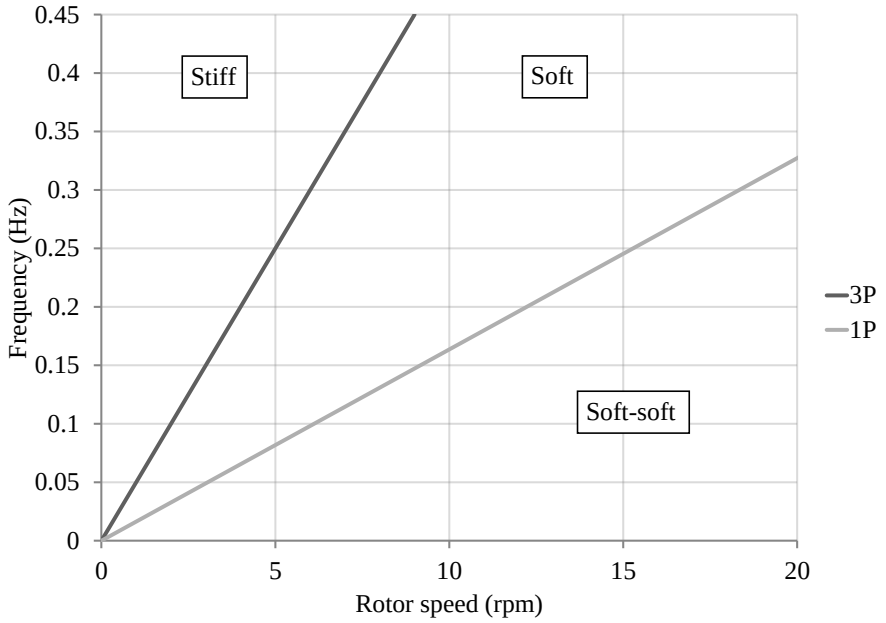

FIGURE 2.11: Typical Campbell diagram for a wind turbine.

2.8.6.2 Vibrations due to vortex shedding

According to Veritas [8] induced vibrations due to vortex shedding can be analysed for wind turbine design. This phenomenon may occur in a situation where the rotor and nacelle has not been mounted on the tower. The analysis might prove that certain velocities should be avoided when erecting the tower. Sensitivity to vortex shedding might be reduced by installing temporary guy wiring or mounting a temporary mass at the top of the tower. Generally, vortex-induced vibrations do not pose any problems once the rotor and nacelle is installed. The weight of the nacelle decreases critical wind speed for vortex-induced vibrations to a low level. This value is typically below $10\,\mathrm{m\,s^{-1}}$, which is within the interval of power production. When rotating blades pass the tower,

it causes turbulence in the wind passing the tower behind the blades. It reduces the wind speed and obstructs generation of vortices. Furthermore, the blades and nacelle produce aerodynamic damping, further reducing vortex induced vibrations.

2.8.7 Prestressing of a tubular concrete tower

It is well known that concrete has a low tension capacity. Steel reinforcement or prestressing is used in tension areas to counter this weakness. For wind turbines prestressing is predominantly used for concrete towers. Large moments produce significant tension forces in the tower cross-section. A tower is prestressed to ensure that the cross-section is either in full compression or has very little tension. This is done to prevent or limit cracking in the concrete. The SABS 0100-1 code [29] and Nawy [27] provides requirements and methods for design and analysis of prestressed concrete.

2.8.7.1 Prestressing reinforcement

According to Nawy [27] effective prestressing can be achieved using high-strength steels of 1862 MPa or higher. These strong steels are adequate in neutralizing losses due to creep and shrinkage in concrete. Furthermore, it has additional strength to sustain a required prestressing force. Prestressing reinforcement are either single wires, single strands consisting of several wires, multi-strand tendons or high-strength bars. For the first three, stress-relieved or low relaxation wires are typically used. It should be noted that wires or strands that are not stress-relieved exhibit higher relaxation losses.

2.8.7.2 Prestressing systems

Nawy [27] states that various systems are used to prestress wires or strands. Pretensioning or post-tensioning is applied against anchorages using hydraulic jacks.

For pretensioning, the prestressing steel is tensioned before casting of the concrete section. This is usually performed at precasting plants using stressing beds anchored to bulkheads or walls. Strands or wires are stretched and the concrete is cast. Bonding between both takes place as the concrete reaches its required strength.

For post-tensioning, stressing is performed after casting and hardening of concrete. Tendons are placed in longitudinal ducts. Forces are transferred through end anchorages. Furthermore, reinforcement should not be grouted or bonded prior to the stressing operation. For bonding the ducts are injected with cement grouting.

Hydraulic jacks transfer initial prestressing forces to the steel tendons. Capacity ranges from 10 t to 20 t with strokes of 152 mm to 1219 mm depending on which of the above methods are used. According to the SABS code [29] jacking forces for prestressing generally should not exceed 75 % of the characteristic strength of the tendon (f_{pu}).

2.8.7.3 Loss of prestress

Initial prestressing forces progressively reduce over a time period of about five years. Therefore, the level of prestressing at each loading stage should be determined. These include transfer to concrete, service load stages, and ultimate load. Force reduction is classified according to two groups [27]:

- immediate elastic loss during manufacture and construction due to elastic shortening of concrete, anchorage and friction, and
- time dependant losses due to creep, shrinkage, temperature and steel relaxation.

Losses for the latter can be determined at SLS, but the exact calculation of both groups is not feasible due to various interrelated factors. Empirical lump-sum methods are generally used [27].

2.8.7.4 Serviceability section analysis

According to the SABS code [29] a SLS section analysis should be performed to ensure prevention or restriction of local damage due to concrete cracking or crushing during operation. Therefore hypothetical elastic limits on the magnitude of tensile and compressive stresses in the concrete are specified. The three classes below apply for flexural tensile stresses.

- Class 1: No tensile stresses.

- Class 2: Tensile stresses, but no visible cracking.
- Class 3: Tensile stresses, but surface width of cracks do not exceed 0.1 mm for elements exposed to aggressive environments. For all other elements, the width should not exceed 0.2 mm.

For the study by LaNier [24], wind turbines are assumed to be class 1 structures for tensile stresses in flexure. Therefore, tension should equal zero in the section under SLS loading. Furthermore, compression stress (f_{cu}) should be less than the limits below.

- 0.33 f_{cu}: Design load in bending for continuous beams and other statically indeterminate structures.
- 0.4 f_{cu}: Increased bending capacity in the range of support moments.
- 0.25 f_{cu}: Design load in direct compression.

The IEC code [35] does not specify partial safety factors for SLS design and requirements from the SANS 10160-1 code [46] were considered. The factors for unfavourable and favourable permanent actions are 1.1 and 1.0 respectively. For wind loading the factor equals 0.6, and all other variable action factors are 1.0.

2.8.7.5 Ultimate section analysis

The SABS code [29] provides a method for analysing the ultimate strength of a concrete section. It is based on the general theory for ultimate flexural behaviour of concrete beams [47]. Mechanical behaviour for a circular cross-section of a tubular tower, as shown in Figure 2.12, is similar to its equivalent for a rectangular section and the same theory applies for it [24]. The following assumptions are made to simplify loading calculations:

- for strain distribution in concrete and steel reinforcement plane sections remain plane,
- concrete stresses are either derived from a stress-strain curve using an appropriate material factor or taken as 0.45 f_{cu} (γ_m included) over the compression zone,
- strain at the outermost compression fibre is 0.0035,

- tensile strength of concrete is ignored, and
- stresses in bonded tendons are derived from appropriate stress/strain curves.

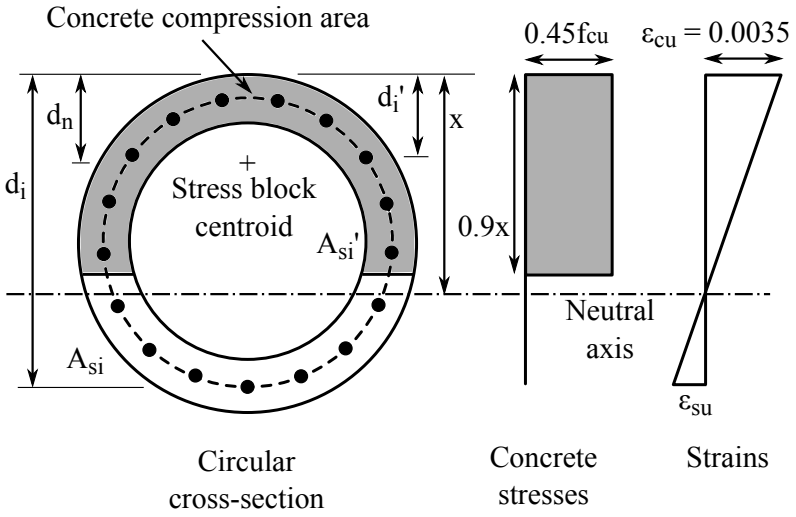

FIGURE 2.12: Stress block for a tubular tower section [29][47].

The symbols d and d' represent the effective depths to the centroids of the tension (A_s) and compression (A'_s) steel reinforcement areas. For a prestressed beam A_s is represented by the tendons in the tension zone. This zone is the white area under the neutral axis. Furthermore, the grey area is the compression zone. The division between the two is determined by the neutral axis depth, x. At this depth the stress and strain curves over the section cross zero. From x the depth to the centroid of the compression zone (d_n) can be determined. For the above procedure x is usually varied iteratively until force equilibrium in the section is reached.

According to Kong and Evans [47] one of three cases should be true when force equilibrium is met: under-reinforcement, over-reinforcement or a balanced section. For the first the steel yields before concrete crushes. The beam still resists the increasing applied moment due to steel ductility. Failure is characterized by large steel strains, causing extensive concrete cracking and substantial deflection. This is the preferred design due to economy and sufficient warning at failure. The second case is the reverse of the first. Concrete ultimate strain and crushing is reached before the steel yields. Failure is accompanied by small deflection and little tension cracking. It is often explosive and occurs with little warning. For the third configuration concrete crushing and steel yielding occurs simultaneously.

The ultimate resistance moment, M_r, for the rectangular beam section is calculated using equation 2.34. For ultimate limit state design M_r should have a higher value than the applied moment.

$$M_r = f_{st} A_s (d - d_n) \tag{2.34}$$

Where:

f_{st} = design tensile stress in tension reinforcement at failure

2.8.8 Modelling of a tubular tower

According to Veritas [8] a computer-based FEM analysis can be performed to determine the strength and stiffness of a wind turbine tower. This procedure should be used if simple calculations are insufficient or cannot be performed. For such an analysis a geometric representation of the tower is created in a two to three dimensional space. Suitable material properties, elements types, boundary conditions and loads are defined for it and a FEM analysis is performed to verify the strength and stiffness.

2.8.8.1 Static analysis

A static analysis is typically used to determine the DLC that controls for stress, strain and deflection response under extreme loading. The general analysis procedure is either linear or nonlinear. For the former unit loads are applied. Response of a single load is determined and DLC's can be examined by using linear combinations (superposition) [8]. However, for the latter nonlinear effects of large displacements and deformations, materials and boundary conditions are accounted for. Global or local buckling may control for a slender wind turbine tower. These are unstable forms of structural failure and examination thereof is also performed using nonlinear static procedures [48].

The most fundamental procedure for verifying global stability of shell structures is path-tracing based on the arc-length method. In Abaqus this is the modified Riks method, which is a special form of the general nonlinear procedure. It predicts unstable geometrically nonlinear collapse of a structure due to unsymmetrical loading and large displacements and deformations. The magnitude of loads do not follow a prescribed

history and stay proportional. Therefore all loading can be scaled with a single parameter. Scaling is done according to increments or load steps along an arc length until convergence or equilibrium is reached. The scaling parameter is defined as the load proportionality factor (LPF). Its full value is typically set as unity. Furthermore, the arc length measures the progress of the solution enabling the analysis to produce results regardless of whether the response is stable or not [48][43].

Local instability cannot be examined using global control methods (such as Riks), because severe nonlinearity can cause instability in the static analysis. Therefore it is inappropriate and the general nonlinear procedure is modified to ensure stability. Damping is used in such a way that viscous forces are sufficiently large to prevent immediate buckling or collapse, but small enough not to influence structural behaviour significantly [48]. A study by Kobayashi and Mihara [43] used the above damping method to model local buckling methods for thin-walled cylindrical shells. The results that are relevant for this study produced the diamond patterns shown in Figure 2.9.

2.8.8.2 Material model and element type

According to Veritas [8] various different material properties can be used for different parts of a specific model. These are included using material models that predict material behaviour. This is crucial to accurately model the response of a structure. Single values or plots can be imported into these models depending on the accuracy required. SI-units (kg-m-N-s) are recommended as a consistent set of units for defining material and model properties. Shell elements are the most suitable for modelling of tubular towers. These are used for parts consisting of plates or constant thickness sub-parts. Wall thickness of structures do not have to be very thin to be represented well. Furthermore, each element node contains 5 to 6 degrees of freedom (DOF's). Therefore good results can be obtained with a small amount of elements.

2.8.8.3 Boundary conditions

For boundary conditions to be realistic, it might be necessary to include element models of other parts. This comes into play where the component of focus has stiffness properties that cannot be well-defined unless they are modelled through other elements

included in the model. This is very relevant for wind turbine towers. Tower stiffness is very dependent on foundation design and results for a frequency analysis cannot be accurately modelled without accounting for foundation effects. Veritas [8] states that 1 T is significantly dependant on the efficiency of the fixing of the tower to the foundation and its stiffness. If the assumption is made that a tower is completely fixed at its bottom, the error in the natural frequency can be up to 20 %.

2.8.8.4 Loads

Structural loads for FEM analysis consists of moments, nodal forces and surface pressures. Application for the first two is simple, but might result in unrealistic local results. This is because in practice loads do not act on single points. Therefore pressure loading is generally more realistic. Furthermore, structural loading is typically applied using various force components. Components may be applied simultaneously or separately as single load cases. The latter is more flexible and generally preferred.

2.9 Cost analysis of wind turbine towers

2.9.1 Overview of engineering economics

According to Blank and Tarquin [49] engineering economy is motivated by the work engineers do in performing analysis and synthesis to make informed choices. It consists of a collection of techniques that simplify economically based comparisons of alternatives.

2.9.1.1 The time value of money

The time value of money is the change in amount over a given time period. Interest represents the difference between the ending and original amount and is expressed as a percentage rate of the latter. The time in which interest is accrued is defined as the interest period, of which one year is most common. For consecutive periods simple and compound interest can be determined. The latter accounts for the time value of money on the interest as well as the principle amount (PA), as shown in equation 2.35. Accumulated interest for each period is determined based on PA plus the total amount

of interest accrued from previous periods. It should be noted that the money accrued over time is denoted as the future worth (FW). The reverse of the equation calculates the present worth (PW).

$$\text{Money accumulated over time} = PA(1+i)^n \tag{2.35}$$

Where:

i = interest rate

n = interest period

Cash flows are inflows and outflows of money. For costing calculations the former is represented by a positive sign and the latter with a negative. Single value amount estimates are generally used to determine these flows. Furthermore, cash flows take place at different times throughout an interest period and for simplification each is assumed to occur at the end. This is called the end-of-period convention.

2.9.1.2 Present worth analysis

A present worth analysis (PWA) is generally used to compare two or more mutually exclusive alternatives. Values for this method are referred to as discounted cash flows. Furthermore, the interest rate is sometimes denoted as the discount rate. For this method all future cash flows are converted into a present monetary value, making it easy to compare alternatives. However, for alternatives to be comparable both should be used in identical capacities for the same time period.

2.9.1.3 Estimating costs

Costs for a project are categorized as direct or indirect. The former is defined for humans, machines and materials. The latter contains costs for utilities, management and taxes. Direct costs can be further divided into first cost, and maintenance and operating costs. The traditional industry method for cost estimation is the bottom-up approach. Cost components and subdivisions are identified and estimated as input. Estimates are then summed to obtain the total direct cost as output. An alternative approach is the design-to-cost (top-down) method, which is fundamentally the opposite.

Techniques for estimation can either be empirical or mathematical. In a professional setting software packages are mostly used. These are linked to updated databases of relevant cost indices.

2.9.2 Life-cycle costing of a wind turbine

According to Blank and Tarquin [49] life-cycle cost (LCC) is an extension of the PWA. This approach is commonly applied to alternatives with cost estimates over its entire life span. It provides insight into the profile of costs and its economic consequences. This method is most effective for projects with a large percentage of operation and maintenance costs relative to initial investment. Most of the total lifetime costs spent on wind turbines are initial or capital costs of up to 80 % [10]. Lifetime costs of a wind turbine are incurred for several phases [50][1]:

- manufacture,
- transport,
- construction and installation,
- operation and maintenance,
- decommissioning and dismantling, and
- disposal and recycling.

2.9.3 Cost breakdown of a wind turbine

Due to the high initial expenditure for wind turbines, research studies generally focus on the estimation of initial capital costs (ICC). Various studies have been preformed regarding the effects of component costs on this total. The tower cost is a very significant factor in this regard and contributes a significant portion to the total cost.

Fingersh et al. [51] created a model using scaling relationships to project the cost of wind turbine components and subsystems. Cost data is based on a mature design and a 50 MW wind farm. Estimations were based on a 1.5 MW baseline wind turbine with a 70 m rotor diameter and 65 m hub height. Table 2.8 shows the results. We see that the

tower cost amounted to 10.5 % of the ICC. Furthermore, with the addition of balance of station (BOS), it increased to 36.7 %. It should be noted that BOS is a conglomerate term for various cost items as shown in Figure 2.13.

TABLE 2.8: ICC percentages of a 1.5 MW baseline wind turbine [51].

Major cost components	Percentage cost of	
	TCC	ICC
Rotor	22.9	16.9
Drive train and nacelle	59.6	44.0
Control, safety system, condition monitoring	3.4	2.5
Tower	14.2	10.5
Wind turbine capital cost	100	73.8
Foundations		3.3
Transportation		3.6
Roads, civil works		5.6
Assembly and installation		2.7
Electrical interface/connections		8.7
Engineering and permits		2.3
BOS cost		26.2
ICC		100

Schmidt [52] used the NREL cost model [51] to estimate the ICC of 1.5 MW, 3 MW and 4.5 MW capacity wind turbines. The 3 MW machine was used as the baseline. Table 2.9 lists the percentage of ICC for main tower components. Here we see the influence of tower cost decline with increase in turbine capacity. The combined contribution of tower and BOS costs are 44.5 %, 38.2 % and 42.1 % for the 1.5 MW, 3 MW and 4.5 MW turbines respectively.

TABLE 2.9: Component percentages of ICC for 1.5 MW, 3 MW and 4.5 MW wind turbines [52].

Main components	1.5 MW	3 MW	4.5 MW
Rotor and hub assembly	14.4	21.5	21.4
Nacelle, drive train and generator	41.1	40.3	36.5
Tower	19.2	12.9	11.1
BOS	25.3	25.3	31.0

Tegen et al. [53] calculated the installed capital cost of a reference wind turbine with: 1.5 MW capacity, 82.5 m rotor diameter and 80 m hub height. Estimations were based on a combination of market and modelled data. Market data consisted of a large sample from 46 000 MW worth of installed and operating capacity for 2011 to provide empirical

data on plant costs and performance. The scaling model by Fingersh et al. [51] was used to provide modelled data for capital cost. Results are shown in Figure 2.13. Tower cost contributed to 16 % of installed capital cost. With the addition of BOS costs its share was 39 %.

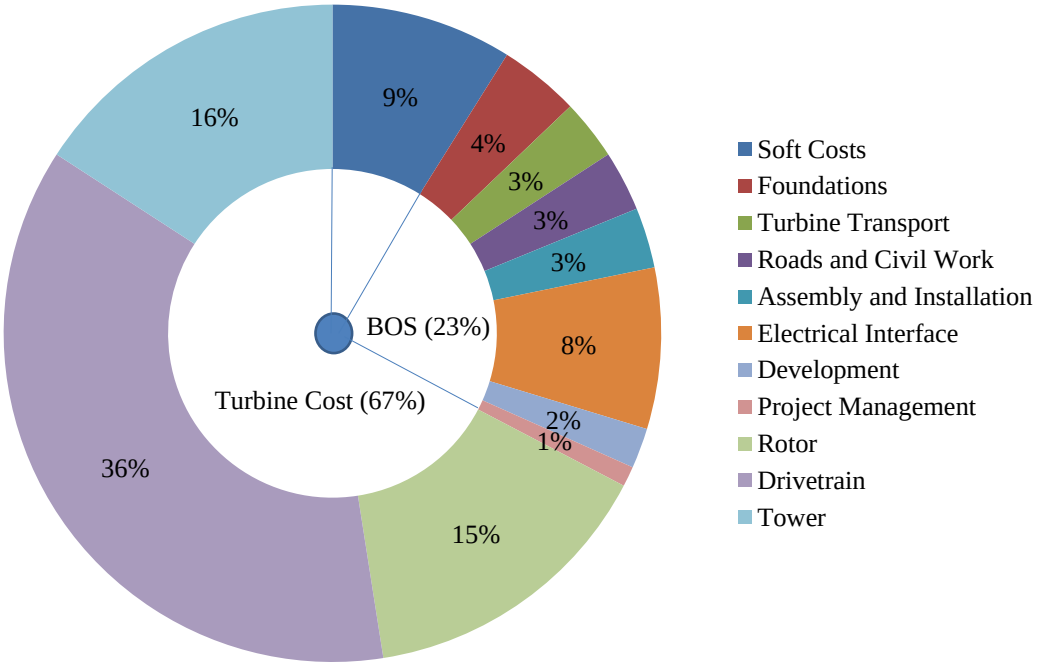

FIGURE 2.13: Installed capital costs for a 1.5 MW reference wind turbine with 82.5 m rotor diameter and 80 m hub height [53].

2.9.4 Cost estimation of a wind turbine tower

A study by Engstrom et al. [30] proposed and investigated candidate types of tall towers for on-shore wind turbines in forests. The scope included machines from 3 MW to 5 MW with hub heights ranging from 80 m to 175 m. In order to be comparable, tower solutions were designed for the same conditions. The following designs were compared:

- conventional steel shell tower with flanges, and longitudinal and transverse welds,
- steel tower with bolted friction joints,
- prestressed concrete tower (for slipformed and precast construction),
- hybrid tower with a concrete bottom section and conventional steel top,

- steel lattice tower, and
- wooden tower.

The NREL 5 MW baseline wind turbine was chosen as the reference machine and scaled down for the 3 MW capacity. Design work was performed according to the IEC standard [35]. One set of loads was calculated for each hub height and applied to each tower design. The main results of the study were presented as specific investment costs. This was calculated by dividing the total investment cost for the wind turbine by the yearly production. Balance of station and maintenance costs were not considered. The results for the 3 MW machine is shown in Figure 2.14. Here we see all the tower designs are competitive up to 100 m in height, with the hybrid being most feasible and the concrete the most expensive. For an increase in height the lattice and wooden towers were the most affordable by a large margin.

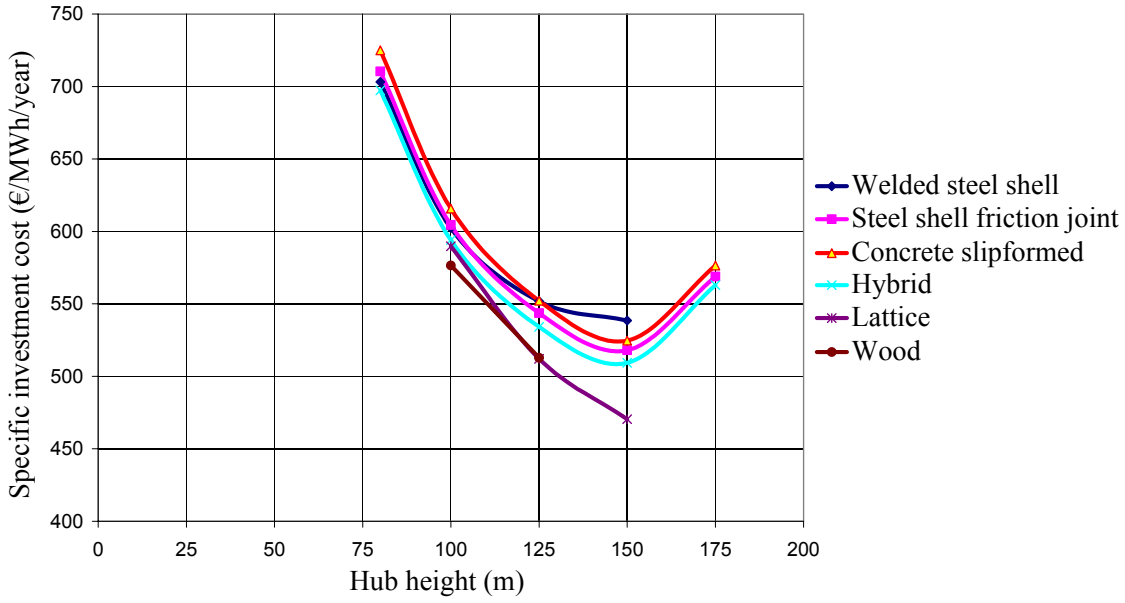

FIGURE 2.14: Specific investment costs for a 3 MW reference wind turbine with differing tower types [30].

LaNier [24] investigated the feasibility of wind turbine towers for a 100 m hub height situated on low wind speed sites. The following designs were compared for 1.5 MW, 3.6 MW and 5 MW capacities.

- a welded tubular steel tower,
- a prestressed concrete tower (for jump forming and precast construction), and

- a self-erecting hybrid tower with a concrete bottom and conventional steel top.

Construction approaches were developed for a baseline 50 tower wind farm in order to determine detailed and comprehensive conceptual cost estimates for all the tower types. Costs were developed for all the significant elements involved with constructing a wind turbine installation:

- factory fabrication,
- transport to site,
- site development for roadways and contractor support offices,
- foundation construction,
- assembly of tower elements on site,
- labour and equipment to support erection and integration of tower elements,
- cranes for lifting of tower segments, nacelle and rotor assembly, and
- mark-up for general contractor field overhead, administrative overhead and profit.

All these elements were included to form a more complete assessment of how important various elements of tower design and construction are for the overall cost of a wind farm. It should be noted that procurement of the rotor assembly, nacelle and electrical work for grid connection was excluded.

Preliminary tower designs were developed according to similar design criteria for estimates to be consistent for comparison. For each tower the required construction procedure was determined first. Next, the involved operations, tasks and equipment requirements were defined. Levels of effort for labour and equipment were then estimated for these requirements. Construction for all the tower concepts were assumed to take place over a 28 month period.

The hybrid tower was used as the baseline for all the cost estimates. Its construction specifications at 1.5 MW capacity was developed in some detail to identify all required operations. The precast tower was estimated according to the same procedures developed for the concrete section of the hybrid. However, erection was assumed to be performed

entirely by mobile crane. An industrial chimney contractor estimated basic costs for the cast-in-place tower. Erection and post-tensioning approximations were also included. The steel tower was estimated based on shop fabrication of formed plate steel shells and delivery to site for assembly and erection. Larger towers were assumed to be transported to site in quartered sections. Erection and crane times, and cost requirements were derived from a study by Smith [54]. Figure 2.15 shows the resulting cost estimates for the tower designs. Both concrete concepts were more viable, with the cast-in-place the most affordable by a large margin. The hybrid solution was the most expensive.

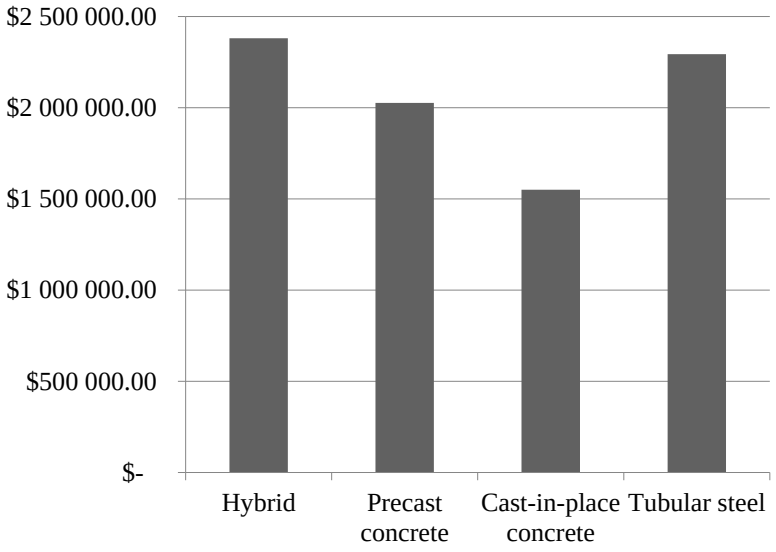

FIGURE 2.15: Installed costs of various tower designs for a 3.6 MW reference wind turbine [24].

2.9.5 Sensitivity analysis

According to Blank and Tarquin [49] every economic study depends on good cost estimation. The uncertainty of variation introduces a degree of risk into a project. Therefore, sensitivity analysis is a vital tool to use. It determines the impact of uncertainty on a cost estimate by varying influential parameters.

Normally independence is assumed and a particular parameter at a time is varied over a range of values. All other parameters are held at their most likely estimate. It is a good approach when one parameter contributes most of the sensitivity. However, it has a detrimental effect where several parameters contribute. Several parameters are usually varied by defining three estimates per parameter: pessimistic, most likely and optimistic. The pessimistic estimate produces the least favourable value and the optimistic estimate

the most favourable. Both approaches can either be performed for a single project or several alternatives.

To perform a sensitivity analysis, firstly the significant variable parameter estimates are identified. Next, the probable range and increment of variation for each is determined. This range can either be numerical or percentage based. Results for each parameter estimate is calculated using a costing method. Lastly, these results are plotted graphically against the parameter range. It should be noted that significant variables can be identified by increasing each parameter individually by a constant percentage while keeping the others fixed. The costs for all parameters for each case is then calculated and the effect of each compared [55].

2.10 Conclusion

This chapter presented and interpreted the basis of literature according to which the study was performed. Wind energy has the potential to be a strong contributor to a more sustainable future. Locally the potential exists and the public sector is being used to utilize it. A typical modern wind turbine has a horizontal axis orientation, three rotor blades, active blade pitch and face into the wind using yaw control. It has a steel monopole tower between 60 m and 80 m high with a reinforced concrete foundation. However, this design presents various problems for structural integrity, manufacturing and viability at heights above 80 m. These constraints have led to a movement towards steel-concrete hybrid and full concrete tower solutions. Such designs present an alternative and possibly more optimal solution for heights over 100 m. For ultimate loading of a wind turbine various design situations and cases should be investigated. However, it is customary to base extreme loading on a static machine. These loads are calculated using aero-elastic or simplified methods and structural verification is performed using an ULS analysis. Financial studies for wind turbines tend to focus on bottom-up initial capital costs (ICC) estimation, because these can be up to 80 % of the project total. The uncertainty of cost variation introduces risk and a sensitivity analysis is thus performed to measure the impact thereof.

Chapter 3

Methodology for Comparative Study

3.1 Introduction

This chapter shows the steps followed to determine whether the concrete tower solution is a viable or more competitive alternative to its steel counterpart for South African conditions. A realistic reference wind turbine shall be presented and a local site assigned to it. Realistic and comparable steel and concrete designs shall be shown and discussed. Methods for comparative loading and testing thereof shall be introduced. The procedures for optimization of structural dimensions and calculation of material mass and volumes shall be investigated. A cost analysis shall be presented for comparison of the local viability of the towers. This analysis shall incorporate the calculated material volumes and masses. The chapter applies the following framework:

- Reference wind turbine and site,
- Support structure designs,
- Considerations for wind conditions,
- Wind turbine tower loading,
- Structural analysis and modelling, and
- Life-cycle cost analysis.

3.2 Reference wind turbine and site

3.2.1 Finding a suitable reference wind turbine

In order to perform the comparative structural and costing analysis of the tower designs, certain technical properties had to be defined beforehand for the wind turbine it would support. For this purpose a reference wind turbine was defined. It was important that the properties of the machine be realistic to ensure accurate calculation and design. Such a machine was assumed to have design parameters that are representative of current industry trends. An empirical study was performed in order to determine these trends for modern wind turbines. A database of available commercial machines was compiled using information from Windpower [56] and technical data was acquired from available brochures and web sites. The rated power, hub height, and rotor diameter [57] were considered to be the three most important design parameters. Various graphs were plotted according to these using the data mentioned above. Parameter ranges for a suitable reference wind turbine design were chosen based on these results.

3.2.1.1 Number of wind turbines per power rating

The number of wind turbines per rated power is shown in Figure 3.1. The total amount of commercial models are 942 ranging from 200 kW to 10 000 kW. We can see four outliers with capacity values and quantity density (in brackets) as follows:

- 1.5 MW (136),
- 2.0 MW (147),
- 2.5 MW (99) and
- 3.0 MW (123).

The number of turbines between 1.5 MW and 3 MW amount to 67 % of the total number. This correlates strongly with literature [10][9]. It is clear that the market currently favours turbines within this capacity range. Therefore it was assumed that a realistic wind turbine should have one of the four above mentioned capacity values.

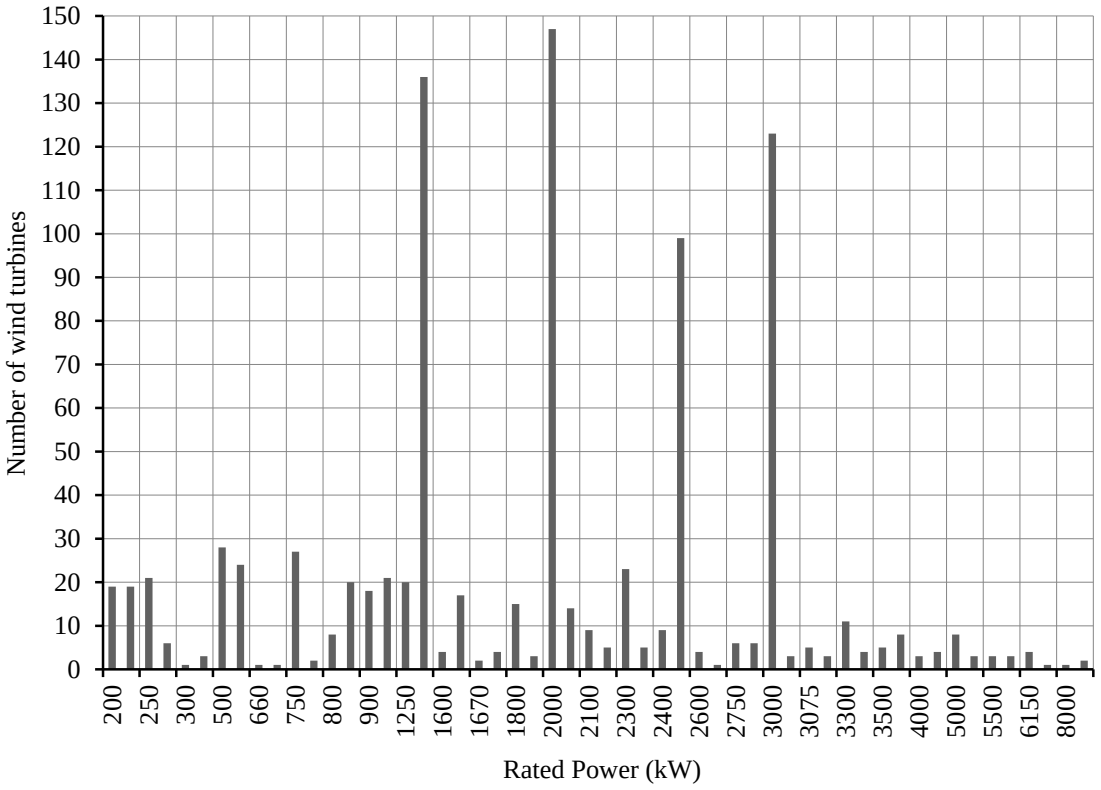

FIGURE 3.1: Distribution of rated power for commercial wind turbines.

3.2.1.2 Rated power versus hub height

Hub heights were plotted according to the favoured capacity range as shown in Figure 3.2. A linear regression line illustrates the overall trend the data follows. Here we see a rise in hub height with the increase in rated power. However, the data is scattered. To account for this a suitable hub height range was established for each of the four capacities. Due to the skewness of the data these intervals were determined using the interquartile range. This measure of spread is less affected by skewness and outliers [58]. Furthermore, the range was defined by the lower and upper quartiles: Q_1 and Q_3. It should be noted that skewness was measured using the 90 % confidence ranges of the adjusted Fisher-Pearson standardized moment coefficient (G_1) [59]. These are shown in Table 2 in Appendix B. The resulting hub height ranges for each of the four capacity values are listed in Table 3.1.

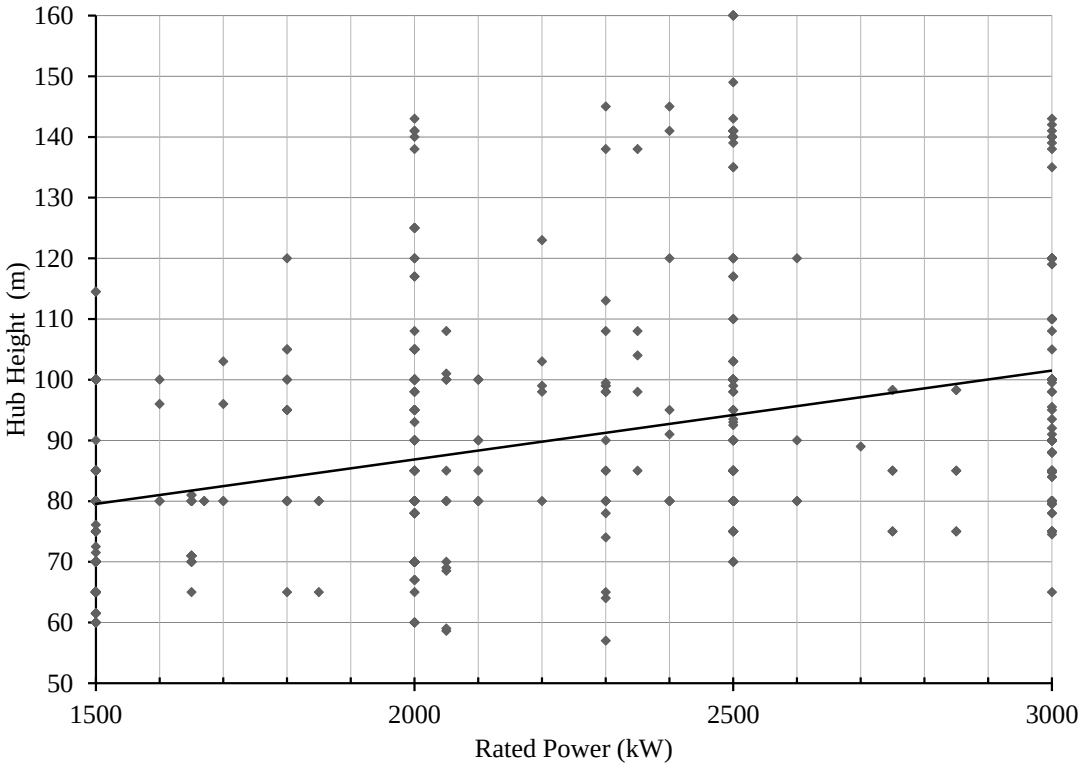

FIGURE 3.2: Distribution of hub heights for capacity range of 1.5 MW to 3 MW.

TABLE 3.1: Statistical properties and hub height ranges for significant capacities.

Rated power (kW)	Sample size	Sample G_1	90 % limit	Q_1 (m)	Q_3 (m)	Hub height range (m)
1500	130	0.937	0.350	69	80	69 - 80
2000	144	1.164	0.330	80	100	80 - 100
2500	99	1.068	0.393	80	110	80 - 110
3000	119	0.964	0.365	84	108	84 - 108

3.2.1.3 Rated power versus rotor diameter

Figure 3.3 shows the rotor diameter for each wind turbine model in the capacity range. Suitable diameter ranges were determined according to the same procedure as above and results are listed in Table 3.2. Values in the last three columns correlate with those for hub heights. According to Veritas [8] this should be expected.

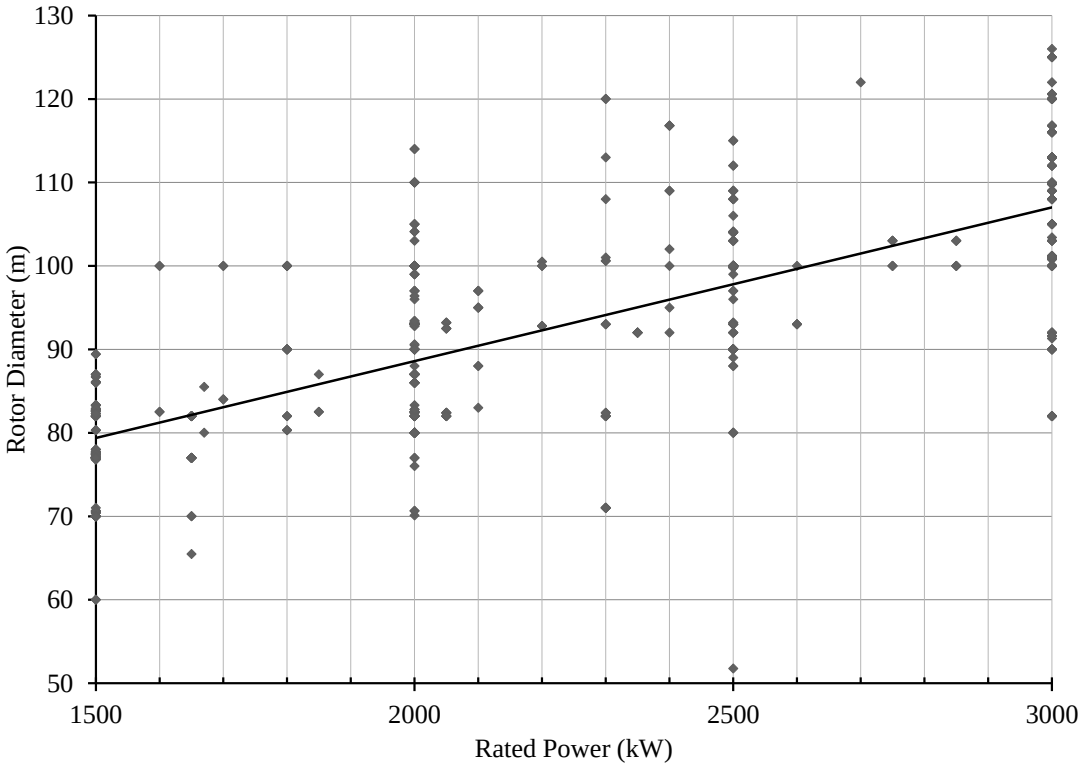

FIGURE 3.3: Distribution of rotor diameters for capacity ranges of 1.5 MW to 3 MW.

TABLE 3.2: Statistical properties and rotor diameter ranges for significant capacities.

Rated power (kW)	Sample size	Sample G_1	90 % limit	Q_1 (m)	Q_3 (m)	Rotor diameter range (m)
1500	136	-0.455	-0.341	77	82.3	77 - 83
2000	147	0.369	0.326	82.5	93.4	82 - 94
2500	99	-1.487	-0.393	90	100	90 - 100
3000	116	-0.395	-0.369	100	116	100 - 116

3.2.2 Suitable site and location

Site location is significant for wind turbine design, because it determines wind conditions, construction considerations and transport distances. Sites for various existing and potential wind projects were considered. The choice depended on whether the specified turbine sizes fell within the limits of the reference wind turbine. Table 3 in Appendix B lists the size parameters as well as the location of each project. From the information at hand, Klipheuwel-Dassiesfontein was chosen as the most suitable for this study. Design parameters fall within limits of the reference turbine. It should be noted that a 100 m hub height was favoured. Site coordinates are 34°13′46″S and 19°22′39″E. Altitude

was estimated as 320 masl. Furthermore, the terrain is rural and assumed to contain a mixture of low and high grass.

3.2.3 Properties of the reference wind turbine

According to Decq and Espejo [60] Sinovel SL3000/113 [61] wind turbines are used at Klipheuwel-Dassiesfontein. The design parameters of these machines fall within the reference wind turbine limits and its technical information was used for this study. However, additional data was needed for blade length, chord and mass of the rotor and nacelle. These were acquired from a brochure for the Siemens SWT 3 MW turbine [62], which has similar design parameters. Furthermore, the blade material was assumed to be glass reinforced plastic (GRP). Significant technical information is listed in Table 3.3.

TABLE 3.3: Technical information for the reference wind turbine [61][62].

Technical parameter	Symbol	Value	Unit
Rated power	P	3	MW
Rotor diameter	D	113	m
Hub height	z_{hub}	100	m
Blade no.	n_b	3	
Cut-out wind speed	v_{out}	25	$\mathrm{m\,s^{-1}}$
Survival wind speed	v_{e50}	52.5	$\mathrm{m\,s^{-1}}$
Control system	Blade independent pitch Active yaw		
Turbine class	IEC IIIA		
Maximum blade chord	$c(r)_{max}$	4.2	m
Blade length	Lb	55	m
Rotor mass	m_R	67 000	kg
Nacelle mass	m_N	78 000	kg

3.3 Support structure designs

3.3.1 Steel monopole

3.3.1.1 Geometric dimensions

A study by ArcelorMittal [63] provides information of the geometric dimensions of a tubular steel tower. The performance and cost of this tower was compared with other

designs (steel lattice, concrete, steel-concrete hybrid) for various hub heights. The dimensions of the 100 m steel tower was used for this study. For dynamic purposes this tower is a soft design. Furthermore, it is divided into six main sections each with flanges at its ends. However, for this study the flanged design was discarded and main sections were assumed to be welded together. This assumption was made to simplify modelling of the tower. Each main section consists of a varying number of ring segments welded together. The tower dimensions are presented in Table 6 in Appendix C.

3.3.1.2 Material properties

South African S355JR structural steel was assumed suitable for design of all structural members. This grade is considered industry standard for wind turbine towers [24]. Characteristic material properties listed in Table 3.4 were acquired from the Red Book [64]. This book provides significant information regarding steel material properties and design for South Africa.

TABLE 3.4: Material properties of structural steel.

Material Property	Value	Unit
Density	7850	$\mathrm{kg\,m^{-3}}$
Modulus of elasticity (Young's modulus)	200	GPa
Poisson's ratio	0.3	
Ultimate tensile strength	470	MPa
Yield stress (3 mm $<$ thickness $\leq$ 16 mm)	355	MPa
Yield stress (16 mm $<$ thickness $\leq$ 40 mm)	345	MPa
Yield stress (40 mm $<$ thickness $\leq$ 63 mm)	335	MPa

To model plastic behaviour of S355JR steel a tensile stress-strain curve of an American equivalent steel was used [65]. The stress values were converted from ksi to MPa. The curves were determined according to the thicknesses in Table 3.4 and are shown in Figure 1 in Appendix E.

3.3.2 Prestressed concrete monopole

3.3.2.1 Geometric dimensions

A suitable prestressed concrete design was obtained using information from a study by LaNier [24]. Three designs were compared for rated powers of 1.5 MW, 3.6 MW

and 5 MW respectively at a hub height of 100 m. Information was given regarding the geometric properties of these towers and dynamic behaviour. The former is shown in Table 4 in Appendix C. Regarding the latter, all were soft designs. Furthermore, linear interpolation was applied to scale these dimensions to a rated power of 3 MW for the reference wind turbine. It was then simplified for modelling by dividing it into 20 sections over its height. For each section and average uniform wall thickness was approximated according to top and bottom thickness. Resulting geometric properties are listed in Figure 5 in in Appendix C.

3.3.2.2 Nominal reinforcement

Nominal reinforcement specifications for handling was acquired from the LaNier [24] study. It was combined with minimum requirements from the SABS concrete code [29] for use in the study. The following schedule was chosen: Four 12 mm mild steel bars over the cross-section at a spacing of 305 mm centre to centre for both horizontal and vertical reinforcement. This is shown in Figure 3.4. Cover was chosen as 40 mm for outdoor conditions in the Cape winter rainfall region [66].

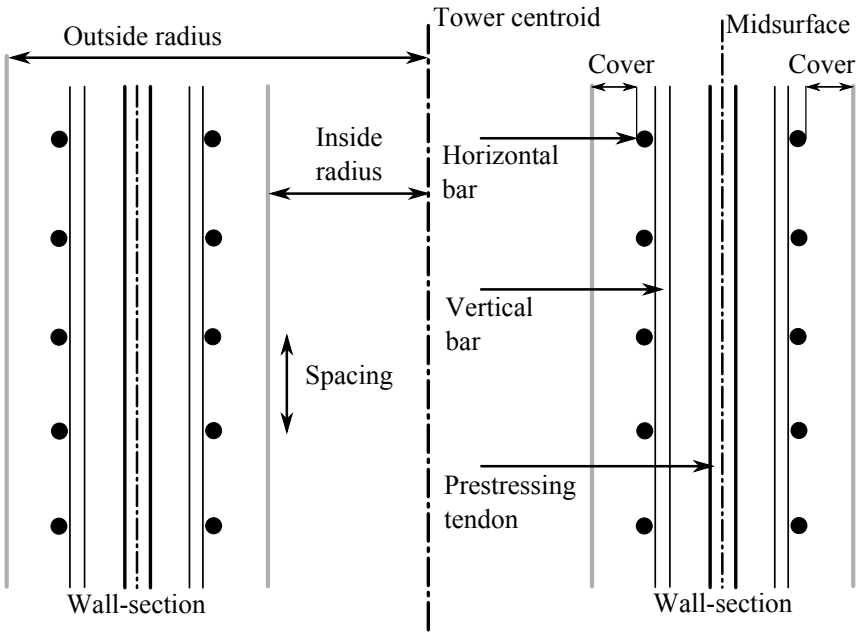

FIGURE 3.4: Placement of nominal and prestressing reinforcement in the tower wall (N.T.S).

3.3.2.3 Prestressing reinforcement

Seven wire low relaxation steel multi-strand tendons were used as prestressing reinforcement. Nominal strand diameter was chosen as 15.2 mm and properties were acquired for a bonded 12 strand post tensioning system [67]. The tendons were assumed to be housed in corrugated polyethylene ducts with 94 mm diameter and 2 mm wall thickness. Furthermore, ducts were assumed to be injected with cement grout for bonding. A type M1 anchorage was assumed to be appropriate for this study and is shown in Figure 3.5. The distance, H, represents the recess needed in order to practically fit a jack onto the anchor. It is dependent on the amount of strands per tendon and was taken as 400 mm. This value was conservatively assumed to be the minimum tendon spacing and complied with the SABS code requirements [29]. To meet specifications for cover, tendons were placed along the middle radius of the wall section as shown in Figure 3.4.

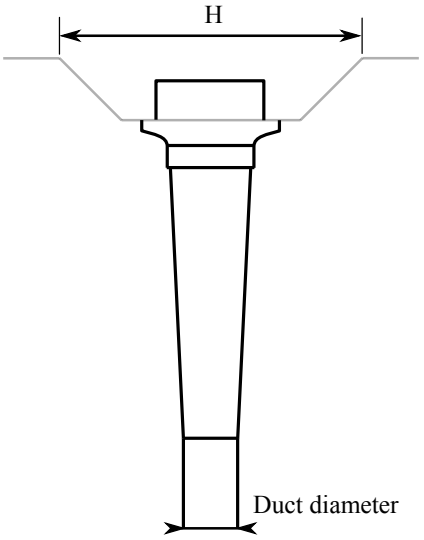

FIGURE 3.5: Prestressing tendon anchorage detail.

3.3.2.4 Material properties

Significant material properties for the prestressed concrete design were acquired from various sources and are listed in Table 3.5. It should be noted that the prestress after losses was acquired from the LaNier [24] study and was assumed to be a factored value. Nawy [27] provides a stress-strain curve for grade 1860 MPa prestressing strands, which was used in this study. Tension stiffening properties of 60 MPa reinforced concrete were determined according to the Abaqus tension stiffening model [48]. The maximum

flexural tensile strength value of the concrete was taken from Bamforth et al. [68]. Furthermore, maximum strain was assumed to be the strain at yielding of the prestressing reinforcement and calculated using the properties in Table 3.5. The compression stress-strain curve was determined using equations 3.1 and 3.2 from Hognestad [69] and values from the SABS [29] code. These equations contributed to the form of the curve and the values from the latter was used as input. All the above mentioned curves are shown in Figure 1 in Appendix E.

TABLE 3.5: Material properties for the prestressed concrete tower design [29][64][68].

Material Property	Value	Unit
Nominally reinforced high strength concrete		
Density	2400	$\mathrm{kg\,m^{-3}}$
Poisson's ratio	0.2	
28 d characteristic cube strength	60	MPa
Mean flexural tensile strength	6.1	MPa
Modulus of elasticity (Young's modulus)	36	GPa
Ultimate compressive strain	0.0035	
Mild reinforcing steel		
Yield stress	250	MPa
7 Wire low relaxation steel strand		
Short term modulus of elasticity	195	MPa
Ultimate tensile strength	1860	MPa
Yield strength	1690	MPa
Factored prestress after losses	1100	MPa

$$f_{c1} = f_c" \left[2\frac{\epsilon}{\epsilon_0} - \left(\frac{\epsilon}{\epsilon_0} \right)^2 \right] \tag{3.1}$$

$$f_{c2} = f_c" \left[1 - 0.15 \left(\frac{\epsilon - \epsilon_0}{\epsilon_{cu} - \epsilon_0} \right) \right] \tag{3.2}$$

Where:

f_{c1} = concrete compression stress value up to $f_c"$.

$f_c"$ = ultimate compression strength ($0.67 f_{cu}$).

ϵ = strain.

ϵ_0 = strain at ultimate strength ($0.00024 \times \sqrt{f_{cu}}$).

f_{c2} = concrete compression stress value from $f_c"$ to ultimate failure.

3.4 Considerations for wind conditions

The ultimate limit state of the tower designs was tested according to extreme wind conditions. This was assumed in order to comply with section 3.5 below. For these conditions, typically the characteristic 50 year return period wind speeds are used. To model South African conditions the local wind code [37] was used in combination with the IEC code [35]. It was found that the extreme wind speed distribution of the latter was more conservative and therefore its steady extreme 50 year model (see subsection 2.5.2) was used for wind speed calculations. However, the fundamental basic wind speed ($v_{b,0}$) of the local code [37] was taken as V_{ref} at the site. We know that V_{ref} acts at hub height and $v_{b,0}$ at 10 m above ground. Therefore $v_{b,0}$ was normalized for the hub height using equation 3.3. It should be noted that this equation was derived from equation 2.5.

$$V_{ref} = V_{b,0}\left(\frac{z_{hub}}{10}\right)^{0.11} \tag{3.3}$$

3.5 Wind turbine tower loading

3.5.1 Critical design load case

Due to time limitations only one critical design load case (DLC) was considered for ultimate loading of the wind turbine. Upon considering subsections 2.7.3 and 2.7.4 a non-operational machine with normal machine state was assumed to be the most critical situation with DLC 6.1 from the IEC code [35] the worst case. For this case the wind turbine is stationary and under extreme wind conditions. Therefore the steady extreme 50 year wind speed model was used for active yaw with up to $\pm 15°$ misalignment.

For critical tower loading Case 2 in subsection 2.7.5 was assumed. Blades were assumed to be at full feather with the wind blowing into the front. One blade was assumed to face vertically upwards and the other two inclined at 30° to the horizontal (see Figure 3.8). It was assumed that this case induces the maximum lift forces for tower base bending and at full feather lift forces act at right angles to the direction of the wind loading. A further assumption was made that full feather reduces drag forces on the blades to the

extent where it becomes negligibly small. The following general assumptions were made to comply with the IEC [35] requirements for extreme tower loading:

1. For operation the blade tip speed is not high relative to the design gust speed.
2. Yaw drive is designed to stay operational in extreme winds.
3. Restraint against yaw slippage is provided.
4. When grid loss occurs, power backup is provided for the control- and yaw system to ensure yaw alignment for at least 6 hours.
5. The reference wind turbine is capable of applying full feather.
6. Feathering results in negligibly small drag loads on blades.
7. The 15° yaw error causes maximum angle of attack, inducing maximum lift forces.

It should be noted that because of the first assumption it is safe to say that operational load cases do not govern for extreme loading. Furthermore, assumptions two and three rules out the possibility of cases where a turbine is side or back-winded.

3.5.2 Critical tower loading

The loads applied to a wind turbine tower fundamentally consists of external loads and own weight. For this study significant loading types were assumed to be represented by six definitive loads. These are shown in Figure 3.6 and listed in Table 3.6. The axial force due to lift was also calculated, but found to be negligibly small. The letter T in the subscripts of the load symbols indicates that it is applied at the top of the tower. Furthermore, h indicates that the load is a function of tower height. These loads shall be discussed below.

3.5.3 Tower loading calculations

Due to unavailability of aero-elastic computer programs, tower load calculations for this study were performed using simplified methods, which shall be discussed below.

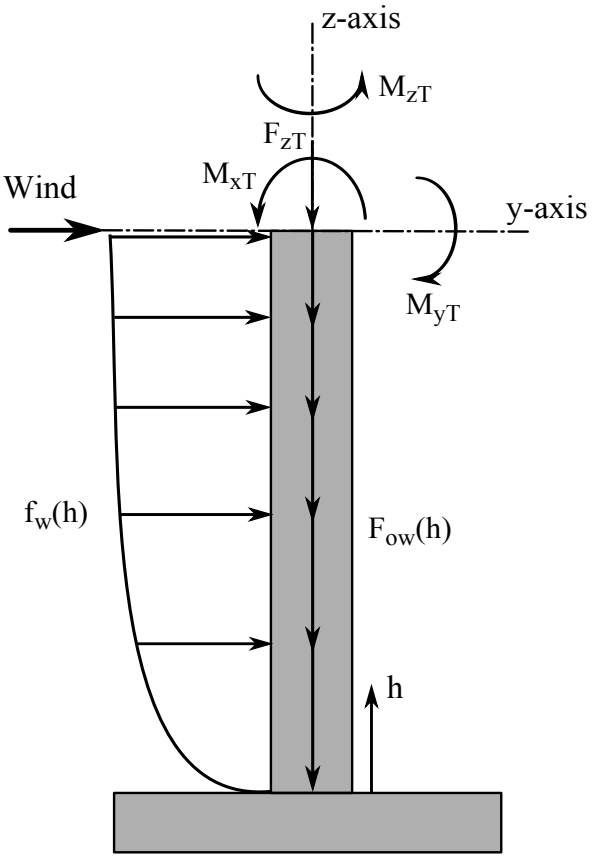

FIGURE 3.6: Assumed critical loads acting on the tower.

TABLE 3.6: Assumed critical loads acting on the tower.

Load description	Assumed cause	Load symbol
Tilt moment around y-axis	wind lift on rotor blades	M_{yT}
Torsion (Yaw) moment around z-axis	wind lift on rotor blades	M_{zT}
Tilt moment around x-axis	rotor mass eccentricity	M_{xT}
Vertical gravity load at tower top	nacelle weight	F_{zT}
Distributed pressure force over tower height	wind drag on tower	$f_w(h)$
Tower own weight	gravity	$F_{ow}(h)$

3.5.3.1 Loading using the Quasi-Static method

The Quasi-static method was used to calculate loads induced on the tower due to wind pressure exerted on the rotor blades. These loads include M_{yT} and M_{zT}. The chord length of the blade has a very significant influence on the magnitude of these loads. Therefore a realistic blade profile was needed. A study by Malhotra [70] provides a complete profile with chord progression over its entire span. However, the blade had to be scaled from 61.33 m to 55 m to be suitable for this study. This was done by decreasing

the station and chord according to (α), which is the ratio of the scaled length (latter) over the nominal length (former) [71]. The blade information is shown in Table 7 in Appendix D.

Table 3.7 lists assumed values for some of the critical parameters for calculations. The logarithmic increment of damping was taken as 0.05 for concrete and GRP, and 0.02 for welded steel [14]. Furthermore, the roughness length accounts for the effect of the terrain on the wind speed. This factor was taken from Buchold and Moossavi Nejad [72] for low and tall grass. Lift and drag coefficients were based on the Danish standard DS 472 (see subsection 2.7.9). The value for f_{bf} was obtained by scaling the resulting frequency obtained for the study by Malhotra [70]. However, according to Griffith and Ashwill [71] the frequency has an inverse scaling relationship and was increased by factor α from a nominal value of 0.695 Hz.

TABLE 3.7: Assumed values of critical parameters for the Quasi-static method.

Description	Symbol	Assumed value	Unit
Roughness length	z_0	0.04	m
Blade drag coefficient	C_d	1.3	
Blade lift coefficient	C_l	1.5	
Blade flapwise frequency	f_{bf}	0.775	Hz

The integral length scale of the Kaimal spectrum, L_u, was calculated using equation 3.4 and values for C and m were acquired from Figure 3.7 [8].

$$L_u = 100Cz^m \tag{3.4}$$

Lift forces were calculated using Microsoft Excel spreadsheets. Blade station is the distance from the hub to a certain point along the length of the blade. It was assumed to be the primary variable and all others were calculated according to it. The load per unit length between station points was calculated according to Equation 2.18. The gust factor, air density and wind speed was varied according to height above ground. Height was determined according to blade position, station in the rotor plane and altitude. Furthermore, the chord length was varied according to station and the lift coefficient kept constant.

For moment calculation, force magnitudes were assumed to progress linearly between station points. Concentrated (point) loads were then determined according to the force

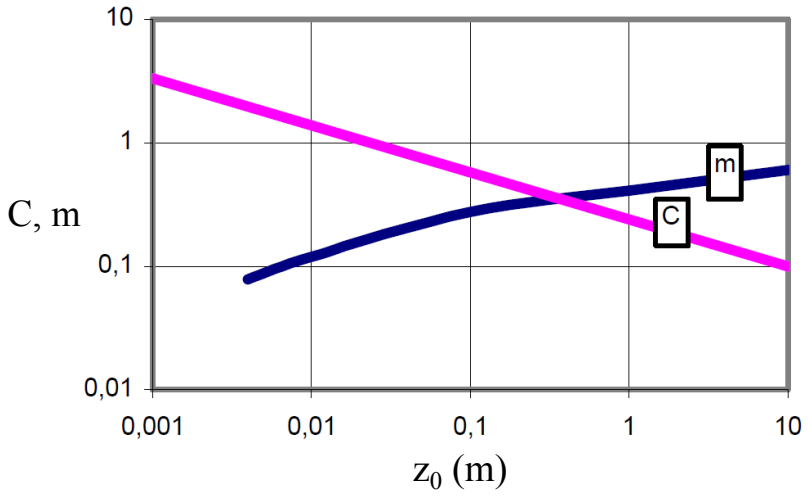

FIGURE 3.7: Values of C and m for integral length scale of Kaimal spectrum [8].

distribution over station length. The lever arm was calculated for and multiplied by each point load to determine section moments. Section moments were summed to obtain the total moment for each blade.

The same blade forces induce both M_{yT} and M_{zT}, as shown in Figure 3.8. However, the lever arms differ. For M_{yT} the lever arm for each blade is calculated as the length from the load to the hub in the direction parallel to that of the blade. The lever for M_{zT} is simply the distance, parallel with the y-axis, between the load application and tower centroid and is the same for all blade loads. It was calculated as the sum of the static clearance and tower radius at the tip of a blade facing vertically downwards. The former shall be discussed further on. Furthermore, the horizontal components of the point loads were used to calculate moments for the inclined blades. It should be noted that the effects of the vertical components neutralize each other concerning M_{xT}.

3.5.3.2 Loads due to nacelle and rotor mass

The mass of the rotor and nacelle induce gravity forces and moments that act on the tower. Loads for this study include M_{xT} and F_{zT}. These were calculated using the principle in equation 2.7. The area of the rotor hub and nacelle is small relative to the tower and rotor blades and wind pressure loading should be negligible.

It should be noted that there was no need to determine the gravity moment regarding M_{yT}, because the net effect of moments induced by the inclined blades are zero.

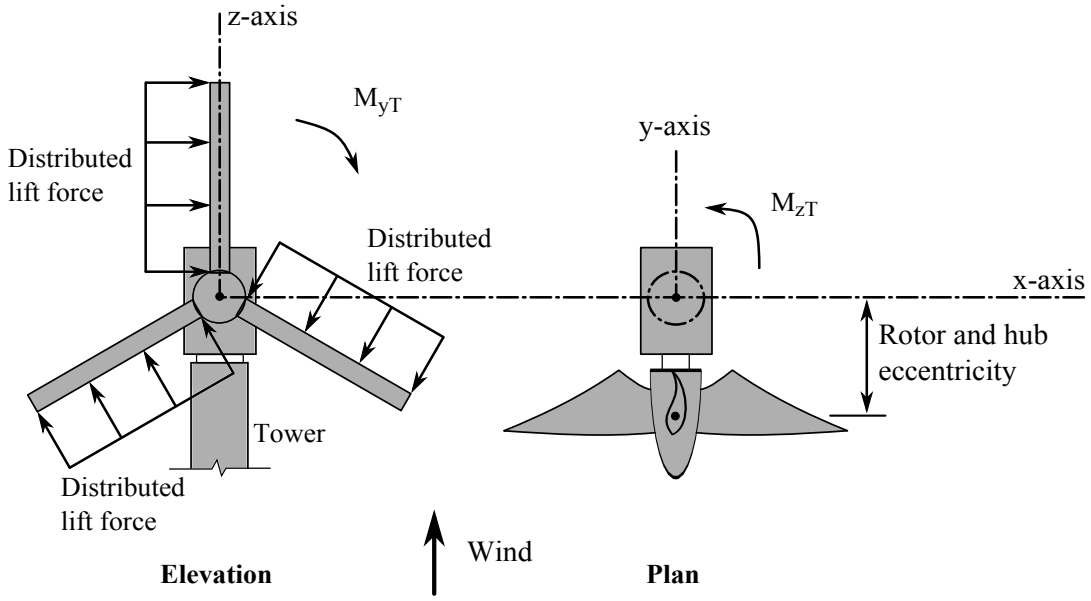

FIGURE 3.8: Lift forces on rotor blades inducing M_{yT} and M_{zT} (N.T.S).

Therefore, there was no need to determine the mass distribution over the blades as suggested in equation 2.7. Alternatively, the mass of the rotor-hub assembly was obtained and used to calculate M_{xT}. This moment is induced by rotor and nacelle eccentricity as shown in Figure 3.8. However, it was assumed that the nacelle eccentricity is designed to be zero. Therefore its mass produces no gravity moment. Furthermore, the eccentricity of the rotor-hub assembly was assumed to be the distance between its centroid and that of the tower. The nacelle mass was used to calculate F_{zT}.

3.5.3.3 Distributed load over tower height

The pressure value for $f_w(h)$ was calculated in Microsoft Excel using force coefficients from the local wind loading code [37]. The tower station was assumed to be the primary variable. It represents the section heights above ground over the tower span. Equation 2.24 was used to calculate the peak pressure loading on the tower. Both the wind speed and air density was varied as a function of height and altitude was taken into account. Furthermore, in addition to height the force coefficients were varied according to tower diameter. To determine the design wind force, equation 2.25 was applied and the structural factor was assumed to be unity. However, A_{ref} was also taken as unity in order for the load to be a pressure force. This was done, because the FEM software used for this study can model pressure fields as loads. These fields shall be discussed

further on in subsection 3.6.4. Effectively then, force coefficient values were multiplied with those for the peak pressure values at tower stations.

3.5.3.4 Tower own weight

The tower own weight was taken into account in the FEM models itself.

3.6 Structural analysis and modelling

FEM modelling has become an integral part of the structural analysis process. The IEC [35] ultimate limit state analysis was performed for each tower to test and prove its structural integrity. All modelling was done using Abaqus and the Finite Element Analysis Services (FEAS) [73] were consulted for guidance. Due to the slender nature of wind turbine towers, large displacements and deformations were expected. Therefore the nonlinear effects thereof were taken into account. This was done by performing non-linear static stress analysis [48]. Hand calculation methods were used for the remaining examinations.

3.6.1 Critical deflection analysis

For the critical deflection analysis mechanical blade-tower interference was assumed to be the only occurrence where deflection affects structural integrity (see subsection 2.8.5). For this study a static analysis was done before tower modelling or loading in order to determine the eccentricity of the rotor mass. The maximum tip deflection was assumed to be 10 % of its radius for extreme wind. This value was calculated for the 113 m rotor diameter of the reference wind turbine. It was assumed to be the maximum deflection after all partial safety factors were taken into account. The value was then used to determine the static clearance according to equation 2.33. Therefore the 10 % value was considered to be equal to γu_{max}. Furthermore, the requirement for the residual clearance between the tower and blade tip was taken as 0.0. From this the static clearance was calculated as 5.65 m. It was assumed to be a conservative value ruling out any interference between the blade and tower.

3.6.2 Fatigue failure analysis

Fatigue design was excluded, because it was considered to be outside the scope of this study.

3.6.3 Dynamic considerations

Based on subsection 2.5.2 the gust factor was assumed to account for the dynamic effects of resonance between wind turbulence and structural vibration [35]. For stiffness design (see subsection 2.8.6) an assumption was made that no significant excitation should occur when 3 P passes through 1 T. Furthermore, for vortex shedding it was assumed that during erection guy wiring would be installed and exciting wind velocities avoided.

3.6.4 General modelling methodology

3.6.4.1 Model architecture and element types

Both tower types have tubular monopole designs. These designs are thin-walled cylinders which are either partially or fully tapered. For each tower a single part was created in a 3 D modelling space. The part was shaped as a shell using the revolution feature in Abaqus. Dimensions were determined according to its geometric data in Appendix C. Next, a geometric outline was drawn in the sketch view and revolved around the centroid axis to form a cylindrical model as shown in Figure 3.9. The part was partitioned according to the tower sections, and material properties and wall thickness were then assigned to each. It should be noted that, where applicable, shell sections with similar thickness were joined to simplify the models. For analysis four node 3 D shell elements were used. The element size was either chosen as 0.25 m or 0.5 m depending on the significance of the analysis. Furthermore, it was assumed that connections will not control with regards to tower failure. Therefore connection design and modelling thereof was not considered.

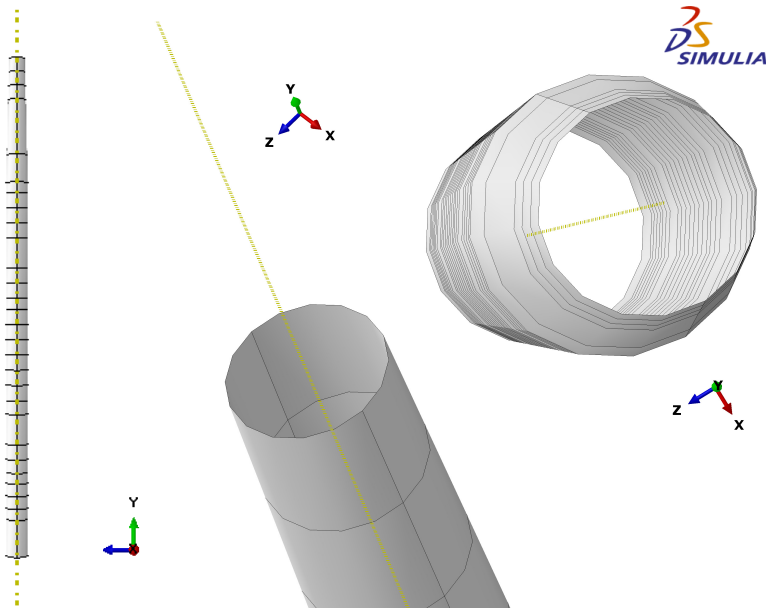

FIGURE 3.9: Representation of tower models used for structural analysis.

3.6.4.2 Boundary conditions and load application

The only boundary conditions applied to the tower was to fully fix it at the bottom for all rotational and translational degrees of freedom. A kinematic coupling constraint was used to apply the tower top loads. The motion of the nodes on the top surface was coupled to a reference node as shown on the right in Figure 3.10. Coupling limits movement of the surface nodes according to the rigid body motion of the reference node [48]. All degrees of freedom of the coupling nodes were constrained in this manner. Furthermore, the first four loads in Table 3.6 were applied at the reference node (RP-2) as shown on the left. The pink arrows represent the moments M_{xT}, M_{yT} and M_{zT} (which follows the right hand rule), and the yellow arrow F_{zT}. It should be noted that the global coordinate system for Abaqus is different than the one specified for the loads in subsection 3.5.2. For the former the y-axis replaces the z-axis and the z-axis is now in the negative y-direction. In effect the coordinate system is rotated by 90° anti-clockwise around the x-axis.

The distributed wind force was applied by using the 'field' and 'load' functions in Abaqus, as shown on the left in Figure 3.10. A mapped analytical field was created requiring a force value and Cartesian coordinates for x, y and z. These were imported directly from Microsoft Excel. The field was applied by using the pressure load function and choosing

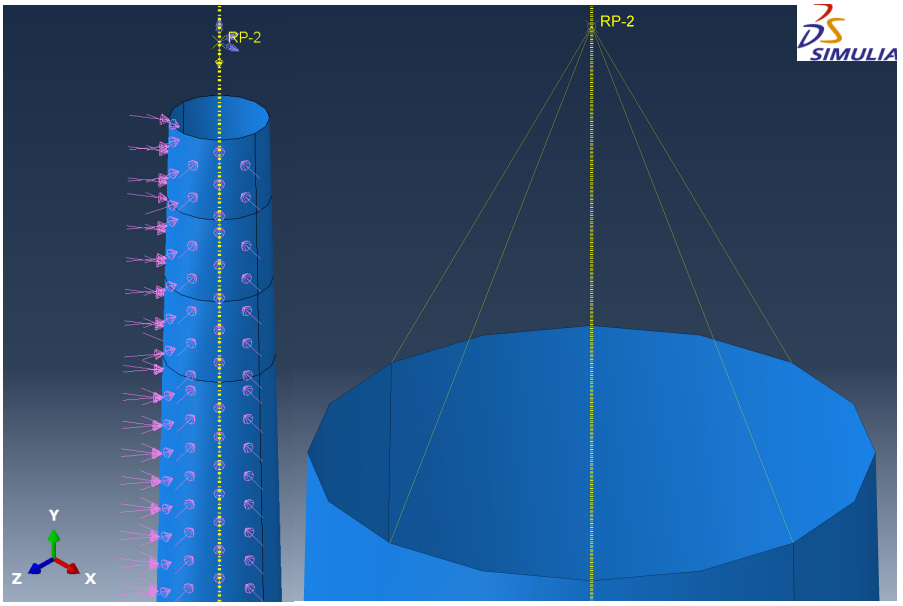

FIGURE 3.10: Kinematic coupling and load application.

the created field as its distribution. Furthermore, γ_f was inserted in this step as the magnitude of the field.

The tower own weight is caused by gravity acceleration of its mass. This force was taken into account in the FEM models by using the gravity load function in Abaqus. As input the gravity acceleration (g) is typically used. However, to convert it to a characteristic load g was first multiplied by the suitable partial safety factor.

3.6.4.3 Material models

Material properties and behaviour of steel and concrete are very complex. For this reason realistic material models were considered very important for obtaining accurate results from structural analyses. Two types were used for this study: elastic and plastic.

The former was implemented for all structural analysis, but only elastic material behaviour was modelled by it. For such behaviour the model used a stress-strain curve following Hooke's law ($\sigma = E\varepsilon$). Therefore no material yielding was accounted for. For example: if this model was implemented in a general static analysis, stress results should (in theory) increase infinitely as the load increases. In Abaqus this was implemented by defining the following elastic properties in the material editor: Young's modulus and Poisson's ratio [48].

Plastic material models were implemented for structural analysis where material yielding and post-failure (plastic) behaviour needed to be tested. It was assumed that after steel yields, strain hardening takes place with the slope of the curve becoming significantly less and decreasing to zero at ultimate strength. For reinforced concrete, compression hardening was assumed to follow a parabolic curve until ultimate stress was reached. From this point onwards the strength would decrease linearly toward ultimate strain [69][74]. Tensile behaviour was assumed to be elastic until cracking occurs. After cracking stress softening would take place until the yield strain of the tension reinforcement was reached [48][74]. The implemented stress-strain curves for the above-mentioned material properties can be viewed in Appendix E. Steel behaviour was modelled in Abaqus by defining additional mechanical plastic properties in the material editor. Values for the respective stress-strain curves were mapped into this property module. For concrete in compression, plastic parameters were mapped similarly to those for steel. The smeared cracking model with tension stiffening was used to simulate tension behaviour. Tension stiffening stress was inserted as the ratio of actual over cracking. It should be noted that Abaqus requires post-failure stress and strain values for plastic material models such as those above. Stress input values ranged from yielding to ultimate failure and for strain plastic values were inserted [48].

Stress-strain curves are usually calculated for engineering strain, ε_e. However, Abaqus requires values of true strain (ε_t) to produce accurate results. Equation 3.5 from Roylance [75] was used to perform the conversion for all stress-strain curves in the study.

$$\varepsilon_t = \ln(1 + \varepsilon_e) \tag{3.5}$$

3.6.5 Steel monopole

3.6.5.1 Ultimate strength analysis

To evaluate ultimate strength of the steel tower a general static analysis (see subsection 2.8.8) was performed in Abaqus. Nonlinear effects of large displacements and deformations were accounted for by activating the large deformation formulation. This was done by selecting the nonlinear geometry (Nlgeom) function as active in the analysis step [48]. For this analysis it was assumed that elastic yielding of the steel resulted in

structural failure. Material failure was assumed to occur when the resulting Von Mises stress values anywhere in the tower were higher than the factored yield stress of the steel. The latter was calculated as the appropriate value from Table 3.4 multiplied with γ_m for structural steel (Table 2.7). The unfavourable normal load factors from the IEC code [35] for aerodynamic and gravity actions were taken as 1.35 and 1.1 (Table 2.6). For consequence of failure the factor was assumed to be unity.

3.6.5.2 Stability analysis

For the stability analysis the global and local buckling strength needed to be verified in Abaqus for ultimate load. Both were considered to be unstable forms of structural failure and examination thereof was performed in Abaqus using nonlinear static procedures. It should be noted that for both the large deformation formation was activated and nonlinear material models used. Verification for global buckling was performed using the modified Riks method (see subsection 2.8.4). In Abaqus it is called static, Riks. For this study it was assumed that structural integrity is achieved when the LPF reaches unity and the analysis completes. To ensure analysis stability for local buckling, the adaptive automatic stabilization scheme was activated in Abaqus. This was initiated in the analysis step, a constant damping factor was specified and default values were used [48]. Failure was assumed to occur when a diamond shaped buckling pattern could be observed (see Figure 2.9(b)), and the analysis aborted. Partial safety factors for loads, materials and consequence of failure were assumed to be the same as for the ultimate strength analysis. However, γ_m was taken as 1.2 for global buckling.

3.6.6 Prestressed concrete monopole

3.6.6.1 Modelling of reinforcement

All reinforcement was modelled in Abaqus by defining rebar layers for each shell section. The following properties needed to be defined for each layer: layer name, cross-sectional area per bar, spacing in the plane of the shell, position in the thickness direction, rebar material and initial angular orientation [48].

In Abaqus the local material orientation of the shell sections follow the convention shown in Figure 3.11. Spacing for horizontal rebar was defined along the '1' direction

at a position within the thickness projection normal to the relative midsurface. Vertical rebar spacing was defined in the same manner along the '2' direction. The position was measured from the midsurface of the shell according to the positive direction of the normal axis [48]. This convention was used to place the rebar layers in the configuration shown in Figure 3.4. Furthermore, the initial angular orientation refers to the material alignment before loading. It was used to distinguish between the horizontal and vertical reinforcement. The former was aligned parallel to the '2' direction at 90° and the latter in the '1' direction at 0°.

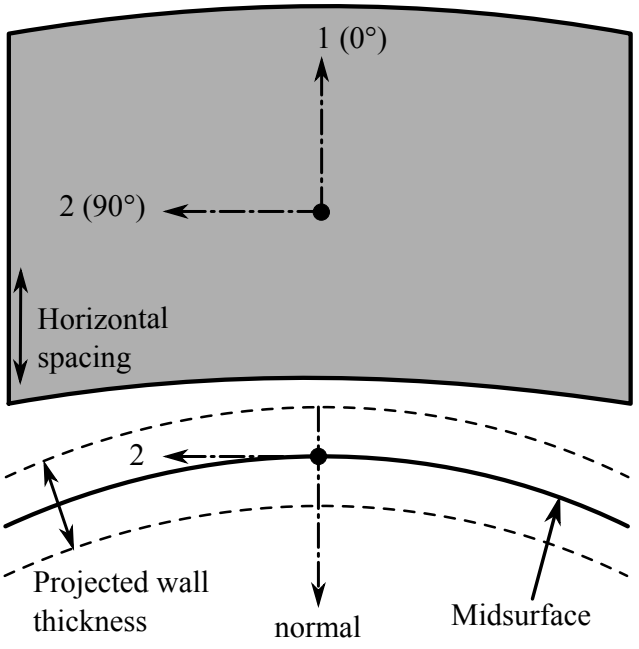

FIGURE 3.11: Material orientation of tower shell sections and reinforcement layers.

To model prestressing forces, initial conditions were used in Abaqus. For this function a constant compression stress was defined for a rebar layer in a shell section by specifying a stress value as an initial condition in the analysis step. For initial conditions this value is solution dependent, meaning it can change during an analysis step. Prestress hold could be applied to keep it fixed, but was deemed not suitable for this study. The stress was assumed to be the factored prestress after losses (Table 3.5) and given a negative sign to induce compression in the concrete. It should be noted that initial conditions can only be implemented in Abaqus for a static analysis [48].

3.6.6.2 Prestressing

Prestressing was applied by performing a SLS section analysis according to the local SABS code [29]. The tower was assumed to be a Class 1 structure. Therefore prestressing forces needed to neutralize all flexural tensile stress at SLS loading anywhere in the tower. However, compression stress also needed to be kept within the SABS [29] limit. The maximum allowable compression was taken as $0.33\, f_{\text{cu}}$ for a prestressed tower.

A nonlinear general static analysis was performed in Abaqus implementing an elastic material model and large deformation formulation. Significant flexural stresses in the section were assumed to be in the vertical direction and two analysis steps were performed. For the first the factored prestress after losses was applied to the tendon layer in each section. However, it was done under permanent action. For the second step complete loading was applied. The spacing of tendons were varied to find the optimal amount. For this number, stress values were kept between the above-mentioned SABS [29] limits. It should be noted that stresses at transfer were not considered.

For prestressing at SLS the partial safety factors for loads were assumed to follow the configuration from the local SANS code [46]:

- M_{yT}, M_{zT} and $F_w(h)$ are forces induced by wind action ($\gamma_Q = 0.6$),
- F_{zT} and $F_{ow}(h)$ are favourable permanent actions ($\gamma_G = 1.0$), and
- M_{xT} is an unfavourable permanent action ($\gamma_G = 1.1$).

Material factors for concrete and steel reinforcement was taken from Table 2.7. Furthermore, for consequence of failure the factor was assumed to be unity.

3.6.6.3 Ultimate strength analysis

The SABS [29] ULS section analysis was performed to examine the ultimate strength of the concrete tower. Calculations were performed in Microsoft Excel and some adjustments were made to account for the circular cross-section shown in Figure 2.12.

Formulae for the segment shown in Figure 3.12 were used to determine the tower section properties. The centroid position and area of the compression block was calculated

using equations 3.6, 3.7 and 3.8 [64]. The first two formulae were used to calculate the parameters in equation 3.8. In this equation the effect of A_2 (the void) was subtracted from the overall segmental area in order to determine the centroid position of the concrete compression block. The second term represents the distance between the bottom of this block and the neutral axis. To determine the section area, A_2 was subtracted from A_1.

$$A = \frac{r^2}{2}\left(\frac{\pi\theta}{180} - \sin\theta\right) \tag{3.6}$$

$$d_x = \frac{c^3}{12A} - r\cos\frac{\theta}{2} \tag{3.7}$$

$$\overline{y}_c = \frac{A_1 d_{x1} - A_2 d_{x2}}{A_1 - A_2} + 0.1x \tag{3.8}$$

Where:

A	=	Area of segment
r	=	Radius of circle
θ	=	Segment angle (in degrees)
d_x	=	Centroid distance of segment
c	=	width of segment
$\overline{y}_c$	=	Distance of concrete compression block centroid to neutral axis
A_1	=	Area of overall tower segment
A_2	=	Area of tower inner segment
d_{x1}	=	Centroid distance of overall tower segment
d_{x2}	=	Centroid distance of inner tower segment

Due to the radial positioning of the prestressing tendons, the centroid depth of those in tension (d_i) had to be calculated separately. Therefore the resistance moments for the tendons were also calculated individually (using equation 2.34) and summed to determine M_r. Stress in each was calculated according to the strain graph in Figure 2.12 and stress-strain curve in Figure 1 in Appendix E. To determine the strain graph the outermost concrete compression fibre was assumed to be at maximum strain at ULS. For the stress-strain curve the appropriate material factor was applied. The top, mid and bottom sections of the tower were assumed to be the most critical and were analysed.

Additionally, a general static analysis was performed in Abaqus. Nonlinear geometry and the plastic material model (with smeared cracking) was implemented. Due to the way

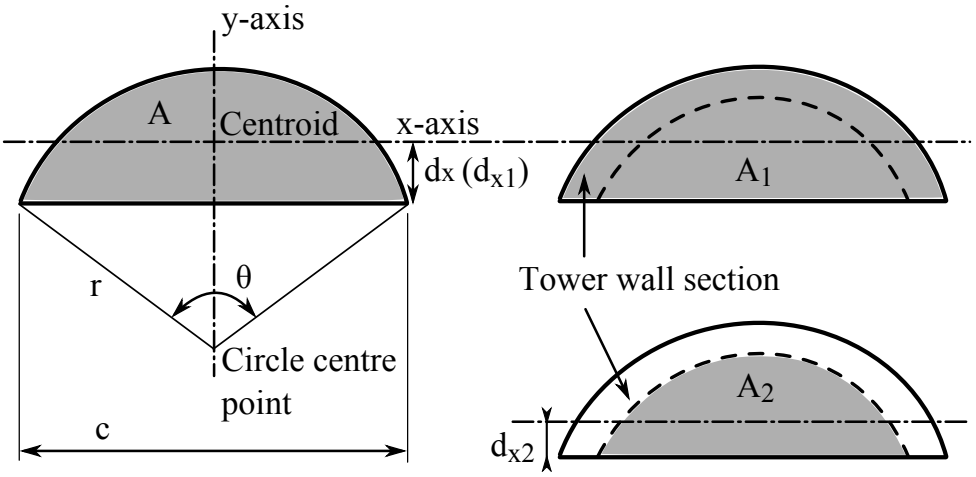

FIGURE 3.12: Representation of a segment [64].

prestressing was modelled, the tendons were loaded in compression. However, in practice these tendons are in tension. Abaqus stress results for tendons would then be less than the factored prestress for tension, and more for compression. To determine the critical tension in the reinforcement the difference between the resulting prestress and tension values was summed with the initial prestress. Critical tension was then compared with the material yield values. Tension failure was considered to occur at tendon ultimate strength. Compression failure was assumed to occur at concrete ultimate stress.

The ultimate applied moment was determined by also performing a general static analysis in Abaqus. Nonlinear geometry and an elastic material model was used. The latter was chosen, because yielding did not need to be tested. Only reaction load values at the tower bottom needed to be extracted. Extraction was performed by creating a kinematic coupling in a similar manner as discussed in subsection 3.6.4. However instead of applying loads, a boundary condition was applied to fix the reference point for all rotations and translations. The resulting reaction moment values at this point were exported from Abaqus and used to determine the applied moment. This was performed by calculating the resultant moment for the couple moment values of the axis in the plane of the tower bottom section (horizontal plane).

Load factors were taken as the same as those for the ultimate strength analysis of the steel monopole tower. Furthermore, for materials and consequence of failure the same factors were taken as those for prestressing.

3.6.6.4 Stability analysis

It is well known that concrete wind turbine towers are not governed by local buckling [24]. For this reason, global stability can still be an issue and was investigated. A Riks analysis was performed in Abaqus. Nonlinear geometry and the plastic material model was applied to it. All partial factors were taken as the same as those for the ultimate strength analysis.

3.6.7 Optimisation and material mass

In order for the tower designs to be comparable, both were optimized according to its governing limit state. Material volume and mass of the optimized designs were calculated and compared with those of the original. Volume of the steel tower was calculated according to equations 3.9 and 3.10 [64]. The former is for a frustrum of a right circular cone and the latter for a right circular cylinder. For the reinforced concrete tower equation 3.9 was used for the concrete. Steel reinforcement area was multiplied with its total length and total bars for each section. The taper angle is small, so the section height was used as the length of the vertical reinforcement. For the horizontal reinforcement the perimeter at the top of each section was used. Furthermore, mass was calculated by multiplying the volumes with material density.

$$V_{frustrum} = \frac{1}{3}\pi h\left(R_{top}^2 + R_{top}R_{bot} + R_{bot}^2\right) \tag{3.9}$$

$$V_{cylinder} = \pi R^2 h \tag{3.10}$$

Where:

$V_{frustrum}$	=	Volume of circular cone frustrum
$V_{cylinder}$	=	Volume of circular cylinder
h	=	Height
R_{top}	=	Top radius of frustrum
R_{bot}	=	Bottom radius of frustrum
R	=	Radius of cylinder

3.7 Life-cycle cost analysis

3.7.1 Cost estimation of life-cycle phases

A "bottom-up" cost estimation was performed for the following life-cycle phases: manufacture, construction and installation, disposal and recycling, and transport. Significant methodology for the study shall be discussed below. In depth details and results are included in Appendix G.

3.7.1.1 Manufacture, construction and installation

Manufacture, construction and installation costs were determined using the conceptual frameworks created by LaNier [24] for a 50 tower wind farm (see subsection 2.9.4). Optimised material mass and volumes for the steel and prestressed concrete designs were supplemented into these frameworks. For the concrete design these values were used to estimate costs for the two construction methods: precast and cast-in-place jump forming. Available local pricing was incorporated into the frameworks where possible. Where local prices were not found, costs from LaNier [24] were linearly interpolated between the values for the 1.5 MW and 3.6 MW turbines. All costs for this phase was assumed to fall under initial capital costs (ICC).

PPiS [76] provides an online database called Merkel's live for pricing of local material, labour and plant cost of various construction operations. For this study Merkel's [76] rates for August 2014 in the Western Cape region was used. Where relevant these rates were inserted into the LaNier [24] cost framework.

Geotechnical and surveying costs were supplied by Dr. Peter Day [77].

Neither LaNier [24] nor PPiS [76] provided data for high strength concrete. Therefore for the concrete tower a typical 60 MPa mix was acquired from Olawuyi [78] and material prices from local suppliers. PPiS [76] labour and equipment rates for 30 MPa/19 mm stone concrete column construction was assumed.

For prestressing reinforcement free construction cost data [79] was used to acquire material and equipment costs, and labour hours per unit distance. PPiS [76] pricing was

applied to the labour hours. To determine the cost of reinforcement its calculated length for this study was multiplied by the unit price.

Macsteel [80] prices were used to estimate material and fabrication cost for the steel tower. Material cost per ton was determined for each section by matching it with a Macsteel [80] plate of similar dimensions. The cost per ton for these plates were multiplied with the mass of each tower section and the products were summed. For fabrication the average difference in price was calculated for a range of plates and welded tube sections with approximately similar dimensions. The latter was found to be 42.69 % more expensive. To determine fabrication cost the material cost was multiplied by this percentage. A welding cost per metre was determined for the fabrication of the six main sections of the tower. Free construction cost data [79] was used to acquire material and equipment costs, and was combined with PPiS pricing [76] for labour cost. The length of weld for all the joined segments was calculated and multiplied by the above unit cost.

3.7.1.2 Disposal and recycling

Total disposal and recycling cost of the tower materials was investigated. The optimized mass and volume discussed in subsection 3.6.7 were used. Municipal solid waste dumping sites were assumed to be used for disposal of tower materials after dismantling. A further assumption was made that a salvage value is given at the dumping site for recyclable waste. According to City of Cape Town [81] disposal of clean builders rubble is free of charge to prevent illegal dumping. Tower materials were assumed to be clean rubble and this cost was taken as zero. Sorting was assumed to take place on site, but its cost was not included. Furthermore, steel was assumed to be cut and concrete broken where necessary for easy transport. An efficiency percentage was determined for salvaging of these materials. This percentage was used to determine a salvage income and transport cost. These values were summed to determine the disposal and recycling costs.

3.7.1.3 Transport

Local manufacturing was assumed for all tower materials and components. Therefore only local transport rates needed to be acquired. Road transport by truck was assumed to be the most probable mode and costs were estimated for the following situations:

- transport of tower materials from the fabrication plant to the site, and
- transport for disposal and recycling of tower materials after dismantling.

For the former the most influential costs were assumed to be transport of fabricated parts and prestressing reinforcement. Fabricated parts were assumed to be precast segments and main steel sections. Site mixing and casting was assumed for the cast-in-place tower and therefore the above-mentioned did not apply for it. Materials for concrete fabrication, nominal reinforcement and common steel components were assumed to be acquired from nearby suppliers of which transport distance was negligible. Prestressing reinforcement was assumed to be manufactured at the same factories as the steel tube sections. Rates were based on an average value of R11.02km^{-1} for a 28 t truck in South Africa [82]. For the precast segments this was suitable, but for the heavier steel tower sections it was linearly extrapolated for a 50 t truck.

Transport costs for the second situation were calculated according to the distance between the installation and dumping sites. The rates were determined for a PPiS [76] 8 t open truck. It was assumed to be a tipper for quick unloading. A fixed cost per 9 hour day was determined consisting of a truck rate, insurance and driver wage. Furthermore, a rate per kilometre and overtime was included. Next, a transport time per trip was calculated for uploading, travel and unloading. The amount of trips per day was determined in order to calculate the total daily mass and cost. The latter values were used to determine a rate per ton. This cost was multiplied with the tower material mass to determine transport cost. It should be noted that overtime was considered if it caused a decrease in cost per ton.

3.7.1.4 Discount and exchange rates

Cost data used for this study were acquired from various different sources. Values differed in time period and type. For this study all estimated costs were calculated as current values for August 2014 South African Rand (ZAR). Value added tax at 14 % was added to prices where necessary.

3.7.2 Comparison with actual costs

Manufacture, construction and installation costs were approximated for large wind projects in South Africa in order to measure the accuracy of the above cost estimation. Eberhard [6] provides a list of farms from the local Renewable Energy Independent Power Project Procurement Program (REIPPPP). The total capacities of none of the listed farms matched the size of the reference wind turbine. Nonetheless, for the ten largest projects information about the number of turbines and machine capacity was acquired (see Table 5.2). Available total costs of these projects were acquired and divided by the amount of wind turbines. These unit costs were scaled for the capacity of the reference wind turbine and multiplied by 38 %. This fraction represents the percentage of total ICC for the tower and balance of station, and was taken as an average from various sources in literature (see subsection 2.9.3) [51][52][53].

3.7.3 Sensitivity analysis

To measure the sensitivity of the life-cycle costs a parameter study was performed for the most significant variables. These parameters were varied according to a percentage based probable range determined from literature. This range was defined by a pessimistic and optimistic value. For each variable all other parameters were kept constant at its most likely values. The results of subsection 3.7.1 were taken as the most likely values. For each key parameter the resulting manufacture, construction and installation (MCI) costs of one tower was varied and compared to low, most likely and high costs of the other towers. Key MCI cost parameters were assumed to be:

- foundation cost,
- material cost,
- fabrication and field erection cost,
- transport cost and
- labour cost.

Transport cost was varied according to a close, most likely and far distance. Furthermore, disposal and recycling estimates were determined according to minimum, most likely

and maximum values. Significant parameters were assumed to be: salvage value and transport cost.

3.7.3.1 Foundation cost

Some scholars suggest that foundation size for the steel tower should be larger than for the concrete designs, due to smaller tower mass. The effect of this was investigated by varying the size related foundation costs of the steel tower up to 150 % of the most likely values of the others. Its upper probable limit was calculated to be 133 %. Furthermore, values from literature were used to determine the general sensitivity of foundation costs. Parameter variation ranged from −32.5 % to 27.4 % of the most likely value [51][52][53]. General sensitivity was applied to the foundation costs of the concrete towers (which was identical) and the lower limit for the steel tower.

3.7.3.2 Material cost

Steel and concrete were assumed to be the most cost intensive materials. The probable range for precast and in-situ concrete was determined using monthly cost data acquired from Klaas [83] for January 2012 through August 2014. All past cash flows were converted into present monetary values, making it easy to compare. The average growth per interest period was calculated and used as discount rate to determine the PW for each monthly cost. For each of these values its deviation from the average PW was calculated as a percentage. The minimum and maximum percentages were used as the low and high estimates for the probable range. Ranges for precast and in-situ concrete were very similar. Therefore its highest and lowest deviations were combined to form a probable range from −2.1 % to 2 % for concrete in general. The range for steel products was calculated similarly as above. Costs were more volatile ranging from −51 % to 45 % from January 2012 to September 2014 [84]. To plot results the steel cost was varied over its probable range while concrete cost was kept constant for its low and high estimates.

3.7.3.3 Fabrication and field erection cost

The probable ranges of fabrication and field erection costs were determined similarly as above. For steel fabrication monthly cost data of manufactured structural metal

products were used to determine a range from −33 % to 25 % [84]. For precast concrete, fabrication, reinforcement and post tensioning was considered [83]. Formwork costs were added for the cast-in-place tower. Probable ranges for both were determined to be −4 % to 2.7 % and −2.4 % to 1.6 % respectively. Field erection data for completed non-residential buildings in the Western Cape was used to determine a range from −94 % to 183 % [84]. Erection costs were varied over its probable range while fabrication costs were kept constant for its low and high estimates.

3.7.3.4 MCI transport cost

For the precast tower the most likely and most distant fabricators were assumed to be located in industrial areas in greater Cape Town. The Cape Concrete precast yard in Blackheath represented the former and Montague gardens industrial was chosen for the latter. Grabouw industrial was taken as the close estimate. The calculated probable cost range was from −51 % to 25 %. Fabrication of the steel tower and prestressing reinforcement was assumed to be performed at one of the main local steel factories. The assumed factories were Cape Town Iron and Steel Works (CISCO) Kuilsriver, Arcelor-Mittal South Africa (AMSA) Saldanha and Hall Longmore Wadeville. These represented close, most likely and far distances and the calculated probable range was from −62 % to 512 %. To plot results steel transport costs were varied while precast MCI costs were kept constant for the close and far estimates. MCI cost for the steel and cast-in-place towers were unaffected by the latter and varied along its most likely values.

3.7.3.5 Labour cost

Labour is complexly integrated into manufacturing, construction and installation. This makes it difficult to measure the exact impact thereof. However, where possible its cost was determined and varied for each tower. Labour cost volatility was estimated by combining quarterly values for gross salaries and wages for construction and manufacture from 2011 to 2014 [84]. The probable range was determined by the method used for material cost and ranged from −5 % to 10 %. Labour costs for the cast-in-place tower was varied across this range while MCI costs for the other two towers were kept constant for its low and high estimates.

3.7.3.6 Disposal and recycling

Values for salvage effectiveness of concrete were acquired from Klee [85]. The pessimistic estimate was assumed to be the lowest value of 10 % and the optimistic value the salvage percentage of 57 % for Australia. This nation was chosen, because it is a large less-populated country like South Africa and for such regions achievable salvage percentages are expected to be lower. Furthermore, because Australia is a developed nation its salvage potential is assumed to be well exploited. The average was taken as the most likely value. Salvage and recycling of steel is a well known practice. The effectiveness of steel was assumed to be deterministic at 98 % for reinforcement and 100 % for structural tubes [86]. A deterministic salvage value for scrap steel was chosen as R2050.00 [87] per ton. For concrete rubble a range from R42.63 to R170.51 was taken [85].

For transport the landfill site just outside Caledon was chosen as close estimate. Large solid waste disposal sites in Hermanus and Kleinmond were taken as the most likely and most distant approximations.

3.8 Conclusion

In this chapter a reference wind turbine was defined and its properties were based on the Sinovel SL3000/113 machine with 3 MW capacity, 100 m hub height and 113 m rotor diameter. Klipheuwel-Dassiesfontein in Caledon was assigned as its location. Realistic and comparable steel and concrete support structure designs were acquired from Arcelor-Mittal [63] and NREL [24], and were tested for a static wind turbine under extreme wind conditions. Loading was calculated using the Quasi-static method and procedures from the local SANS [37] code. Furthermore, an IEC [35] ULS structural analysis was performed using Abaqus and hand calculations. Structural parameters were optimized and material mass and volume were determined for the towers. A cost estimation and sensitivity analysis was performed for the following tower life-cycle phases: manufacture, construction and installation, transport, and disposal and recycling. Material volume and mass of the designs were incorporated where necessary.

Chapter 4

Results for Structural Analysis

4.1 Introduction

In this chapter the structural soundness of the steel and prestressed concrete towers shall be analysed and proved for local conditions. The calculated loads for a stationary wind turbine in extreme conditions shall be shown and discussed. Furthermore, the results of the ultimate limit state analysis and optimal design adjustments of both towers shall be presented and discussed. Resulting material volume and mass for the optimized designs shall then be presented.

4.2 Results for steel monopole

4.2.1 Loading

The nominal loading and partial factors for loads in Table 4.1 were used to perform the ULS analysis for the steel tower. These were multiplied to calculate the ULS loads. For the load eccentricity of M_{zT} and M_{xT} the tower radius at the blade tip was determined to be 2.15 m. By summing this value with the static clearance (5.65 m), the eccentricity was calculated as 7.8 m. It should be noted that $f_w(h)$ is a mapped array of loads and its values over the tower height are listed in Table 8 in Appendix F.

TABLE 4.1: Loading and partial factors for steel tower design.

Load symbol	Nominal value	γ_f	ULS load	Unit
M_{yT}	46 369	1.35	62 958	kN m
M_{zT}	301	1.35	407	kN m
M_{xT}	5127	1.10	5639	kN m
F_{zT}	765	1.10	842	kN
$f_w(h)$		1.35		
$F_{ow}(h)$*	9.81	1.10	10.79	$\mathrm{m\,s^{-2}}$

*For this load the gravity acceleration is inserted into Abaqus.

4.2.2 Ultimate strength analysis

For the ultimate strength analysis the critical stress region was identified as the tower zone above 65 m. As shown in Figure 4.1 the tower wall was subject to large stresses. We see the tower bending towards the right due to the large magnitude of M_y, inducing tension and compression stresses as shown on the left and right. Red and blue represents the highest and lowest Von Mises stresses respectively. The maximum was located at the tension side as indicated with the arrow. Maximum tension and compression in the tower section followed respective paths along its height (as shown) and were plotted on the left in Figure 4.2. We see that induced Von Mises stresses exceeded elastic yielding limits from 71 m upward. Structural failure should occur along this section.

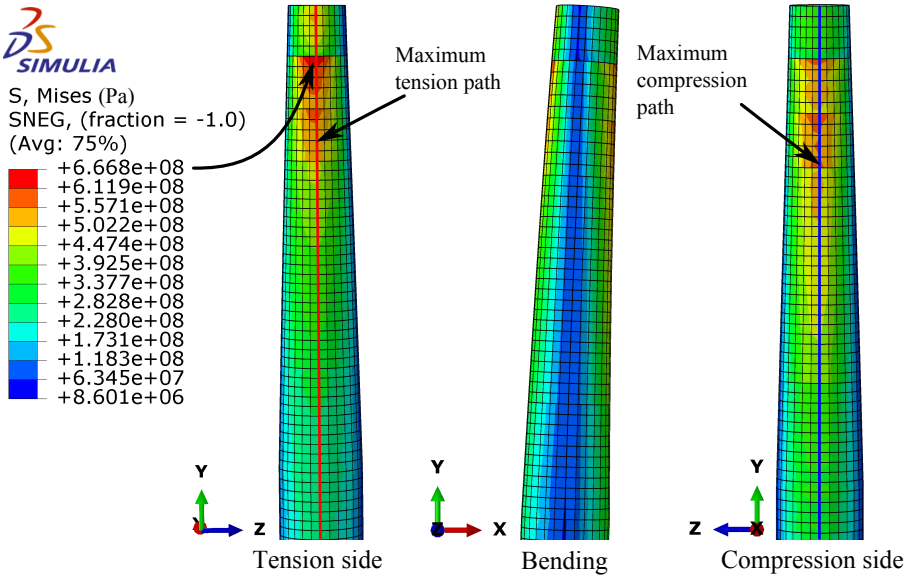

FIGURE 4.1: Stress distribution for the ultimate strength analysis of the steel tower.

The tower geometry was adjusted to decrease critical stress values. Firstly the top diameter was increased to 3.6 m with a constant taper down to the top of flange 3. This size was chosen in order for the steel and concrete tower geometries to be more relatable. From flange 3 to the bottom the diameter was kept the same. Furthermore, the wall thickness was changed as shown in Table 4.2. The right side of Figure 4.2 shows the stresses for the adjusted geometry. Here we see that critical stresses were neutralized to less than or equal to the factored yield strength. It should be noted that at some isolated points values still slightly exceeded the yield limit. It was assumed that for any of these cases a value within 5 % of the limit is permissible.

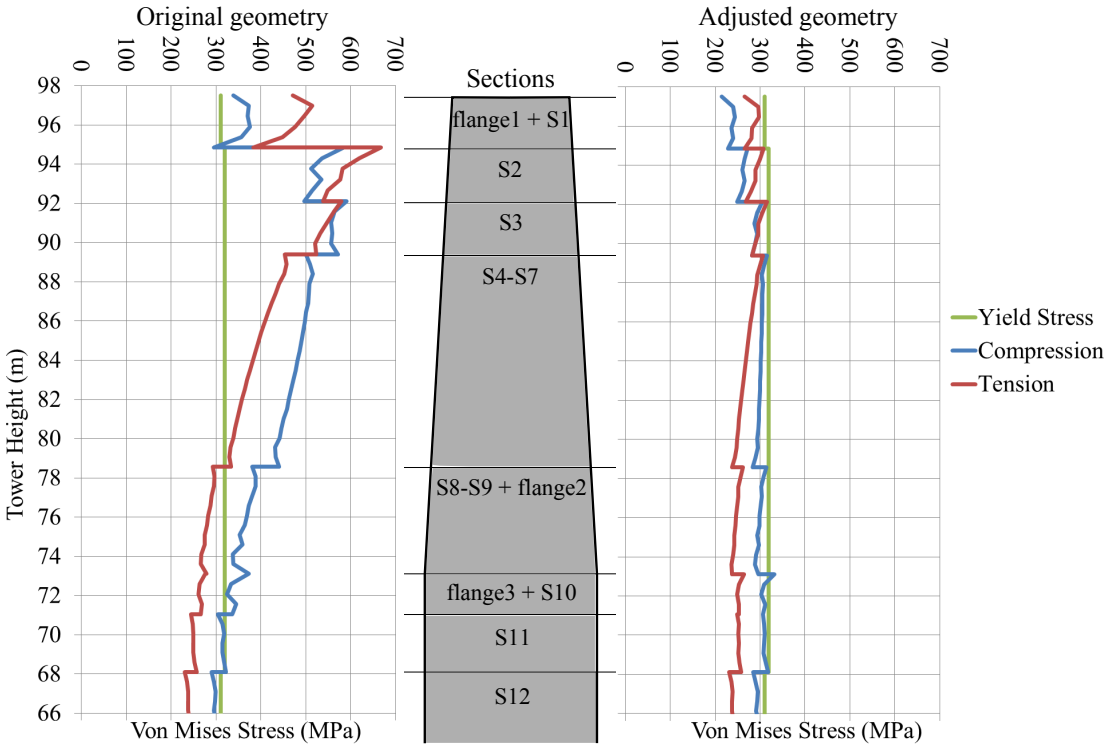

FIGURE 4.2: Stress path results for ultimate strength analysis of the steel tower (above 65 m height).

4.2.3 Global buckling analysis

A global buckling analysis was first performed for the original tower geometry. As shown in Figure 4.3 the tower buckled under the applied loading with the critical zone located within section S3 between 89 m and 92 m. This is the section with the smallest wall thickness at 13 mm and stresses in this zone was similar to the factored yield value of 288 MPa for global buckling. Convergence of the equilibrium equation was not reached

and the analysis aborted. Figure 4.4 shows the increase in load proportion along the arc length (see subsubsection 2.8.8.1). Here we see that a maximum 57.82 % of ULS loading was applied before termination and it was assumed that a stability failure occurred.

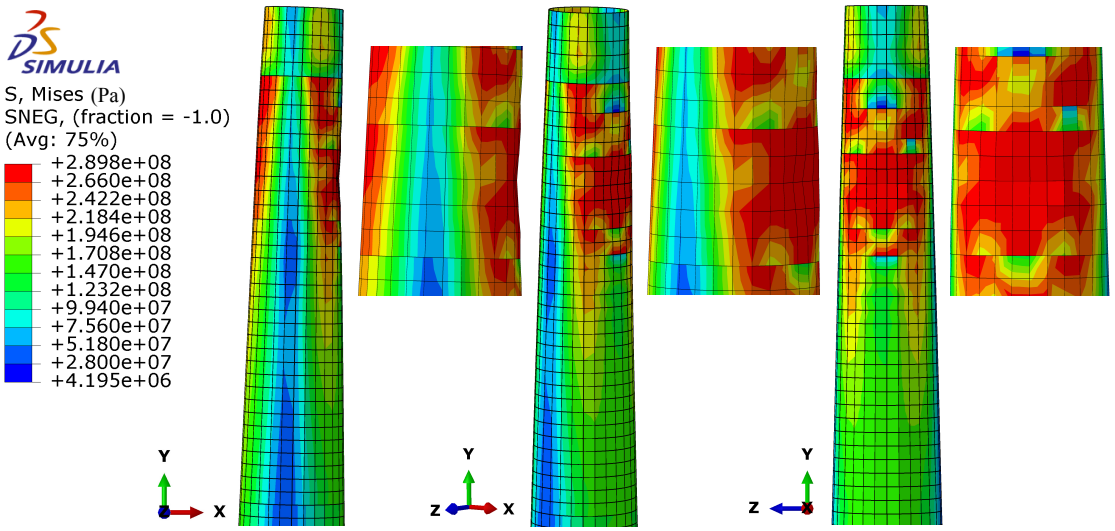

FIGURE 4.3: Global buckling failure of the original steel tower design.

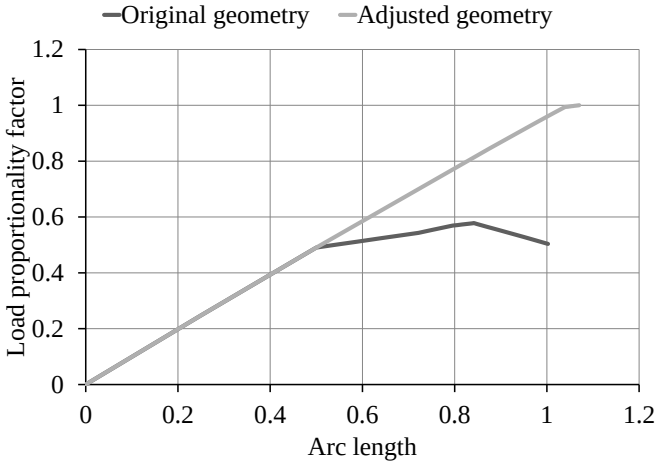

FIGURE 4.4: Increase in LPF for global buckling analysis of the steel tower.

The tower top diameter was increased similarly to the ultimate strength analysis and wall thickness were adjusted as shown in Table 4.2. In Figure 4.4 we see that the LPF for the adjusted geometry increased linearly until just before unity. At this point the steel started to yield. However, the LPF did reach unity and the analysis completed successfully. Figure 4.5 shows the stress results for the adjusted geometry. Stresses

mostly remained just under or equal to the factored limit over the whole height. Segment S11 was deemed critical with a buckling zone forming in the red region. However, the tower did not fail and the adjusted design was assumed to be safe.

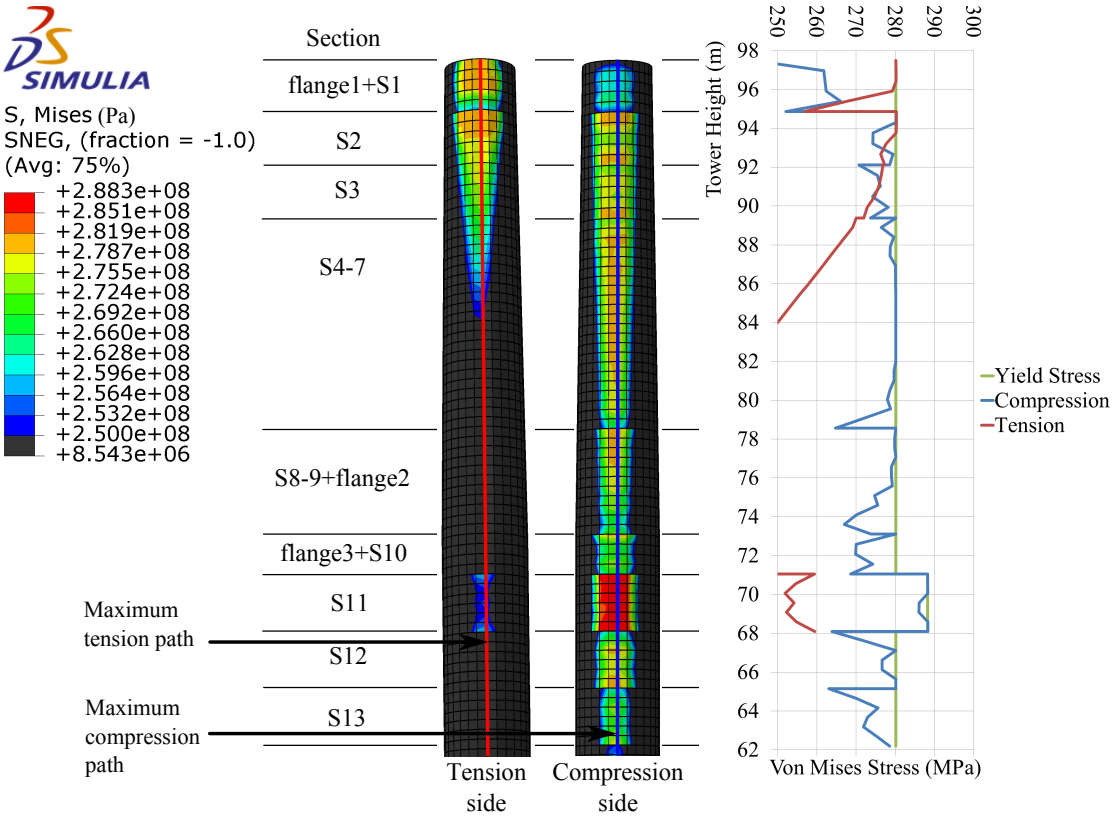

FIGURE 4.5: Stress results for global buckling analysis of the adjusted steel tower.

4.2.4 Local buckling analysis

The local stability of the steel tower was first tested for its original geometry. Figure 4.6 shows the Von Mises stress results for the analysis. No diamond shaped buckling patterns were observed throughout its duration and it aborted when the factored yield stress (312 MPa) was reached for section S2. From this we can conclude that the material yielded before the local buckling capacity was reached. The tower geometry was adjusted and the diameter was changed in the same manner as the above two analysis. Furthermore, thickness was increased to the values in Table 4.2 for optimal stress distribution. In Figure 4.7 we see adjusted stresses optimally distributed near and equal to the factored limit.

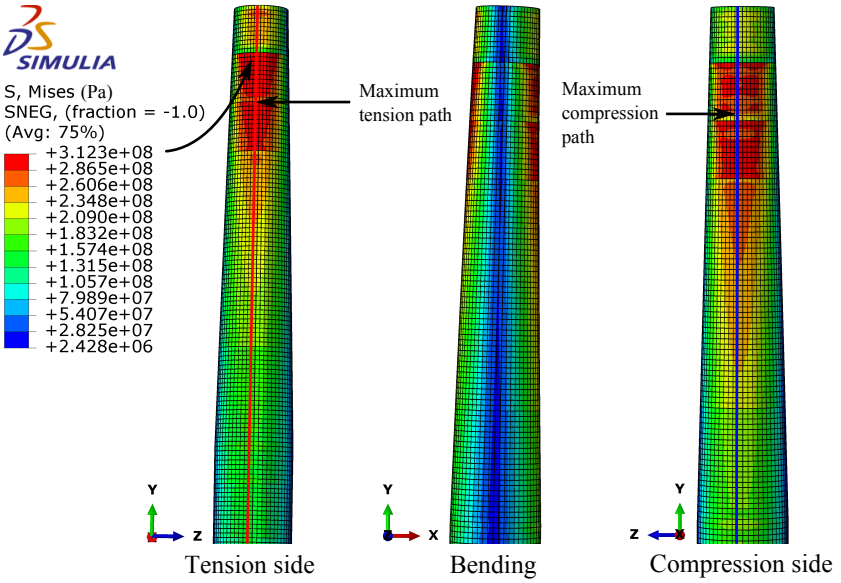

FIGURE 4.6: Stress distribution for the local buckling analysis of the steel tower.

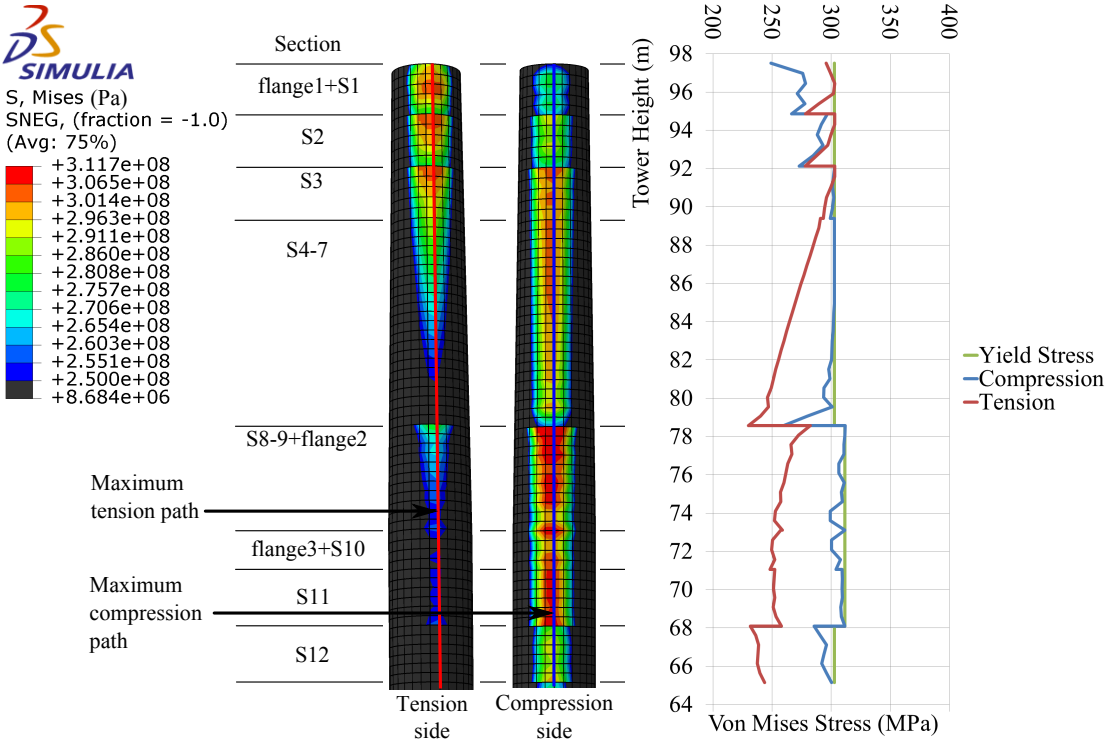

FIGURE 4.7: Stress results for local buckling analysis of the adjusted steel tower.

4.2.5 Optimal design and material mass

The most conservative wall thickness results from the three above mentioned analysis were used to determine the optimum values of the tower as shown in Table 4.2. It should

be noted that wall thickness for the rest of the tower were kept the same as the original. The material volume and mass was calculated for the original and adjusted geometry and listed in Table 4.3. Geometric adjustments increased the volume and mass by 2.7 %.

TABLE 4.2: Optimum wall thickness change (in mm) of steel tower.

Section	Original	Ultimate strength	Global buckling	Local buckling	Optimal
flange1 + S1	20	23	20	20	23
S2	14	21	19	19	21
S3	13	19	19	18	19
S4-7	14	18	19	18	19
S8-9 + flange2	15	17	18	16	18
flange3 + S10	15	16	17	16	17

TABLE 4.3: Material volume and mass of original and adjusted steel tower design.

Section	Original		Adjusted	
	Volume (m^3)	Mass (t)	Volume (m^3)	Mass (t)
Tapered	4.08	32.05	5.70	44.78
Cylindrical	28.85	226.50	28.91	226.94
Total	32.94	258.55	34.61	271.71

4.3 Results for concrete monopole

4.3.1 Loading

The calculated loads for the prestressed concrete tower design were factored for SLS and ULS and are listed in Table 4.4. Tower radius at the blade tip was calculated to be 2.51 m and added to the static clearance to determine the eccentricity of M_{zT} and M_{xT} at 8.16 m. Load values for $f_w(h)$ were modelled in a mapped array over the tower height, which is listed in Table 9 in Appendix F. It should be noted that the same tower design was analysed for the precast and in-situ concrete construction methods.

TABLE 4.4: Loading and partial factors for the prestressed concrete tower design.

		γ_f		Factored values		
Load symbol	Nominal value	SLS	ULS	SLS	ULS	Unit
M_{yT}	46 369	0.6	1.35	27 821	62 958	kN m
M_{zT}	315	0.6	1.35	189	407	kN m
M_{xT}	5361	1.1	1.10	5897	5639	kN m
F_{zT}	765	1.0	1.10	765	842	kN
$f_w(h)$		0.6	1.35			
$F_{ow}(h)$*	9.81	1.0	1.10	9.81	10.79	$\mathrm{m\,s^{-2}}$

*For this load the gravity acceleration is inserted into Abaqus.

4.3.2 Prestressing

Serviceability loading was first applied to a nominally reinforced tower. This was done to assess the stresses in the tower before prestressing was applied. Results for the vertical flexural stresses are shown in Figure 4.8. Here we see that maximum compression (blue) and tension (red) stresses were located in the top region of the tower. The former complied with the elastic limits of the SABS [29] code. However, the latter was well above the tensile limit and needed to be decreased.

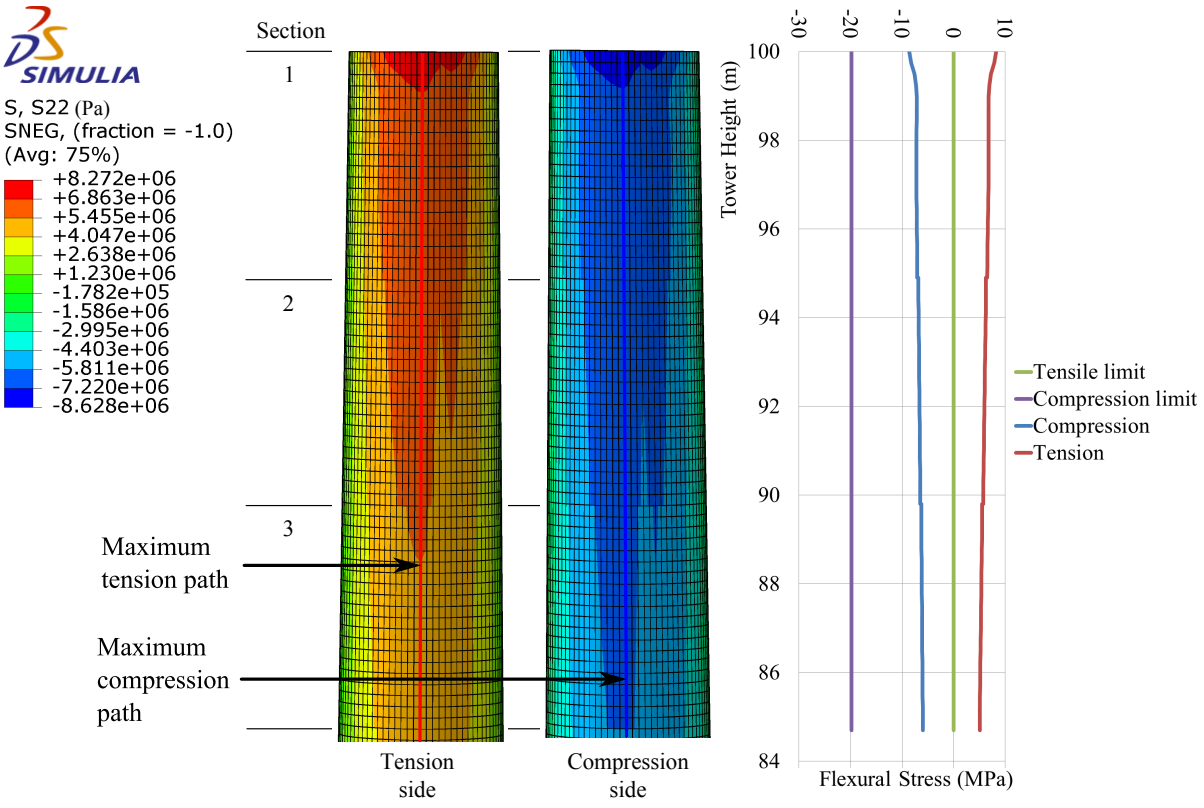

FIGURE 4.8: Flexural stress for SLS loading in the concrete tower prior to prestressing.

Prestressing was applied to the tower in order to decrease the maximum tension to a value of zero or less. For optimum design 19 prestressing tendon units were placed in the tower at a minimum spacing of 492 mm and were stressed to the factored prestress after losses. Resulting flexural stresses in the tower is shown in Figure 4.9. Here we see that these stresses complied with the SABS [29] limits and that tension controlled by a small margin.

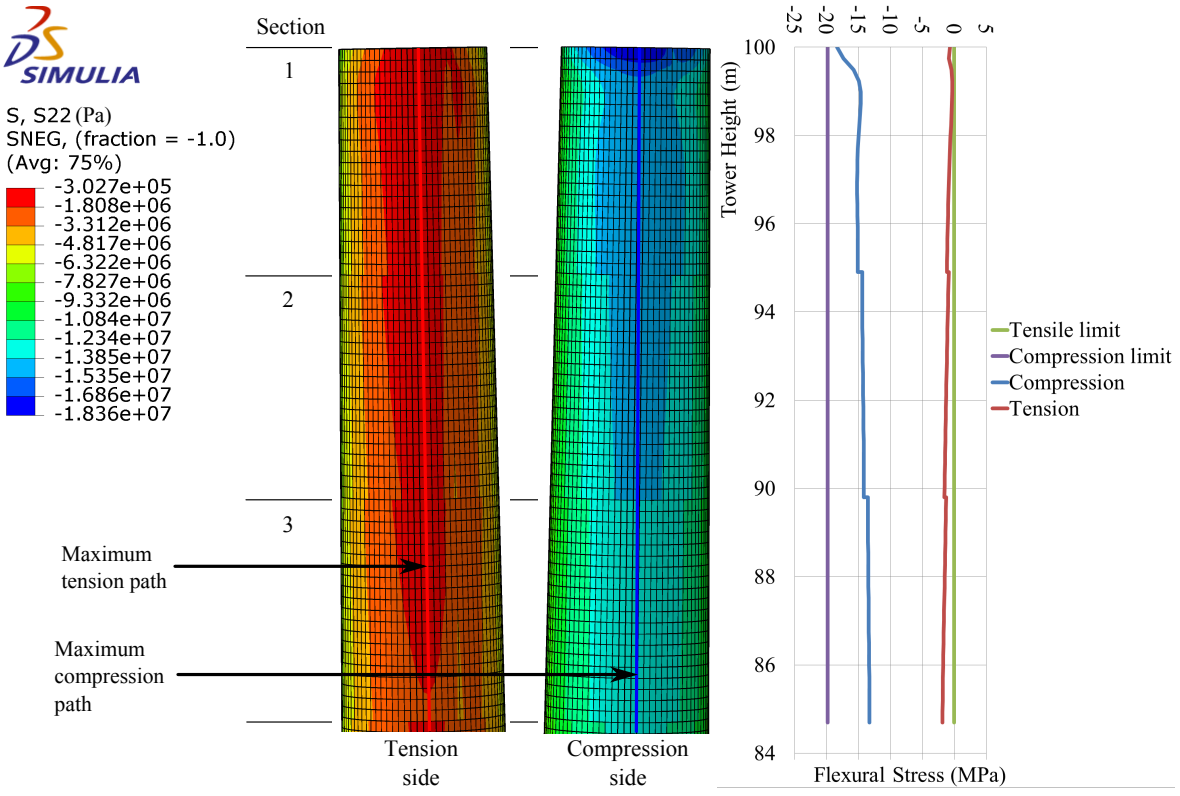

FIGURE 4.9: Flexural stress for SLS loading in concrete tower after prestressing.

4.3.3 Ultimate strength analysis

Abaqus results for the ultimate applied moment at the base are shown in Table 4.5. Here we see that the moment around the z-axis contributed almost entirely to M_u.

TABLE 4.5: Ultimate applied moment for the prestressed concrete tower.

Moment	Value	Unit
M_{ux}	11 490	kN m
M_{uz}	65 684	kN m
M_u (M_{xz})	66 681	kN m

An ultimate section analysis was performed and results for the tower top, base and mid-height are shown in Table 4.6. For all sections strain in the tension reinforcement exceeded the yielding value. This indicates that the tower was under-reinforced, which is ideal for design and economy. For the top section we see that M_r was calculated as marginally less than M_{yT}. However, for the Abaqus analysis this did not lead to failure and was deemed conservative. At the base we see that maximum strain in the original tendon configuration exceeded its value for factored ultimate stress. This indicates ultimate tensile failure of the design. To prevent failure the number of tendons was increased to 29 from base to mid-height. For this configuration maximum strain was kept just under the ultimate limit. Furthermore, M_r was much higher than M_u with a safety factor of 3.08. For the section at mid height we see maximum strain complying with ultimate limits for cracking and crushing. Due to the increased prestressing forces of the adjusted design, compression stress at mid height was also investigated for SLS loads. The maximum resulting stress was 11.5 MPa, which complies with SABS [29] limits.

TABLE 4.6: Significant parameter values for ultimate strength analysis of the pre-stressed concrete tower.

Parameter	Top	Bottom		Middle	Unit
		Original	Adjusted		
Number of tendons	19	19	29	29	
Neutral axis depth	700	622	799	855	mm
Maximum actual tendon strain	0.0124	0.0307	0.0232	0.0150	
Tendon yield strain		0.00776			
Ultimate tendon strain		0.0236			
Force equilibrium check					
Compression	27 272	37 028	52 419	45 223	kN
Tension	27 272	37 028	52 419	45 223	kN
Ultimate resistance moment	58 332	141 758	205 481	135 469	kN m

The adjusted design was analysed in Abaqus and the analysis completed successfully. Flexural stress results in the concrete are shown in Figure 4.10. For tension the maximum values followed two distinct paths as shown in red, both yielding similar results. Tension cracking did not occur by some margin indicating that the tower was conservatively designed as a class 1 SLS structure. However, we see that compression stresses in the concrete were close to its ultimate crushing value. This correlates with serviceability results and show that compression controls for ultimate strength.

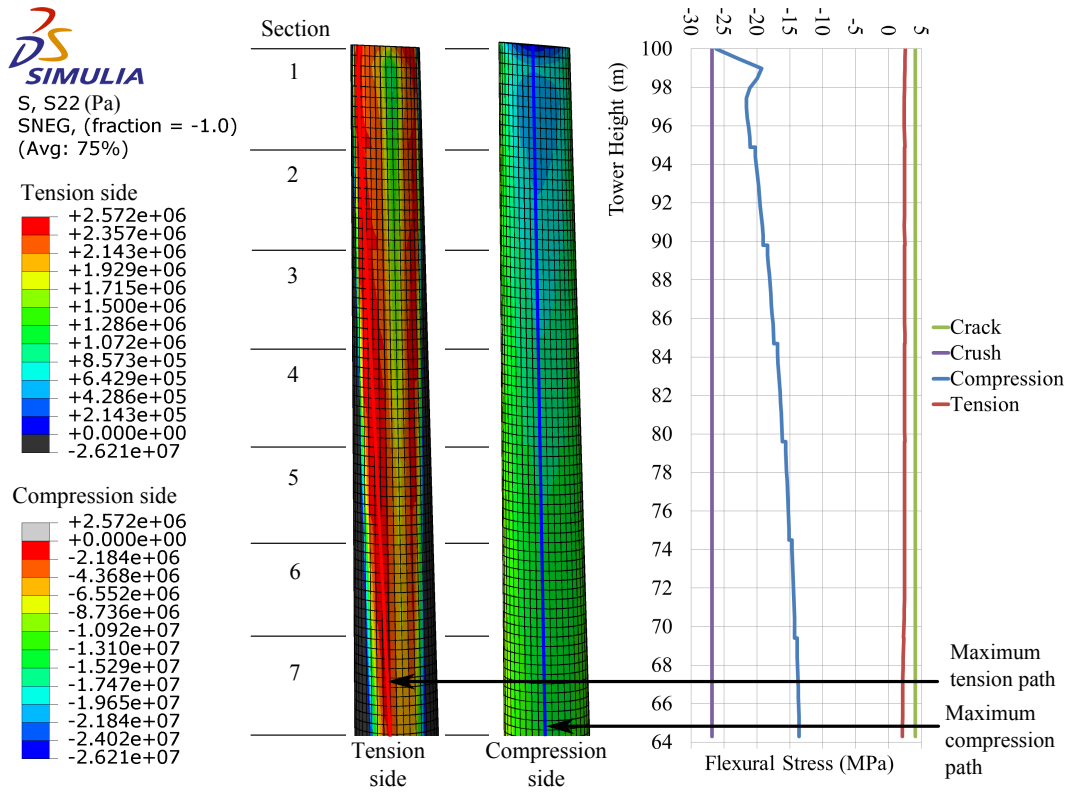

FIGURE 4.10: Flexural stress in the concrete for the ultimate strength analysis of the prestressed tower.

The Abaqus results for maximum ultimate strain of the tension reinforcement was calculated and is shown in Table 4.7. Here we see that the maximum strain in the tension reinforcement was less than the factored yield limit. This indicates that plasticity has not been reached, correlating with and confirming the results in Figure 4.10.

TABLE 4.7: Strain in tension reinforcement for Abaqus ultimate strength analysis of the prestressed concrete tower.

Parameter	Value	Unit
Initial prestressing strain	0.00564	$\mathrm{mm\,mm^{-1}}$
Minimum tendon stress	868.5	MPa
Change in stress	231.6	MPa
Change in strain	0.00119	$\mathrm{mm\,mm^{-1}}$
Maximum strain in tension reinforcement	0.00683	$\mathrm{mm\,mm^{-1}}$

4.3.4 Global buckling analysis

The original geometry and adjusted tendon configuration was verified for global buckling using the Riks analysis. It completed successfully with the LPF reaching unity, as shown in Figure 4.11. Abaqus results for flexural stresses in the concrete are shown in

Figure 4.12. Tendon strains are listed in Table 4.8. Results for both are very similar to those for the ultimate strength analysis. However, maximum compression stress is marginally less by 0.3 % and tension more by 13.3 %.

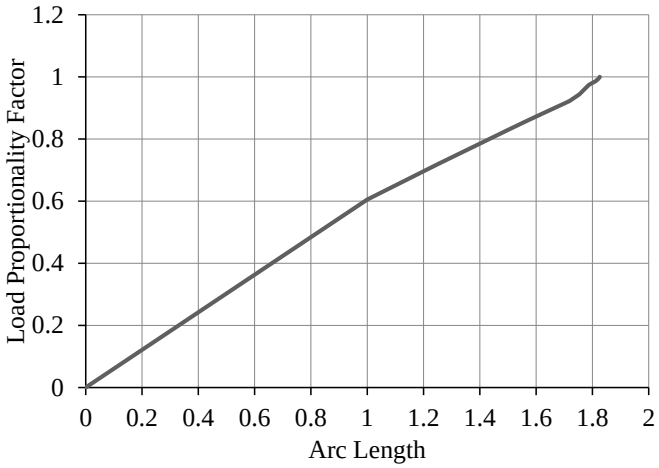

FIGURE 4.11: Increase in LPF for the global buckling analysis of the prestressed concrete tower.

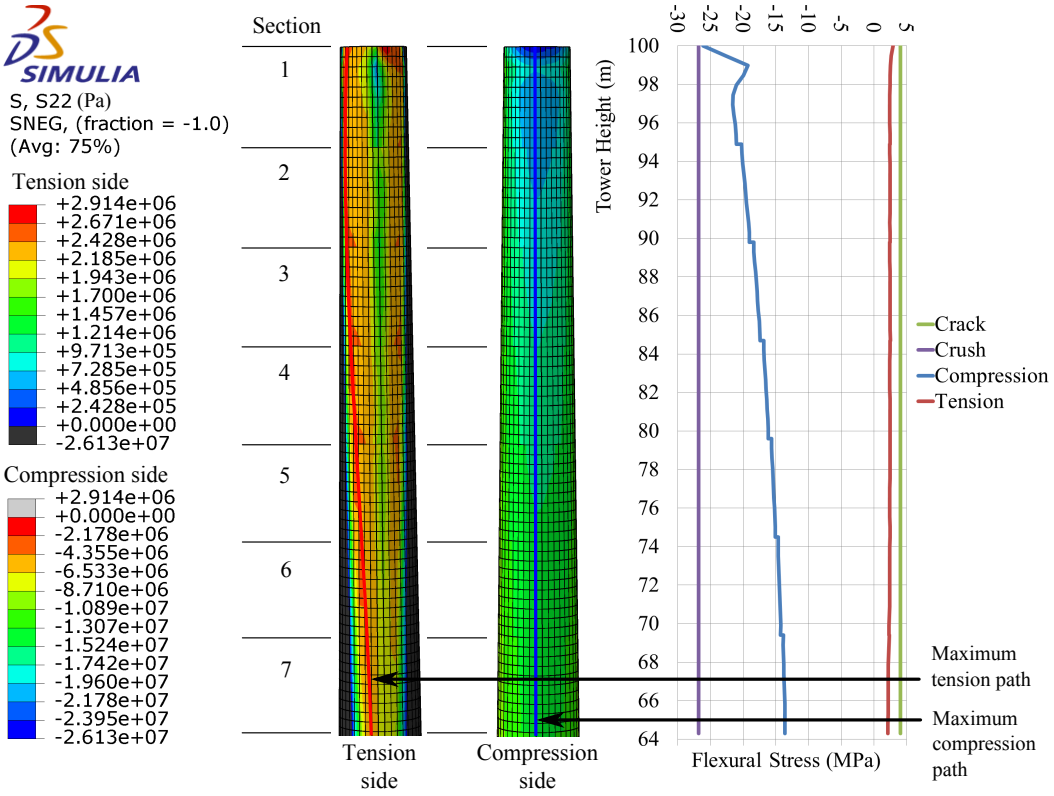

FIGURE 4.12: Flexural stress in concrete for global buckling analysis of the prestressed tower.

TABLE 4.8: Strain in tension reinforcement for Abaqus global buckling analysis of the prestressed concrete tower.

Parameter	Value	Unit
Initial prestressing strain	0.00564	$\mathrm{mm\,mm^{-1}}$
Minimum tendon stress	868.7	MPa
Change in stress	231.3	MPa
Change in strain	0.00119	$\mathrm{mm\,mm^{-1}}$
Maximum strain in tension reinforcement	0.00683	$\mathrm{mm\,mm^{-1}}$

4.3.5 Optimal design and material mass

From the above results we see that the prestressed concrete tower was optimally designed in the following manner: for tension in serviceability and compression in ultimate strength. The volume and mass was calculated for the concrete and reinforcement is shown in Table 4.9. Total material mass of the concrete tower was 605 % more than that of the steel design.

TABLE 4.9: Material volume and mass of the prestressed concrete tower.

Section	Volume ($\mathrm{m^3}$)	Mass (t)
Nominally reinforced concrete	778.1	1867.4
Nominal reinforcement	1.97	15.5
Prestressing reinforcement	4.02	31.5
Total	796.7	1914.5

4.4 Conclusion

The structural soundness of the steel and prestressed concrete towers were successfully tested and proved. For the steel design the geometry was adjusted for each analysis and the most conservative changes were combined for an optimum solution. The geometry of the concrete tower was kept constant, but tension reinforcement was adjusted for optimal tension and compression at serviceability and ultimate strength. Furthermore, material volumes for both towers were determined and compared. The mass and volume of the prestressed concrete tower was found to be considerably larger than that of its steel counterpart.

Chapter 5

Findings for Life-cycle Costing Analysis

5.1 Introduction

This chapter presents the results for the life-cycle cost analysis of the steel and concrete tower solutions. The aim is to convey whether the latter is competitive and more viable in South Africa at a height of 100 m. Results for the cost estimation and sensitivity analysis will be presented according to the relevant life-cycle phases. These are manufacturing, construction, installation, disposal and recycling. Significant parameters shall be varied and implications discussed.

5.2 Manufacture, construction and installation

5.2.1 Estimated costs

Estimated costs for manufacturing, construction and installation (MCI) of the precast, cast-in-place and tubular steel towers are listed in Table 5.1 (see subsection 3.7.1). These are considered to be the most likely values for South African conditions. Main cost items and total cost shall be discussed and compared for the tower alternatives. Furthermore, the latter shall be compared with values for other local wind projects.

TABLE 5.1: Estimated manufacturing, construction and installation costs for towers.

	August 2014 costs in ZAR per tower		
Cost item	Precast concrete	Cast-in-place concrete	Steel
Mobilization and site development	4 636 677	1 194 071	3 372 397
Foundation construction	3 818 272	3 817 471	2 628 301
Tower fabrication	5 158 360	411 959	8 687 213
Tower field erection	3 737 591	8 671 401	907 466
Erect nacelle and rotor	74 304	74 304	72 806
Finishing and clean-up	565 204	565 204	243 240
Contractor mark-up	30%	30%	30%
Total MCI cost	23 387 530	19 154 733	20 698 265
% difference	113 %	92.5 %	100 %

The first item covers setup of temporary offices and access roads, and mobilization of construction equipment. Its most significant cost parameters are for mobilization and rental of big cranes. Crane cost for the cast-in-place design is low at 3.8 % of MCI. This accounts for rotor and nacelle lifting, because the tower is self-erecting. However, cranage for the precast design is the most expensive at 17.8 %, because an additional amount of heavy arc segments (93 in total) are lifted for tower erection. Further lifting of six heavy sections for the steel tower increases crane costs to 14 %.

Foundation construction costs are mostly influenced by concrete and steel reinforcement. Costs for these materials are closely related to the foundation size. For the precast and cast-in-place towers these are the same and contribute 13.7 % and 16.72 % to MCI respectively. The cost for the steel tower is lower at 9.9 % due to a smaller foundation.

Fabrication is the most influential cost item for the precast and steel towers. Its share of MCI costs is 20.3 % and 42 % respectively. The main costs for the precast solution are concrete supply and placing at 5.71 %, and shop overhead and profit at 7.2 %. Contributors for the steel tower are steel supply, rolling and welding of segments, and welding for main sections at 22 %, 9.4 % and 3.3 % respectively. Combined, these parameters contribute just over a third of total MCI cost. The fabrication cost for the cast-in-place tower is for the steel connection ring between the concrete and nacelle at the top of the tower. This is also included for the precast design.

Field erection costs contribute significant amounts for the precast and cast-in-place towers at 16 % and 45.3 % of MCI. Here we see that this item is by far the most influential for the latter. It is expected, because tower fabrication is performed on site. For the

steel tower the cost is much lower at 4.4 % of MCI, because erection is simple and mainly consists of tower segment lifting and field welding. Furthermore, crane cost for lifting was already considered earlier on and should increase costs considerably for both the steel and precast towers if considered here. Prestressing reinforcement is also a significant expenditure for the precast and cast-in-place designs at 11.4 % and 8.75 % respectively. This is the most influential erection cost for the precast design. For the latter other costs are for direct labour and nominally reinforced concrete at 19.45 % and 9.19 %. Field welding at 4.24 % is the most influential for the steel tower.

Erection costs for the nacelle and rotor is practically equal for all three tower designs. For finishing and clean up the main cost difference between concrete and steel solutions are due to the installation of ladders and platforms. These are fixed onto the steel tower during fabrication.

Total estimated MCI cost for the designs suggest that the concrete cast-in-place solution is the most viable alternative. However, it is only 7.5 % cheaper than the steel tower. The precast solution is the least viable and 13 % more expensive. Margins of cost between the towers are low enough for all to still be considered competitive alternatives.

5.2.2 Comparison with actual costs

The approximated MCI costs for large wind projects in South Africa are listed in Table 5.2. Here we see that estimated costs for this study fall within the range presented in the list. Furthermore, the average scaled MCI cost is only 18 % higher than that of the towers for this study. Also, Gouda has the most similar specifications to the reference project and it differs by less than 5 %. We can conclude that estimated MCI costs for this study are realistic, because it relates strongly to values for real local projects.

TABLE 5.2: Manufacturing, construction and installation costs for local wind farms.

Project name	Project cost (ZAR)	Capacity (MW) Total	Capacity (MW) Per turbine	Scaled MCI cost (ZAR)	Source
Amakhala Emoyeni	3 700 000 000	134.4	2.4	31 383 929	[16][88][89]
Cookhouse	2 500 000 000	138.6	2.1	20 562 771	[88][90]
Dorper	2 050 000 000	100	2.5	23 370 000	[88][91]
Gouda	2 670 000 000	135.5	3.0	22 056 522	[88][92]
Jeffreys Bay	2 267 732 000	138	2.3	18 733 438	[93]
Red Cap Gibson Bay	2 250 000 000	111	3.0	23 108 108	[94]
Red Cap Kouga	1 700 000 000	80	2.5	24 225 000	[88][95]
Tsitsikamma	2 900 000 000	93	3.0	35 548 387	[88][96]
Average	2 578 773 200	116.3	2.6	24 873 519	

5.2.3 Foundation cost variation

Figure 5.1 shows the MCI cost change with variation of foundation cost (see subsubsection 3.7.3.1). Shaded areas represent the influence of the latter on MCI costs for the relevant parameters. We see that a steel tower foundation cost increase of 40 % and more, causes its MCI costs to fall within the probable range of the precast design. Therefore it stays competitive for a larger foundation. Compared to the cast-in-place tower it is certainly more expensive. However, for a cost decrease to −10 % and lower it becomes competitive with the cast-in-place design. It should be noted that there is no point at which the steel tower is the most viable alternative. Furthermore, probable ranges of the concrete towers do not overlap. This means that foundation cost uncertainty has no effect on the fact that the precast tower is more expensive than its concrete counterpart.

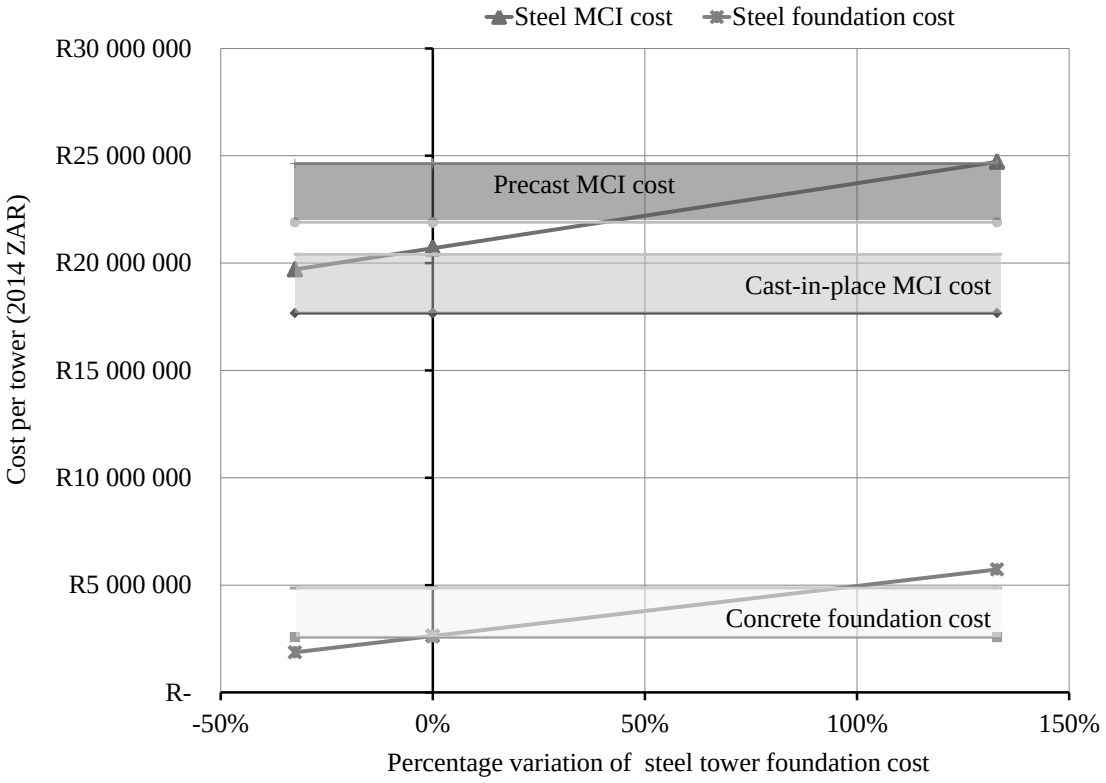

FIGURE 5.1: Influence of foundation cost variation on MCI cost.

5.2.4 Material cost variation

Figure 5.2 shows the influence of material cost on total MCI per tower (see subsubsection 3.7.3.2). Shaded areas represent the effect of concrete cost change and we see that it is very small to negligible. However, steel cost variation has a significant impact on all towers. Over the probable range MCI costs for the precast, cast-in-place and steel towers vary by 26 %, 11 % and 37 % respectively. As expected, it varies the most for the steel design. The main difference between the two concrete solutions are due to prestressing reinforcement. The precast design employs additional horizontal bars for joining the arc segments. Furthermore, this design remains the most expensive over the entire probable range. If steel costs drop lower than −36 % the steel tower is the most viable, becoming more competitive than the cast-in-place solution.

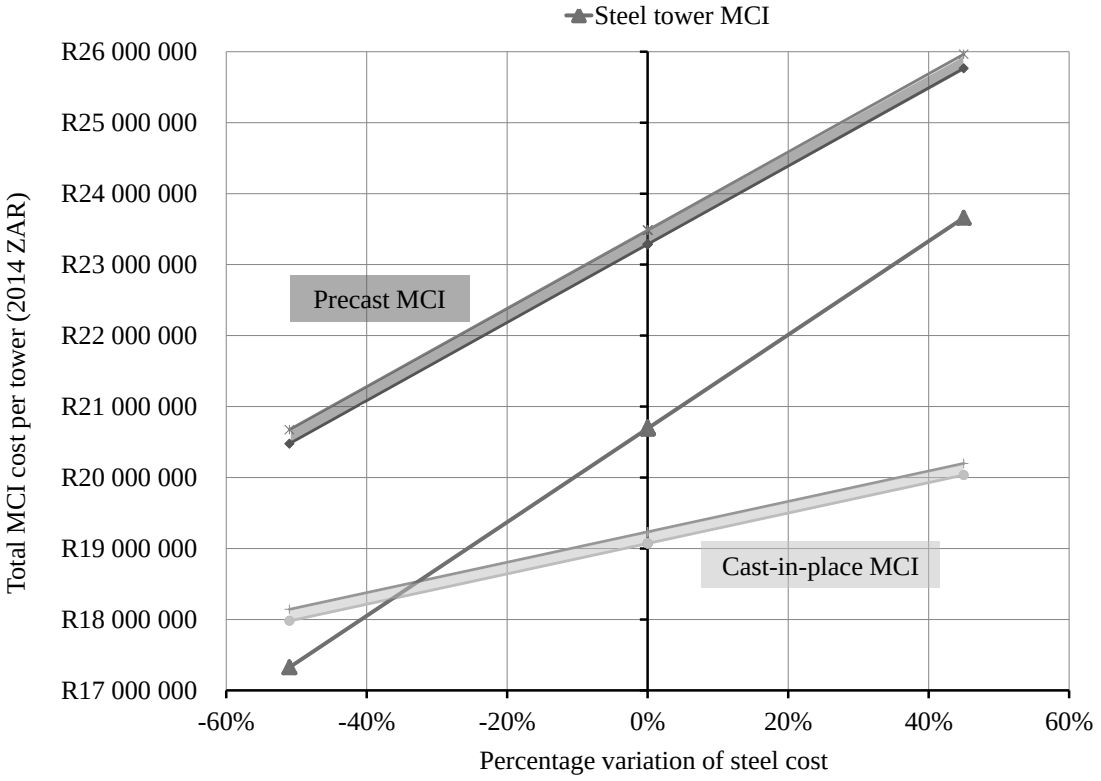

FIGURE 5.2: Influence of material price variation on MCI cost.

5.2.5 Fabrication and field erection cost variation

Figure 5.3 shows the influence of fabrication and field erection costs on MCI values (see subsubsection 3.7.3.3). The shaded regions represent the probable cost range for fabrication. We can see it has a significant influence on MCI costs of the steel tower with a general difference of 16 % between upper and lower limits. However, for the precast and cast-in-place solutions it is small and negligible respectively. It should be noted that if erection cost remains unchanged and steel fabrication cost is low, the steel tower is the most viable by a small margin. As expected, cast-in-place MCI values are very sensitive to change in erection cost. Due to the volatility of these costs, the effect is magnified. Cast-in-place costs vary by 97 % over the probable range. This poses an apparent financial risk, because erection cost is very dependent on site conditions. It is well known that during construction, site conditions are uncontrollable and often change. For erection cost lower than −6 % the cast-in-place tower is certainly the most viable. However, above 73 % the steel tower becomes a better alternative. For a cost increase above 104 %, the cast-in-place tower is the most expensive.

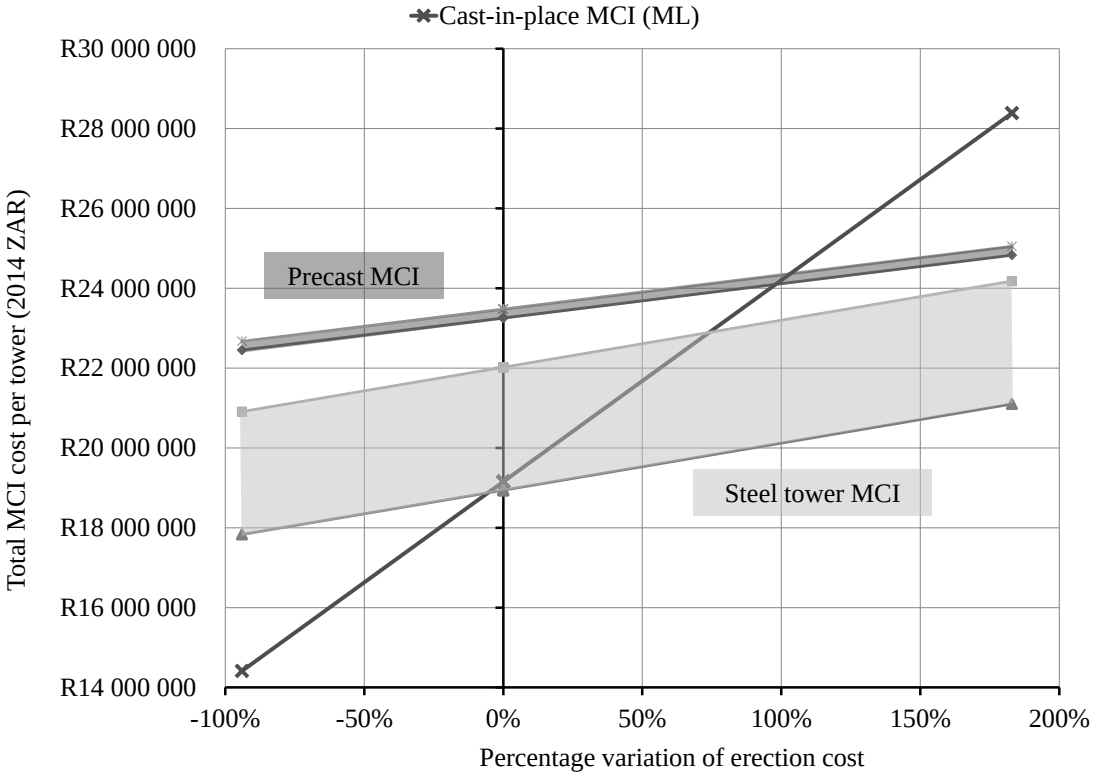

FIGURE 5.3: Influence of fabrication and field erection cost variation on MCI cost.

5.2.6 Transport cost variation

Figure 5.4 shows the influence of transport on MCI costs for the towers (see subsubsection 3.7.3.4). The shaded area represents the probable range for the transport cost of the precast concrete segments from the fabrication plant to the site. Here we see it has a negligible effect on MCI costs at less than 1 %. Furthermore, transport from the steel plant also has very little impact at less than 2 % for all three towers. We can conclude that transport from the fabrication plant has an almost negligible impact on MCI costs for local conditions. However, this is not a fair representation of total transport costs. These costs were not considered for items such as raw materials, equipment and labour. Variation thereof should have a significant impact, but transport to site are provided for and costs are included in price quotes.

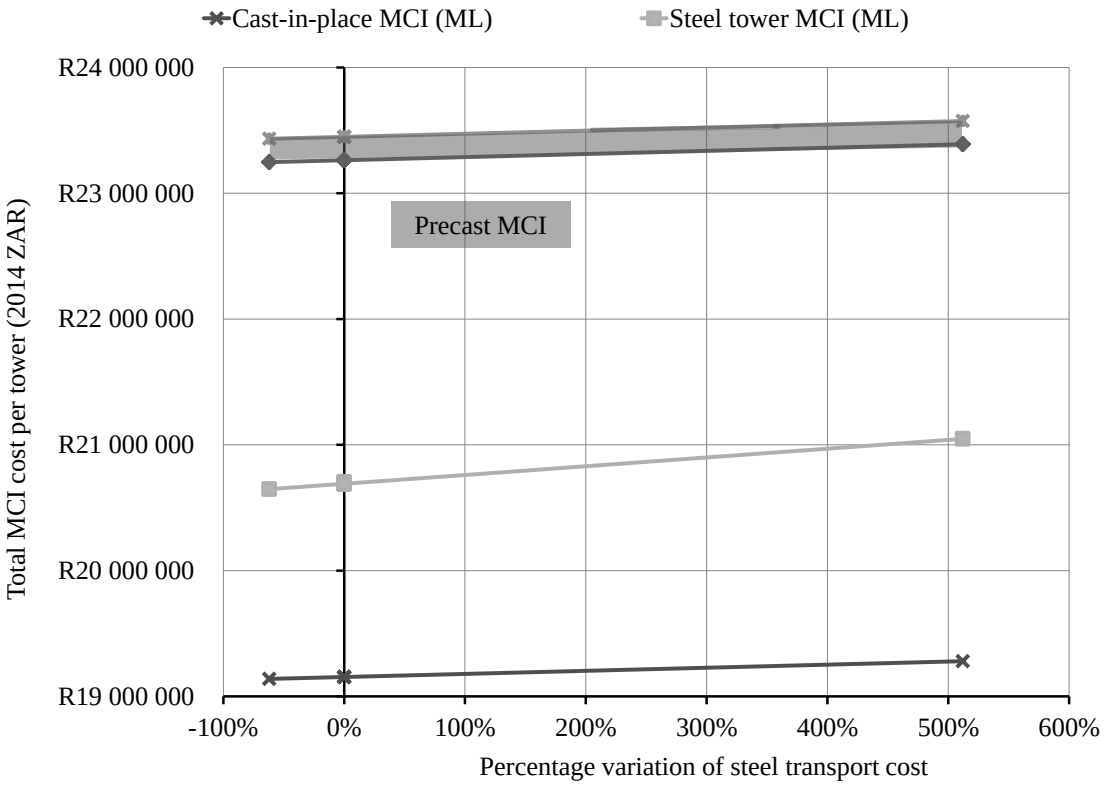

FIGURE 5.4: Influence of transport on MCI cost.

5.2.7 Labour cost variation

Figure 5.5 shows the influence of labour cost on the total MCI cost (see subsubsection 3.7.3.5). The shaded regions represent the probable range of labour cost for the precast and steel towers respectively. We see that for these designs labour cost variation has a negligible effect on MCI costs at less than 1 %. However for the cast-in-place solution it induces a small change of 4 %. It is expected, because this design is more labour intensive than the others. Furthermore, the overall low influence of labour cost can be attributed to relatively low wages for local workers.

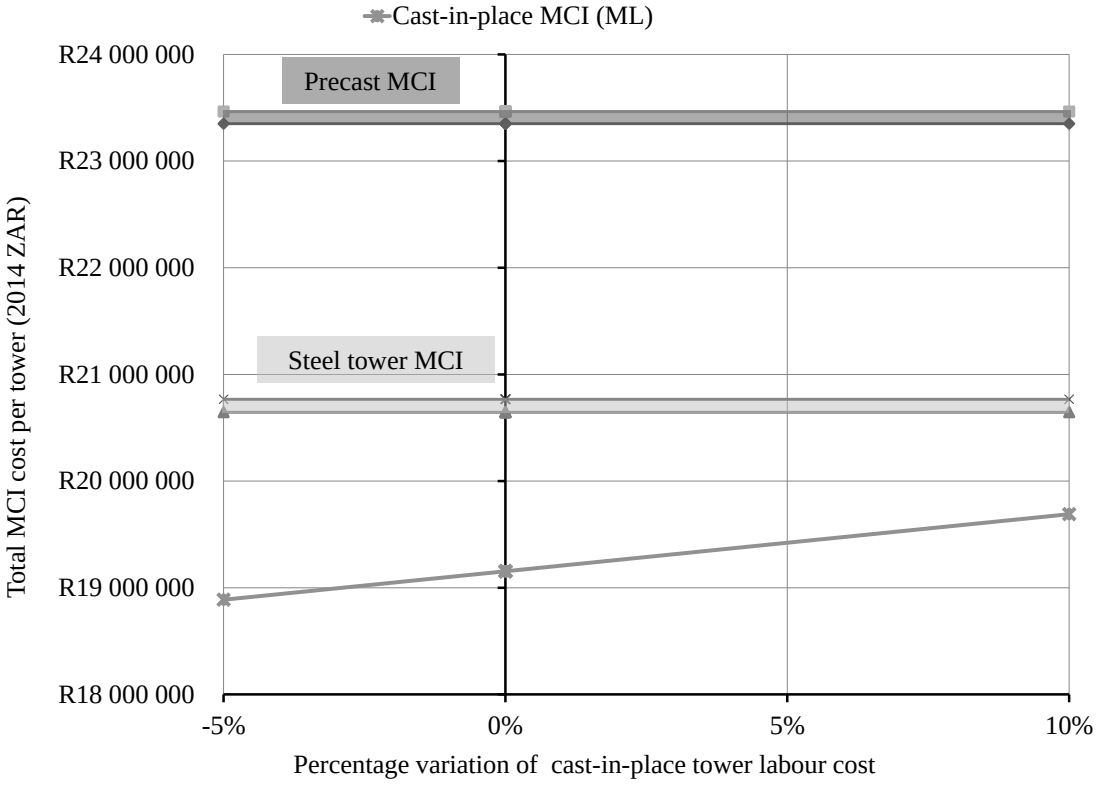

FIGURE 5.5: Influence of variation of labour cost on MCI cost.

5.3 Disposal and recycling

Figure 5.6 shows the salvage values for the concrete and steel tower solutions (see subsubsection 3.7.3.6). Here we see that the income for the steel design is considerably higher. The most likely salvage total for the concrete tower is only 29 % of the steel and at best approximately 50 %. It should also be noted that reinforcing steel contributes a most likely 59 % to total salvage for the concrete solution.

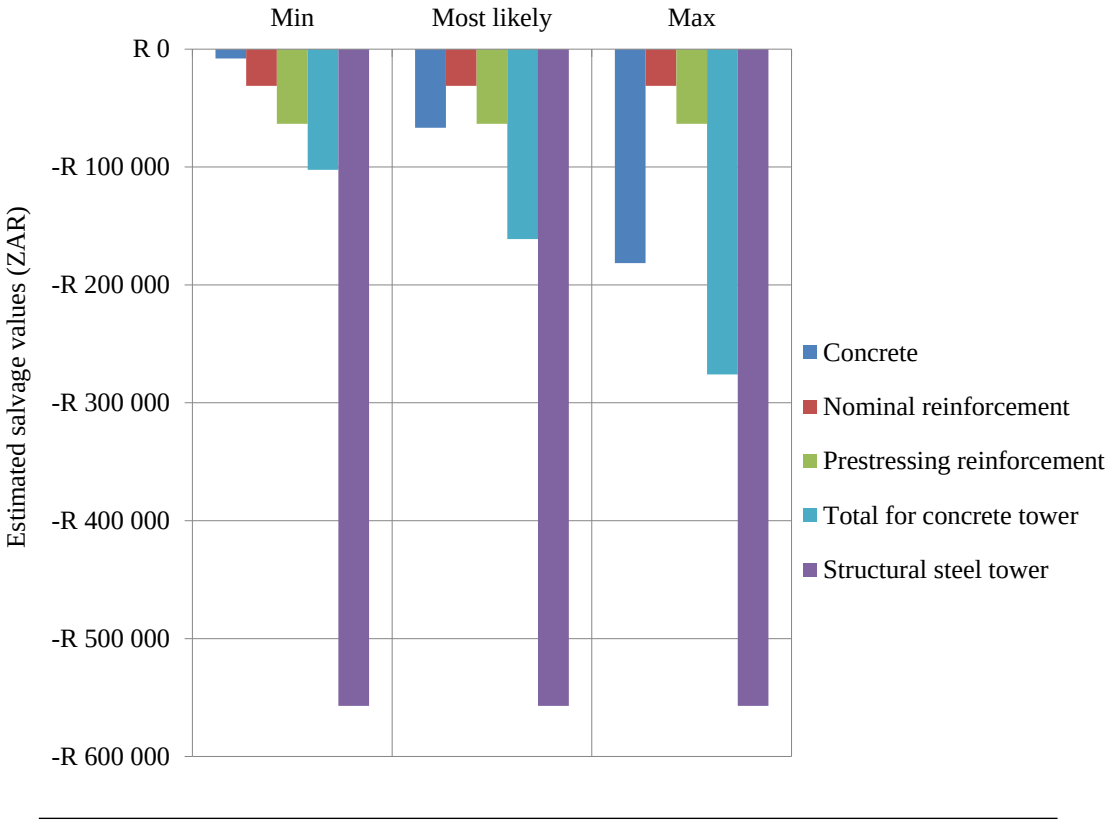

FIGURE 5.6: Estimated salvage values for the concrete and steel towers.

Figure 5.7 shows the transport costs for disposal of recyclable materials for the concrete and steel towers. Here we see that these costs are much higher for the former. This is expected, because the volume and mass of materials utilized for this design is much more in magnitude than that for the steel solution. Concrete is the main cost contributor at 98 %. Furthermore, the distance between the construction and disposal site has a significant effect on the transport cost. The increase from the minimum to the maximum estimates are 310 %.

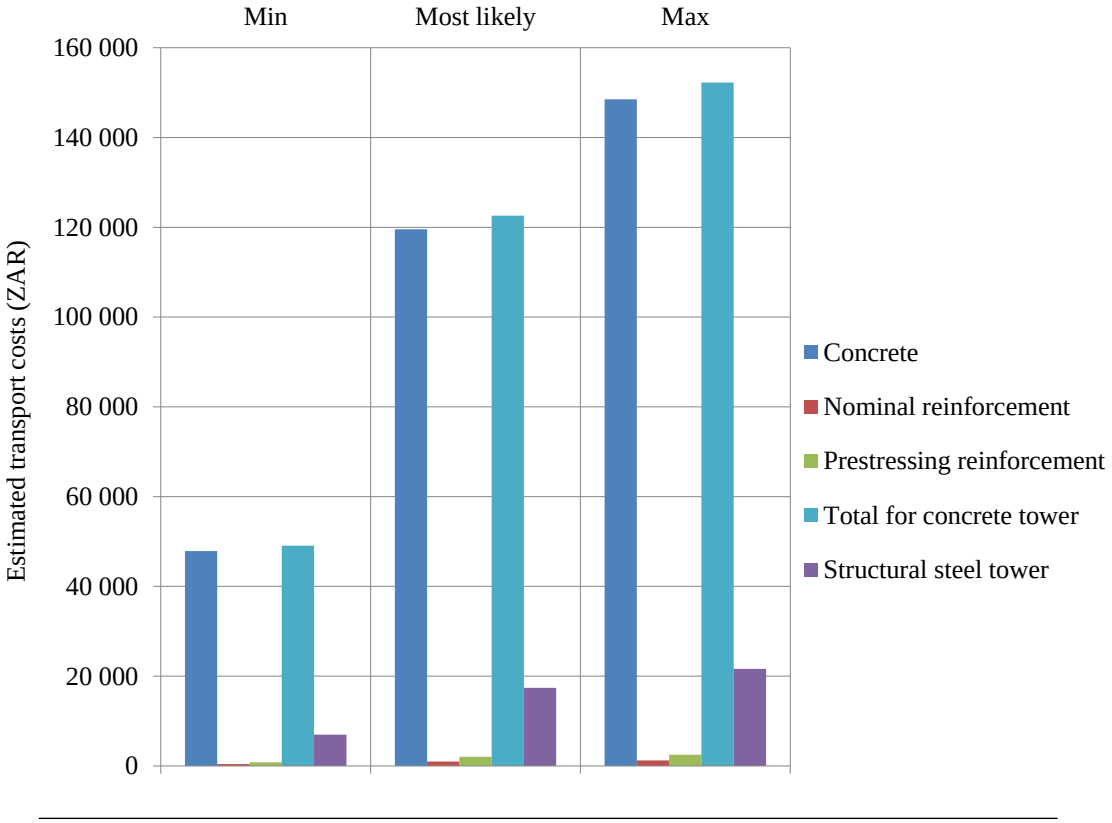

FIGURE 5.7: Estimated transport costs for disposal of recyclable materials for the concrete and steel towers.

Figure 5.8 shows the total disposal and recycling costs for the concrete and steel towers. We see that results are very favourable for the latter. All the estimates suggest a net income of over R500 000. For the concrete design the most favourable estimate (minimum cost) is an income at only 41 % of the steel equivalent. Furthermore, it would at least cost R49 875 to dispose and recycle the concrete tower and there would most likely be a small gain of R38 526. It should be noted that these values are negligibly small compared to the MCI costs of the entire tower. We can still conclude that for disposal and recycling the steel solution would financially be a more favourable alternative.

However, to fairly assess end-of-life costs, dismantling of the towers and sorting of the waste should also be accounted for. One can assume that, compared to the steel design, the addition of these should pose more unfavourable for the concrete solution. Furthermore, the net income for the steel tower is at most only 2.7 % of total MCI costs. It would then be fair to dispute whether it contributes a significant gain.

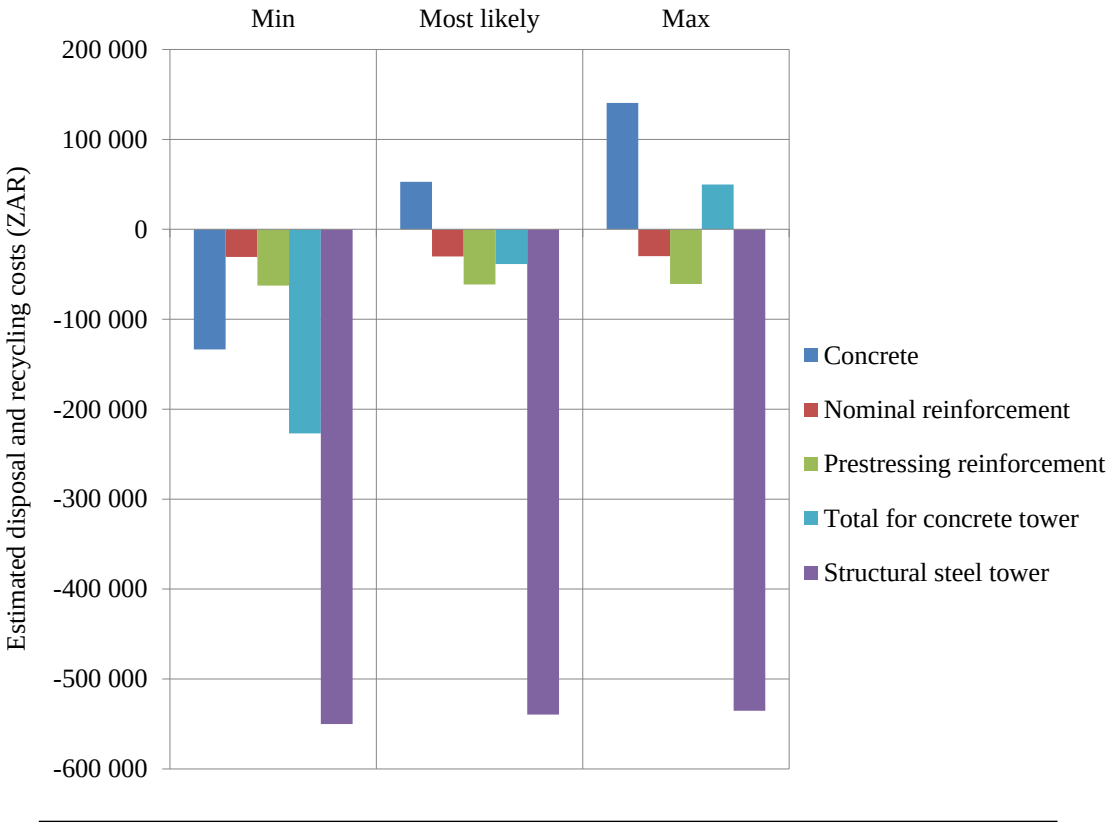

FIGURE 5.8: Estimated disposal and recycling costs for the concrete and steel towers.

5.4 Conclusion

This chapter presented the results for the life-cycle cost analysis of the steel and concrete solutions. The accuracy of estimated manufacture, construction and installation (MCI) costs were proven through comparison with real projects in South Africa. Furthermore, it suggested that the two concrete designs were competitive alternatives to the steel solution and the cast-in-place tower the most viable. The sensitivity analysis also showed the same general trend. However, the steel tower was the most viable if local steel prices were low or erection costs high. This was never the case for the precast tower. Transport and labour cost did not have a significant impact on MCI values and the steel tower was still competitive for larger foundations. Results for disposal and recycling costs were much more favourable for the steel tower, producing a net income for all estimates.

Chapter 6

Conclusion

6.1 Summary of findings

Total manufacture, construction and installation (MCI) costs for the precast, cast-in-place and steel towers were estimated to be R23 387 530, R19 154 733 and R20 698 265. These estimates fell within the range of values that were approximated for real local wind farms and the average for the farms was only 18 % higher. Also, Gouda had the most similar specifications to the reference project and it differed by less than 5 %.

A steel tower foundation cost increase of 40 % to its upper probable limit, caused its MCI costs to fall within the probable range of the precast design. However, for this increase it was certainly more expensive than the cast-in-place tower. For a decrease between −10 % and the lower limit the steel tower cost fell within the range of the cast-in-place design. It should be noted that there was no point at which the steel or precast towers were the most affordable.

Concrete cost variation was found to be very small for the concrete solutions and negligible for the steel. However, steel cost variation had a significant impact on all three designs. MCI costs for the precast, cast-in-place and steel towers varied by 26 %, 11 % and 37 % over the probable range. The main difference between the concrete solutions were for prestressing reinforcement. For steel costs lower than −36 % the steel tower was the most viable, becoming more competitive than the cast-in-place solution. The precast design remained the most expensive over the entire range.

Fabrication enjoyed a significant share of MCI costs for the precast and steel towers at 20.3 % and 42 % respectively. Its variation had a significant influence on MCI costs of the steel design with a general difference of 16 %. However, for the precast and cast-in-place solutions it had a negligible impact. Field erection costs contributed considerably to MCI costs of the cast-in-place tower at 45.3 %. These MCI values were also very sensitive to change in erection cost. Due to the volatility of these costs the effect was magnified and tower costs varied by 97 % over the probable range. For erection costs lower than −6 % the cast-in-place tower was certainly the most viable. However, above 73 % the steel tower was more affordable. For a further increase above 104 % the cast-in-place tower became the most expensive, surpassing its precast alternative.

In general, transport and labour cost had little influence on tower MCI values. Transport sensitivity for both precast segments and steel was negligible at less than 2 % for all three the towers. Labour cost variation had a negligible effect on the precast and steel towers at less than 1 %. However for the cast-in-place solution it induced a slight change of 4 %.

Results for total disposal and recycling costs were very favourable for the steel tower. All the estimates suggested a net income of over R500 000. For the concrete design the most favourable estimate was an income at only 41 % of the steel equivalent. Furthermore, it would at least cost R49 875 to dispose and recycle the concrete tower and there would most likely be a small gain of R38 526. However, these values were negligibly small compared to the total MCI costs of the respective towers. Furthermore, the net income for the steel tower was at most only 2.7 % of total MCI costs.

6.2 Main conclusions

We can conclude that estimated MCI costs for this study were realistic, because it related strongly to values for real local projects. Cost margins between tower designs were low enough for all three to still be considered competitive alternatives. Therefore prestressed concrete wind turbine towers are viable local alternatives to steel at 100 m heights.

The cast-in-place concrete design was estimated to be the most affordable solution of the three. This was confirmed by the general trends in the sensitivity analysis. It is not an unexpected result, because the in-situ solution suits the South African context very well. As we know local construction labour requires low wages and mostly have low

skill levels. This design needs the least expertise of the three and is labour intensive, enforcing job creation. However, its high sensitivity to variation in erection cost causes it to be very dependent on site conditions. During construction these conditions are uncontrollable and often change. Therefore there is a higher financial risk in using this design. Furthermore, the steel tower was the most viable for low steel prices and high erection costs. For a larger foundation size it still remained a competitive alternative to the concrete towers. Overall the precast design was the most expensive, with the exception for high erection costs.

We can conclude that transport from the fabrication plant has a negligible influence on MCI costs for local conditions. However, this is not a fair representation of total transport costs. These costs were not considered for items such as raw materials, equipment and labour. Variation thereof should have a significant impact, but transport to site are provided for and costs are included in price quotes. The overall low influence of labour cost can be attributed to low wages for local workers. Furthermore, the higher impact for the cast-in-place tower is expected, because this design is more labour intensive.

For disposal and recycling the steel solution was a much more favourable alternative to the concrete design. However, to fairly assess end-of-life costs, dismantling of the towers and sorting of the waste should also be accounted for. One can assume that, compared to the steel design, the addition of these should pose even more unfavourable for the concrete solution. It is also fair to dispute whether salvage income contributes a significant gain when compared to overall cost.

6.3 Recommendations for future research

With the doubts in the industry about the performance of the steel monopole design at higher heights, the steel lattice tower has re-emerged as a viable alternative. Structural performance and costing of this design should be investigated for local conditions.

Further cost analysis should be performed for life-cycle phases that were not covered in this study. Research results for all the phases should be combined in a final study to perform a complete comparative life-cycle costing analysis. The use of a material price database such as Merkel's [76] is recommended for future research involving such studies. However, a more specialized product should be acquired. As a part of end

of life costs local reuse and recycling strategies should be developed for wind turbine towers. Furthermore, research should be conducted for the development of high strength concrete for local wind turbine towers using recycled concrete aggregates [97].

Comprehensive and in-depth structural loading, modelling and analysis should be performed for steel monopole and lattice, and prestressed concrete towers of 100 m in height for local conditions. A separate study should be done for each tower type including fatigue, dynamic, foundation and connection design. Resulting dimensions, masses and volumes should be used to aid the above cost studies.

South Africa has a vast coastal region with favourable wind conditions, especially in the Eastern Cape and KwaZulu Natal. Therefore the viability of local offshore wind turbine solutions should be investigated [5]. Furthermore, the development of small off-grid wind turbine tower technology should be researched for rural areas in Southern Africa.

Bibliography

[1] E. Martnez, F. Sanz, S. Pellegrini, E. Jimnez, and J. Blanco. Life cycle assessment of a multi-megawatt wind turbine. *Renewable Energy*, 34:667 – 673, 2009. ISSN 0960-1481.

[2] Manfred Lenzen and Jesper Munksgaard. Energy and co¡ sub¿ 2¡/sub¿ life-cycle analyses of wind turbinesreview and applications. *Renewable energy*, 26(3):339–362, 2002.

[3] S Teske. The advanced energy revolution: A sustainable energy outlook for south africa. Technical report, European Renewable Energy Council and Greenpeace, 2011.

[4] S Gsanger and JD Pitteloud. World wind energy report 2012. Technical report, World Wind Energy Association, 2013.

[5] D Holm, D Banks, J Schäffler, R Worthington, and Y Afrane-Okese. Renewable energy briefing paper. *Available at: reeep-sa. org/docs/doc_download/38-renewable-energy-briefing-paper (Accessed: 16 September 2009)*, 2008.

[6] Anton Eberhard. South africas renewable energy ipp procurement program: Success factors and lessons. May 2014.

[7] Robert Thresher, Michael Robinson, and Paul Veers. To capture the wind. *Power and Energy Magazine, IEEE*, 5(6):34–46, 2007.

[8] Det Norske Veritas. *Guidelines for design of wind turbines*. DNV, 2009.

[9] Wei Tong. *Wind power generation and wind turbine design*. WIT press, 2010.

[10] María Isabel Blanco. The economics of wind energy. *Renewable and Sustainable Energy Reviews*, 13(6):1372–1382, 2009.

[11] C Petcu and A Marí-Bernat. Concept and design of tall reinforced and prestressed wind towers [tesina]. *Barcelona: Universidad Politécnica de Cataluña*, 2007.

[12] Reinhard Harte and Gideon PAG Van Zijl. Structural stability of concrete wind turbines and solar chimney towers exposed to dynamic wind action. *Journal of Wind engineering and industrial aerodynamics*, 95(9):1079–1096, 2007.

[13] Erich Hau and Horst Von Renouard. *Wind turbines: fundamentals, technologies, application, economics*. Springer, 2013.

[14] Tony Burton, Nick Jenkins, David Sharpe, and Ervin Bossanyi. *Wind energy handbook*. John Wiley & Sons, 2011.

[15] A Quilligan, A O'CONNOR, and V Pakrashi. Fragility analysis of steel and concrete wind turbine towers. *Engineering structures*, 36:270–282, 2012.

[16] Amakhala emoyeni wind farm. Online, 2014. URL http://www.windlab.com/projects/amakhala.

[17] Industry growth. Online, December 2014. URL http://www.sawea.org.za/.

[18] Sandra Eriksson, Hans Bernhoff, and Mats Leijon. Evaluation of different turbine concepts for wind power. *Renewable and Sustainable Energy Reviews*, 12(5):1419–1434, 2008.

[19] Andrew Tryon. Wind turbine and snow at gordonbush wind farm. This work is licensed under the Creative Commons Attribution-Share Alike 2.0 Generic Licence, February 2014. URL http://www.geograph.org.uk/photo/3848718. Image Copyright Andrew Tryon. To view a copy of this licence, visit http://creativecommons.org/licenses/by-sa/2.0/ or send a letter to Creative Commons, 171 Second Street, Suite 300, San Francisco, California, 94105, USA.

[20] Peter J Schubel and Richard J Crossley. Wind turbine blade design. *Energies*, 5 (9):3425–3449, 2012.

[21] IRENA Secretariat. Renewable energy technologies: Cost analysis series. Technical report, The International Renewable Energy Agency, June 2012. URL www.irena.org/Publications.

[22] The inside of a wind turbine. Online, September 2014. URL http://energy.gov/eere/wind/inside-wind-turbine-0. The EERE states that materials on its web sites are public domain: (URL) http://www1.eere.energy.gov/webpolicies/.

[23] PH Halberstadt, BJ Magee, and AH Tricklebank. Concrete towers for onshore and offshore wind farms. *The Concrete Centre*, 2007.

[24] Michael W LaNier. Lwst phase i project conceptual design study: Evaluation of design and construction approaches for economical hybrid steel/concrete wind turbine towers; june 28, 2002–july 31, 2004. Technical report, National Renewable Energy Lab., Golden, CO (US), 2005.

[25] AN Singh. Concrete construction for wind energy towers. *The Indian Concrete Journal, August*, pages 43–49, 2007.

[26] V Marshall and JM Robberts. *Prestressed concrete design and practice*. Concrete Society of Southern Africa, 1 edition, 2000.

[27] EG Nawy. *Prestressed concrete: a fundamental approach*. Pearson Prentice Hall, 5 edition, 2010.

[28] Thomas James Lewin. *An investigation of design alternatives for 328-ft (100-m) tall wind turbine towers*. Iowa State University, 2010.

[29] Sabs 0100-1*: The structural use of concrete: Part 1: Design.

[30] S Engstrom, T Lyrner, M Hassanzadeh, T Stalin, and J Johansson. Tall towers for large wind turbines. Technical report, Elforsk, 2010.

[31] Jairo A Paredes, Alex H Barbat, and Sergio Oller. A compression–tension concrete damage model, applied to a wind turbine reinforced concrete tower. *Engineering Structures*, 33(12):3559–3569, 2011.

[32] C Von der Haar. Design aspects of concrete towers for wind turbines. September 2014.

[33] J Jimeno. Concrete towers for multi-megawatt turbines.

[34] Henrik Svensson. *Design of foundations for wind turbines*. PhD thesis, Masters Dissertation, Division of Structural Mechanics, Department of Construction Sciences, Lund University, Sweden, 2010.

[35] International Electrotechnical Committee et al. Iec 61400-1: Wind turbines part 1: Design requirements. *International Electrotechnical Commission*, 2005.

[36] WASA. About wind atlas for south africa. Online, November 2013. URL http://www.wasaproject.info/about_wind_energy.html.

[37] Sans 10160-3:2010:basis of structural design and actions for buildings and industrial structures:part 3: Wind actions, 2010.

[38] Welcome to the wasa download site. Online, September 2014. URL http://wasadata.csir.co.za/wasa1/WASAData.

[39] W Winkler, M Strack, and A Westerhellweg. Scaling and evaluation of wind data and wind farm energy yields. *Hämtat*, 2010:18–01, 2010.

[40] AC Kruger, JV Retief, and AM Goliger. Strong winds in south africa: Part 2 mapping of updated statistics. *Journal of the South African Institution of Civil Engineering*, 55(2):46–58, 2013.

[41] Germanischer Lloyd. Regulations for the certification of offshore wind energy conversion systems. *Germanische Lloyd, Hamburg*, 1995.

[42] Sans 10162-1:2011: The structural use of steel: Part 1: Limit-states design of hot-rolled steelwork, 2011.

[43] Takaya Kobayashi and Yasuko Mihara. Postbuckling analyses of elastic cylindrical shells under axial compression. In *ASME 2009 Pressure Vessels and Piping Conference*, pages 745–754. American Society of Mechanical Engineers, 2009.

[44] David Bushnell. Buckling of shells-pitfall for designers. *AIAA Journal*, 19:1183–1226, 1981.

[45] John Corbett Nicholson. Design of wind turbine tower and foundation systems: optimization approach. 2011.

[46] Sans 10160-1:2010:basis of structural design and actions for buildings and industrial structures:part 1: Basis of structural design, 2010.

[47] FK Kong and RH Evans. *Reinforced and Prestressed Concrete*. Spon Press, 3 edition, 2001.

[48] *Abaqus Analysis User's Manual*. Dassault Systems, October 2012. Version 6.12.

[49] L Blank and A Tarquin. *Basics of Engineering Economy*. McGraw-Hill, 2008.

[50] Fulvio Ardente, Marco Beccali, Maurizio Cellura, and Valerio Lo Brano. Energy performances and life cycle assessment of an italian wind farm. *Renewable and Sustainable Energy Reviews*, 12(1):200–217, 2008.

[51] Lee Jay Fingersh, M Maureen Hand, and Alan S Laxson. *Wind turbine design cost and scaling model*. National Renewable Energy Laboratory Golden, CO, 2006.

[52] Michael Frank Schmidt. The economic optimization of wind turbine design. 2007.

[53] S Tegen, E Lantz, M Hand, B Maples, A Smith, and P Schwabe. 2011 cost of wind energy review. Technical report, National Renewable Energy Laboratory, 2013.

[54] Kevin Smith. Windpact turbine design scaling studies technical area 2: Turbine, rotor, and blade logistics. *National Renewable Energy Laboratory, NREL/SR-500-29439*, 2001.

[55] SK Fuller and SR Petersen. Life-cycle costing manual for the federal energy management program, 1995 edition. *NIST handbook*, 135, 1996.

[56] The Windpower. Turbines list. Online, 2013. URL http://www.thewindpower.net/manuturb_turbines_en.php?tri=2.

[57] GR Collecutt and RGJ Flay. The economic optimisation of horizontal axis wind turbine design. *Journal of wind engineering and industrial aerodynamics*, 61(1): 87–97, 1996.

[58] Laerd Statistics. Measures of spread. Online, October 2013. URL https://statistics.laerd.com/statistical-guides/measures-of-spread-range-quartiles.php.

[59] David P Doane and Lori E Seward. Measuring skewness: a forgotten statistic. *Journal of Statistics Education*, 19(2):1–18, 2011.

[60] Philippe Decq and Andres Espejo. Dassieklip wind energy facility in south africa. Validation report, Det Norske Veritas AS, 2012.

[61] Sinovel Wind Group. Sl 3000 series wind turbines. Online, 2013. URL www.sinovel.com.

[62] Wind turbine swt-3.0-113 / swt-3.2-113. Online, October 2014. URL http://www.energy.siemens.com/hq/en/renewable-energy/wind-power/platforms/d3-platform/wind-turbine-swt-3-2-113.htm#content=Technical%20Specification.

[63] Arcelormittal: Support lattice tower marketing. Technical report, ArcelorMittal, 2012.

[64] South African Institute of Steel Construction. Southern african steel construction handbook. 7, 2010.

[65] Therese McAllister and Gene Corley. *World Trade Center Building performance study: Data collection, preliminary observations, and recommendations.* Federal Emergency Management Agency, 2002.

[66] G Owens, editor. *Fulton's concrete Technology.* Cement & Concrete Institute, 9 edition, 2009.

[67] Structural Systems. Prestressing technology. Online, October 2014. URL http://www.structuralsystemsuk.com/downloads/downloads.php.

[68] P Bamforth, D Chisholm, J Gibbs, and T Harrison. Properties of concrete for use in eurocode 2. *The Concrete Center Report (www. concretecenter. com) CCIP-029: UK*, 2008.

[69] Eivind Hognestad. Study of combined bending and axial load in reinforced concrete members. 1951.

[70] Puneet Malhotra. *Advanced blade testing methods for wind turbines.* PhD thesis, University of Massachusetts Amherst, 2010.

[71] D Todd Griffith and Thomas D Ashwill. The sandia 100-meter all-glass baseline wind turbine blade: Snl100-00. *Sandia National Laboratories Technical Report*, 2011.

[72] HA Buchold and SE Moossavi Nejad. *Structural Dynamics for Engineers.* ICE Publishing, 2 edition, 2012.

[73] Finite element analysis services. 2014. URL http://www.feas.co.za/.

[74] S V Chaudhari and M A Chakrabarti. Modeling of concrete for nonlinear analysis using finite element code abaqus. *International Journal of Computer Applications*, 44(7):14–18, 2012.

[75] David Roylance. Stress-strain curves. *Massachusetts Institute of Technology study, Cambridge*, 2001.

[76] *Merkel's live: builder's pricing and management manual*. PPiS, November 2014. URL www.ppis.co.za. Online database.

[77] Dr. P Day. Land surveying and geotechnical investigation for wind turbine. Adjunct Professor of Geotechnical Engineering at the University of Stellenbosch, November 2014.

[78] Babatunde James Olawuyi. Typical mix proportions for 60mpa concrete. PhD candidate for Structural Engineering, Department of Civil Engineering at the Stellenbosch University, November 2014.

[79] Free construction cost data. Online, 2014. URL http://www.allcostdata.info/index.html.

[80] Document downloads: Price lists. Online, September 2014. URL http://www.macsteel.co.za/.

[81] Solid waste management. Online, 2014. URL www.capetown.gov.za.

[82] Supee Teravaninthorn and Gaël Raballand. *Transport prices and costs in Africa: a review of the main international corridors*. World Bank Publications, 2009.

[83] R Klaas. Contract price adjustment provisions (cpap) work groups and selected material indices. *Statistics South Africa*, 2012-2014.

[84] P Lehohla. Bulletin of statistics. *Statistics South Africa*, 48, 2014.

[85] H Klee. Recycling concrete. Technical report, WBCSD, July 2009.

[86] Recycling and reuse. Online, 2014. URL http://www.steelconstruction.info/Recycling_and_reuse.

[87] Price list. Online, 2014. URL http://www.scrapmetalsolutions.co.za/price_list.php.

[88] Infrastructure, energy, telecommunications. Online, 2014. URL http://www.capital.nedbank.co.za/capital/deals-infrastructure-energy-telecommunications.

[89] Bedford celebrates start of r3.5bn wind farm. Online. URL http://www.heraldlive.co.za/bedford-celebrates-start-r3-5bn-wind-farm/.

[90] First turbines for cookhouse wind farm arrives in sa. Online, 2013. URL http://www.engineeringnews.co.za/article/first-turbines-for-cookhouse-wind-farm-arrive-in-sa-2013-04-08.

[91] Dorper wind farm, south africa. Online, 2014. URL http://www.engineeringnews.co.za/article/dorper-wind-farm-south-africa-2014-06-13.

[92] Gouda wind park project, south africa. Online, 2014. URL http://www.engineeringnews.co.za/article/gouda-wind-park-project-south-africa-2014-09-19.

[93] Project fact sheet. Online, 2014. URL http://jeffreysbaywindfarm.co.za.

[94] Developments: Gibson bay wind farm. Online, 2013. URL http://redcap.co.za/developments/gibson-bay-wind-farm-1/.

[95] Developments: Kouga wind farm. Online, 2011. URL http://redcap.co.za/developments/kouga-wind-farm.

[96] Tsitsikamma community wind farm project, south africa. Online, 2013. URL http://www.engineeringnews.co.za/article/tsitsikamma-community-wind-farm-project-south-africa-2013-07-05.

[97] Derick Wade Immelman. *The influence of percentage replacement on the aggregate and concrete properties from commercially produced coarse recycled concrete aggregate*. PhD thesis, Stellenbosch: Stellenbosch University, 2013.

Appendix A: Mast Information for the Wind Atlas of South Africa

Table 1 lists the mast name, closest town, location coordinates, altitude and start date of wind measurements.

Table 1: Mast information for Wind Atlas of South Africa [38]

Site	Closest Town	Coordinates	Altitude (m.a.s.l)	Data Start Date
WM01	Alexander Bay	28° 36' 06" S 16° 39' 51" E	152	2010/06/23
WM02	Calvinia	31° 31' 29" S 19° 21' 38" E	824	2010/06/30
WM03	Vredendal	31° 43' 49" S 18° 25' 11" E	241	2010/06/24
WM04	Vredenburg	32° 50' 46" S 18° 06' 33" E	22	2010/05/18
WM05	Napier	34° 36' 42" S 19° 41' 32" E	288	2010/05/20
WM06	Sutherland	32° 33' 24" S 20° 41' 28" E	1581	2010/09/17
WM07	Beaufort West	32° 58' 00" S 22° 33' 24" E	1047	2010/05/28
WM08	Humansdorp	34° 06' 35" S 24° 30' 51" E	110	2010/08/04
WM09	Noupoort	31° 15' 09" S 25° 01' 42" E	1806	2010/09/01
WM10	Butterworth	32° 05' 26" S 28° 08' 09" E	925	2010/08/05

Appendix B: Reference Wind Turbine and Site

TABLE 2: The 90 % range for adjusted Fisher-Pearson standardized moment coefficient [59].

Sample Size	Lower Limit	Upper Limit	Sample Size	Lower Limit	Upper Limit
25	-0.726	0.726	90	-0.411	0.411
30	-0.673	0.673	100	-0.391	0.391
40	-0.594	0.594	150	-0.322	0.322
50	-0.539	0.539	200	-0.281	0.281
60	-0.496	0.496	300	-0.230	0.230
70	-0.462	0.462	400	-0.200	0.200
80	-0.435	0.435	500	-0.179	0.179

TABLE 3: Wind farming projects and locations in South Africa.

Project Name	Capacity (MW)	Hub height (m)	Rotor diameter (m)	Location
Amakhala Emoyeni	2.4	80	116.8	Bedford
Coega	1.8	95	90	Port Elizabeth
Darling	1.3	50	62	Darling
Dorper	2.5	80	80	Malteno
Hopefield	1.8	80		Hopefield
Jeffreys Bay	2.3	80	101	Jeffreys Bay
Klipheuwel	0.7, 0.8, 1.8	40, 46, 60	47, 48, 66	Klipheuwel
Klipheuwel-Dassiesfontein	3	100	113	Caledon
Metrowind van Stadens	3	90	113	Port Elizabeth
Noblesfontein	1.8, 3	80 to 125	100, 112	Victoria West
Red Cap Kouga	2.5	80	90	Jeffreys Bay
Sere	2.3	80 to 100	108	Vredendal
West Coast One	2	80	90	Western Cape

Appendix C: Geometry of Support Tower Designs for Study

Table 4: Pre-stressed concrete tower design dimensions in metres

Tower geometric design parameters	Tower designs from literature 1.5 MW	3.6 MW	5 MW	Scaled design 3 MW
Outside diameter at top	2.896	3.658	3.658	3.440
Wall thickness at top	0.4572	0.4572	0.4572	0.457
Tower mid height	49	49	49	49
Outside diameter at mid height	3.962	5.182	5.639	4.833
Wall thickness at mid height	0.5334	0.6096	0.6858	0.588
Outside diameter at base	5.791	6.706	7.620	6.445
Wall thickness at base	0.6096	0.6858	0.762	0.664

TABLE 5: Modelled pre-stressed concrete tower design dimensions in metres.

Tower section	Top height	Bottom thickness	Top thickness	Average thickness
1	100	0.470	0.457	0.464
2	94.9	0.483	0.470	0.477
3	89.8	0.496	0.483	0.490
4	84.7	0.509	0.496	0.503
5	79.6	0.523	0.509	0.516
6	74.5	0.536	0.523	0.529
7	69.4	0.549	0.536	0.542
8	64.3	0.562	0.549	0.555
9	59.2	0.575	0.562	0.568
10	54.1	0.588	0.575	0.581
11	49	0.596	0.588	0.592
12	44.1	0.603	0.596	0.599
13	39.2	0.611	0.603	0.607
14	34.3	0.618	0.611	0.615
15	29.4	0.626	0.618	0.622
16	24.5	0.634	0.626	0.630
17	19.6	0.641	0.634	0.637
18	14.7	0.649	0.641	0.645
19	9.8	0.656	0.649	0.653
20	4.9	0.664	0.656	0.660

TABLE 6: Steel tower design dimensions in metres.

Tower section	Section top height	Section length	Top diameter	Top wall thickness
flange 1	97.5	0.2	3	0.02
S1	97.3	2.44	3	0.02
S2	94.86	2.74	3.132	0.014
S3	92.12	2.73	3.28	0.013
S4	89.39	2.72	3.427	0.014
S5	86.67	2.71	3.574	0.014
S6	83.96	2.7	3.72	0.014
S7	81.26	2.69	3.866	0.014
S8	78.57	2.68	4.011	0.015
S9	75.89	2.67	4.156	0.015
flange 2	73.22	0.11	4.3	0.015
flange 3	73.11	0.11	4.3	0.015
S10	73	1.95	4.3	0.015
S11	71.05	2.95	4.3	0.016
S12	68.1	2.95	4.3	0.017
S13	65.15	2.95	4.3	0.018
S14	62.2	2.95	4.3	0.019
S15	59.25	2.95	4.3	0.019
S16	56.3	2.95	4.3	0.02
S17	53.35	2.95	4.3	0.021
S18	50.4	1.95	4.3	0.023
flange 4	48.45	0.12	4.3	0.023
flange 5	48.33	0.12	4.3	0.023
S19	48.21	2.95	4.3	0.023
S20	45.26	2.95	4.3	0.024
S21	42.31	2.95	4.3	0.025
S22	39.36	2.95	4.3	0.026
S23	36.41	2.95	4.3	0.028
S24	33.46	2.95	4.3	0.03
flange 6	30.51	0.13	4.3	0.03
flange 7	30.38	0.13	4.3	0.03
S25	30.25	2.45	4.3	0.03
S26	27.8	2.95	4.3	0.032
S27	24.85	2.95	4.3	0.032
S28	21.9	2.95	4.3	0.035
S29	18.95	2.45	4.3	0.038
flange 8	16.5	0.15	4.3	0.038
flange 9	16.35	0.15	4.3	0.038
S30	16.2	1.95	4.3	0.038
S31	14.25	2.45	4.3	0.04
S32	11.8	2.45	4.3	0.045
S33	9.35	1.95	4.3	0.05
flange 10	7.4	0.175	4.3	0.05
flange 11	7.225	0.175	4.3	0.05
S34	7.05	2.45	4.3	0.05
S35	4.6	2.45	4.3	0.05
S36	2.15	1.95	4.3	0.05
flange 12	0.2	0.2	4.3	0.05

Appendix D: Blade Profile and Scaling

TABLE 7: Blade profile and scaling in metre.

63.33 m baseline blade				Scaled blade			
Station over length		Chord		Station over length		Chord	
0.000	32.111	3.358	3.730	0.000	28.797	3.034	3.370
0.199	34.106	3.501	3.654	0.179	30.586	3.163	3.302
1.197	36.100	3.643	3.580	1.073	32.374	3.292	3.235
2.194	38.095	3.786	3.505	1.967	34.163	3.421	3.167
3.191	40.089	3.929	3.430	2.862	35.951	3.550	3.099
4.188	42.083	4.073	3.355	3.756	37.740	3.680	3.031
5.185	44.078	4.219	3.280	4.650	39.529	3.813	2.964
6.183	46.072	4.390	3.205	5.545	41.317	3.967	2.896
7.180	48.068	4.528	3.130	6.439	43.107	4.092	2.828
8.178	50.061	4.586	3.055	7.334	44.894	4.143	2.760
9.174	52.056	4.624	2.980	8.227	46.683	4.178	2.692
10.172	54.050	4.647	2.904	9.122	48.472	4.199	2.624
11.169	55.047	4.648	2.829	10.016	49.366	4.200	2.556
12.166	56.045	4.601	2.754	10.910	50.260	4.158	2.489
13.164	57.042	4.526	2.679	11.806	51.154	4.090	2.421
14.160	57.540	4.454	2.604	12.699	51.602	4.025	2.353
15.158	58.040	4.393	2.529	13.593	52.050	3.969	2.285
16.155	58.538	4.329	2.456	14.488	52.496	3.912	2.219
18.151	59.036	4.264	2.384	16.277	52.943	3.852	2.154
20.144	59.535	4.194	2.302	18.065	53.390	3.789	2.080
22.139	60.033	4.120	2.215	19.854	53.837	3.723	2.001
24.133	60.532	4.045	2.095	21.643	54.284	3.655	1.893
26.128	61.031	3.968	1.868	23.431	54.732	3.585	1.687
28.123	61.330	3.888	1.516	25.220	55.000	3.513	1.370
30.117		3.808		27.008		3.441	

Appendix E: Stress-Strain Curves

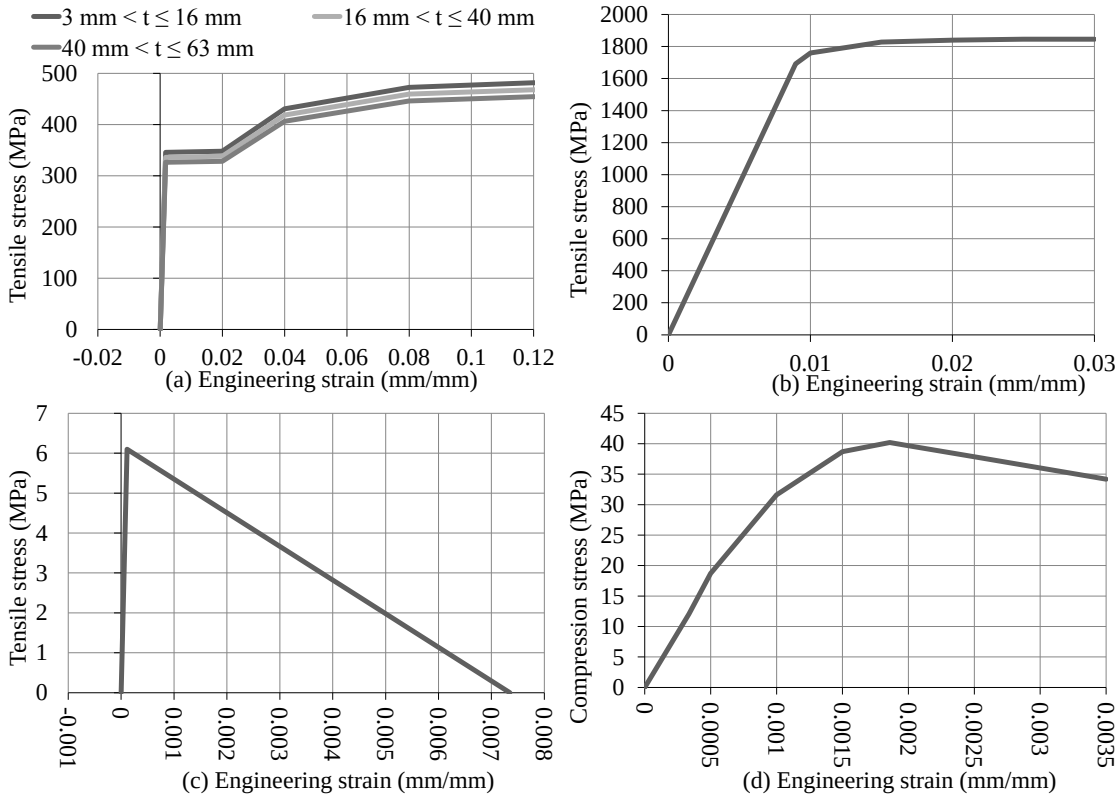

FIGURE 1: Stress-strain curves for: (a) S355 structural steel [65]. (b) 1860 MPa steel prestressing strands [27]. (c)-(d) 60 MPa reinforced concrete [48].

Appendix F: Distributed Load Over Tower Height

The values for $f_w(h)$ in Tables 8 and 9 were used as input into an analytical field for Abaqus and determined according to global axis coordinates for the model.

TABLE 8: Nominal values of the distributed wind load over the steel tower height.

X (m)	Y (m)	Z (m)	Nominal field value ($\mathrm{N\,m^{-2}}$)	X (m)	Y (m)	Z (m)	Nominal field value ($\mathrm{N\,m^{-2}}$)
0	97.5	0	769.1	0	42.31	0	660.5
0	97.3	0	768.7	0	39.36	0	650.0
0	94.86	0	767.5	0	36.41	0	638.7
0	92.12	0	765.9	0	33.46	0	626.7
0	89.39	0	763.9	0	30.51	0	613.8
0	86.67	0	761.6	0	30.38	0	613.2
0	83.96	0	759.0	0	30.25	0	612.6
0	81.26	0	756.1	0	27.8	0	601.1
0	78.57	0	753.0	0	24.85	0	586.1
0	75.89	0	749.5	0	21.9	0	569.5
0	73.22	0	745.8	0	18.95	0	551.2
0	73.11	0	745.6	0	16.5	0	534.1
0	73.0	0	745.3	0	16.35	0	533.0
0	71.05	0	740.9	0	16.2	0	531.9
0	68.1	0	734.0	0	14.25	0	516.6
0	65.15	0	726.9	0	11.8	0	494.8
0	62.2	0	719.6	0	9.35	0	469.2
0	59.25	0	711.9	0	7.4	0	444.8
0	56.3	0	703.9	0	7.225	0	442.3
0	53.35	0	695.5	0	7.05	0	439.9
0	50.4	0	686.8	0	4.6	0	398.8
0	48.45	0	680.8	0	2.15	0	334.9
0	48.33	0	680.4	0	0.2	0	193.6
0	48.21	0	680.1	0	0	0	0
0	45.26	0	670.6				

TABLE 9: Nominal values of the distributed wind load over the concrete tower height.

X (m)	Y (m)	Z (m)	Nominal field value ($N\,m^{-2}$)	X (m)	Y (m)	Z (m)	Nominal field value ($N\,m^{-2}$)
0	100	0	891.7	0	47.04	0	755.5
0	97.96	0	887.7	0	45.08	0	748.4
0	95.92	0	883.6	0	43.12	0	741.0
0	93.88	0	879.5	0	41.16	0	733.4
0	91.84	0	875.3	0	39.20	0	725.5
0	89.80	0	871.0	0	37.24	0	717.3
0	87.76	0	866.6	0	35.28	0	708.7
0	85.72	0	862.2	0	33.32	0	699.7
0	83.68	0	857.7	0	31.36	0	690.3
0	81.64	0	853.1	0	29.40	0	680.4
0	79.60	0	848.3	0	27.44	0	670.0
0	77.56	0	843.5	0	25.48	0	658.9
0	75.52	0	838.6	0	23.52	0	647.2
0	73.48	0	833.6	0	21.56	0	634.7
0	71.44	0	828.5	0	19.60	0	621.3
0	69.40	0	823.2	0	17.64	0	606.7
0	67.36	0	817.8	0	15.68	0	590.9
0	65.32	0	812.3	0	13.72	0	573.3
0	63.28	0	806.7	0	11.76	0	553.8
0	61.24	0	800.9	0	9.80	0	531.4
0	59.20	0	794.9	0	7.84	0	505.3
0	57.16	0	788.8	0	5.88	0	473.4
0	55.12	0	782.5	0	3.92	0	431.9
0	53.08	0	776.0	0	1.96	0	369.0
0	51.04	0	769.3	0	0	0	0
0	49.00	0	762.4				

Appendix G: Cost Estimation of Life-cycle Phases

This appendix provides a visual representation of the excel sheets that was used to perform the life cycle costing analysis for this study. The data is listed as shown below.

- Page 147 to 150: Most likely manufacture, construction and installation costs for the prestressed precast concrete tower.
- Page 151 to 155: Most likely manufacture, construction and installation costs for the prestressed cast-in-place concrete tower.
- Page 156 to 158: Most likely manufacture, construction and installation costs for the prestressed precast concrete tower.
- Page 159 to 163: Miscellaneous calculations and data used as input for the main calculation sheets for manufacture, construction and installation costs.
- Page 164: Disposal and recycling cost estimations and sensitivity analysis.
- Page 165: Transport cost estimations.

Detailed conceptual cost estimates of the all precast concrete tower manufacture and construction. The structure of the NREL costing model was used and local prices was inserted where possible. Original costs are for a 3.6MW turbine with a tower of 100m in height. Where necessary, quantities was linearly interpolated between values for the 1.5MW and 3.6MW towers. Construction is on a 28 month schedule. Furthermore, costs were determined and a percentage of the total, so that NREL costs can be integrated easily where local values could not be found. Inflation rate calculations were calculated using the site http://fxtop.com/en/inflation-calculator.php. The time of the NREL study is aassumed to be 31 July 2004 and for this study as August 2014.

No	Item (3.6MW description unless stated otherwise)	Quantity for 1.5MW	Quantity for 3.6MW	Quantity for 3MW	Units	NREL unit cost (2004 $)	Quantity	Units	Study cost (2014 Rand) Per unit	Per tower	% per tower	Comments
1	**Mobilization and site development for 50 towers**											
	Access road				lump sum		-	-	-	R 262 534.05	1.12	Access road allowance - after windPACT Area 4 balance of station study
	Site offices and office equipment				lump sum		-	-	-	R 53 726.40	0.23	
	Management & supervision recruitment and relocation				lump sum		-	-	-	R 26 863.20	0.11	
	Design/develop special pedestal cranes 30t capacity			N/a								
	Fabricate, assemble 2 special pedestal cranes for erecting precast elements			N/a								
	Equipment move-in and setup						-	-	-	R 26 863.20	0.11	
	other mobilization and site development cost						-	-	-	R 26 863.20	0.11	
	Mobilize/demobilize (6) LTL-600 crane to site	5	6	6	lump sum	R 415 091.00	-	-	-	R 669 040.35	2.86	
	Rental for (6) Lampson LTL-600 crawler cranes for precast segment unload and erection to 100m	105	132	124.29	months	R 78 000.00	124.29	months	-	R 2 604 195.36	11.13	Crane selection from windPACT Area 2 turbine rotor and blade logistics.
	Labour cost to assemble crane per turbine	1	1	1	per turbine	R 3 685.00	1.00	per turbine	-	R 49 495.45	0.21	
	Labour cost to relocate crane per turbine	1	1	1	per turbine	R 1 560.00	1.00	per turbine	-	R 20 953.30	0.09	
	Crane cribbing cost per turbine	1	1	1	per turbine	R 538.00	1.00	per turbine	-	R 7 226.20	0.03	
	Meals and lodging for crew per turbine	1	1	1	per turbine	R 605.00	1.00	per turbine	-	R 8 126.12	0.03	
	Fuel cost per month	105	132	124.29	per month	R 4 222.00	124.29	per month	-	R 140 960.42	0.60	
	Mobilize/demobilize (1) LTL-850 crane	1	1	1	lump sum	R 484 727.00			-	R 130 213.18	0.56	
	Rental for (1) Lampson LTL-850 Crane for nacelle, hub and blade erection at 100m level	10.4	15	13.69	months	R 88 667.00	13.69	months	-	R 357 281.90	1.53	
	Labour cost to assemble crane per turbine	1	1	1	per turbine	R 7 332.00	1.00	per turbine	-	R 98 480.49	0.42	
	Labour cost to relocate crane per turbine	1	1	1	per turbine	R 2 730.00	1.00	per turbine	-	R 36 668.27	0.16	
	Crane cribbing cost per turbine	1	1	1	per turbine	R 808.00	1.00	per turbine	-	R 10 852.73	0.05	
	Meals and lodging for crane crew per turbine	1	1	1	per turbine	R 1 161.00	1.00	per turbine	-	R 15 594.09	0.07	
	Fuel cost per month	10.4	15	13.69	per month	R 4 222.00	13.69	per month	-	R 15 521.85	0.07	
	Other equipment rental	28	28	28	months	R 10 000.00	28.00	months	-	R 75 216.96	0.32	
										R 4 636 676.72	**19.83**	
2	**Foundation construction per tower (Precast)**											
	Survey layout and location						1	lump sum		R 8 000.00	0.03	Use data by Dr. peter day.
	Geotechnical investigation (per tower location)	50	50	50	each	R 1 000.00	50	wind farm	R 500 000.00	R 10 000.00	0.04	Use data by Dr. Peter day: R500000 fixed cost for wind farm.
							1	lump sum		R 200 000.00	0.86	Use data by Dr. Peter day: R200000 WTG cost per site.
	Excavation	1725	2455	2246.43	cubic yards	R 8.00	1717.51	m^3	R 134.19	R 230 472.26	0.99	With large excavator. Merkel's pricing for earthworks.
	Supply and install concrete forms (19.2m by 19.2m by 3.66m deep)	2200	3027	2790.71	sq Ft	R 2.50	259.26	m^2	R 341.78	R 88 608.98	0.38	Use Merkel's rough formwork for sides of bases.
	Supply, place and consolidate foundation concrete	1008	1588	1422.29	cubic yards	R 89.90	1087.41	m^3	R 1 525.09	R 1 658 395.89	7.09	Use 90% of gross foundation volume to account for central thickening of foundation. Merkel's 30MPa/19mm RC base mixing at site.
	Reinforcing steel	143200	231500	206271.43	Lbs	R 0.45	93.56	t	R 16 509.95	R 1 544 721.60	6.60	Assume Merkel's R12 mild reinforcement bars
	A-490 anchor bolts and couplers (reuse upper bolts)			N/a								
	Precision locating template for anchor bolts and post tensioning anchors and ducts	4	4	4	each	R 12 500.00	-	-	-	R 13 431.60	0.06	
	Backfill and tamp (after post tensioning)	650	650	650	cubic yards	R 6.00	497	m^3	R 47.81	R 23 759.54	0.10	Tamp 10ft around footing. Merkel's 93% Mod AASHTO compacted earth filling obtained from excavations on site.
	Untamped backfill	1200	1200	1200	cubic yards	R 1.00	917	m^3	R 44.56	R 40 882.02	0.17	Merkel's uncompacted earth filling obtained from excavations on site.
										R 3 818 271.89	**16.33**	

3	**Shop fabrication of steel (Concrete top connection ring) (Precast)**												
Tube section material													
Tube section fabrication, rolled and welded				N/a									
Base flange ring (Dim 3.96mOD x 3.45mID x 0.127m thk)				N/a									
Cut, weld, stress relieve				N/a									
Drill holes, mill after welding first tube section				N/a									
Top flange ring (Dim 3.66mOD x 2.64mID x0.127m thk)													
Cut, weld, stress relieve	11132	14684	13669.14	lbs	R	2.00	6.20	t	-	R	367 196.92	1.57	Weight include 33% waste
Drill holes, mill after welding first tube section				lump sum			-	-	-	R	40 294.80	0.17	
Concrete tower top connection ring (Dim 5.23mOD x 2.56mID x 0.152m thk)				N/a									
Cut, weld, stress relieve				N/a									Weight include 33% waste
Drill holes to match tower flange, mill to match tube flange				N/a									
Fabricate and install internal galvanized ladders				N/a									Use 30 ib per vertical ft
Surface preparation, prime and paint				N/a									
2 Coats primer on interior surfaces				N/a									
Primer and epoxy finish coats on exterior				N/a									
Truck delivery (see note 3) $27 per kW*(49m/86m)=15.38/kW for 1.5MW tower				N/a									
Truck delivery of top flange plate only				lump sum			1	load	R 4 466.96	R	4 466.96	0.02	Use transport rates for 28t truck delivery from steel fabrication plant to site.
										R	**411 958.67**	**1.76**	
4	**Field erection of steel tube & pedestal crane (Precast)**												
Fabricate jack-up frame and base supports (4)				N/a									
Install base support system and jack-up frame				N/a									
Rig, erect and fit 3 tube sections (labour)				N/a									
Weld (3) field joints with track-mounted welder ($1.67/kW)*(49m/86m)=$0.95/kW				N/a									
Grout and torque tower base (labour)	40	40	40	man hours	R	40.30	40.00	man hours	R 25.32	R	1 012.80	0.00	Merkel's hour rate for semi-skilled labourer.
Grout and torque tower base (Material and equipment)				lump sum			-	-	-	R	11 416.86	0.05	
Erect special pedestal crane on top of steel tube (assume 5 days with crew of 8 to fully install)				N/a									
										R	**12 429.66**	**0.05**	
5	**Precast concrete operation - Includes 1200 A segments, 750 B segments, 900 C segments, 900 D segments, 1050 E segments, 150 F segments**												
Design and Fabricate (4) A forms	-		4	Each	R	16 000.00	-	-	-	R	17 192.45	0.07	Divide total form costs by 50 towers
Design and Fabricate (2) B forms	-		3	Each	R	16 000.00	-	-	-	R	12 894.34	0.06	Divide total form costs by 50 towers
Design and Fabricate (2) C forms	-		2	Each	R	15 000.00	-	-	-	R	8 058.96	0.03	Divide total form costs by 50 towers
Design and Fabricate (2) D forms	-		2	Each	R	15 000.00	-	-	-	R	8 058.96	0.03	Divide total form costs by 50 towers
Design and Fabricate (4) E forms	-		4	Each	R	15 000.00	-	-	-	R	16 117.92	0.07	Divide total form costs by 50 towers
Design and Fabricate (1) F form	-		1	Each	R	15 000.00	-	-	-	R	4 029.48	0.02	Divide total form costs by 50 towers
Install 16 forms and start-up at precast plant	-		16	Each	R	2 000.00	-	-	-	R	8 596.22	0.04	Divide total form costs by 50 towers
Precast (99) A, B, C, D, E and F segments per tower													
Daily strip and set up forms	1	1	1	Segment	R	120.00	-	-	-	R	159 567.41	0.68	Outer form = 3.566m x 5.18m with 15 ties
Supply end plates and weld to horizontal rebar	48	48	48	Welds	R	6.00	-	-	-	R	382 961.78	1.64	
Supply and install rebar (nominal)	947	850	877.71	Lbs	R	0.35	7.75	t	R 16 509.95	R	127 902.58	0.55	Merkel's straight R12 mild steel bars for vertical reinforcement. Use calculated mass of nominal reinforcement for modelled tower.
							7.75	t	R 16 613.36	R	128 703.70	0.55	Merkel's curved R12 mild steel bars for horizontal reinforcement. Use calculated mass of nominal reinforcement for modelled tower.
Supply and install embedments (7) per segment	1	1	1	Segment	R	220.00	-	-	-	R	292 540.25	1.25	Include male/female alignment
Supply duct for erection post tensioning bars (4) per segment	4	4	4	Segment	R	20.00	-	-	-	R	106 378.27	0.45	
Install strand post tensioning duct sleeves (13) average per segment	13	13	13	Ducts/slve	R	7.00	-	-	-	R	121 005.28	0.52	
Install bar post tensioning anchor plates and trumpets (12) per ring	12	12	12	Anchors	R	25.00	-	-	-	R	132 972.84	0.57	33 rings
Supply and place concrete	10.75	11.05	10.96	Cubic yard	R	80.00	683.30	m^3	R 1 954.87	R	1 335 754.46	5.71	Volume calculated from tower dimensions. 60MPa concrete mixed by J Babs and priced by combination of Merkel's and local suppliers. Profit and sundries markup included in section 5.
Strip, handle, cure and store segments	1	1	1	Segment	R	150.00	-	-	-	R	199 459.26	0.85	
Total cubic yards of PC concrete	838	1094	1020.86							R	3 062 194.16	13.09	
Supervision, quality control, maintenance shop overhead	30	30	30	%						R	918 658.25	3.93	
General and administrative and profit	25	25	25	%						R	765 548.54	3.27	
										R	**4 746 400.95**	**20.29**	

Truck delivery (99 precast segments per tower)	78	99	93	loads	R	1 100.00	93	loads	R	1 871.16	R	174 018.09	0.74	Note 5. Segment weights range from 57.3 kips (57300 lbs) (26t) to 32.4 kips (32400 lbs)(14.7t) for 3.6MW tower. Calculate cost for round trip per segment between precast factory and site.
Fabricate joint closure forms (8 sets of 3 forms)	1600	1600	1600	sq ft	R	20.00	148.64	m^2	R	932.10	R	2 770.95	0.01	Include re-usable tie-bolt hardware. Assume Merkel's special formwork for rectangular columns.
Erect 34 rings of 3 segments each	78	99	93	segments										
Strip, clean and oil (3) top fixtures and (6) forms	26	33	31	sets	R	250.00	46.50	h	R	118.54	R	5 512.11	0.02	Concurrent with leveling and shimming
Set shims with level and glue gaskets	26	33	31	rings	R	175.00	46.50	h	R	118.54	R	5 512.11	0.02	0.5 crew hour per segment
Hoist and set 99 segments	78	99	93	segments	R	175.00	46.50	h	R	118.54	R	5 512.11	0.02	0.5 crew hour per segment - hoist directly from delivery truck
Supply post tensioning bars and couplers	24998	31728	29805	lbs	R	1.50	13.5194	t	-		R	600 496.14	2.57	0.5 crew hour per 4 bars (1.5 MW hybrid X factor 100m/49m=2.04 x ration by no. of segments).
Install and stress 168 post tensioning bars with couplers	24998	31728	29805	lbs	R	0.50	13.5194	t	-		R	200 165.38	0.86	0.5 crew hour per 4 bars (1.5 MW hybrid X factor 100m/49m=2.04 x ration by no. of segments).
Install top positioning fixtures	78	99	93	each	R	58.00	15.50	h	R	118.54	R	1 837.37	0.01	0.5 crew hour per 3 segments
Place and weld rebar splices and ties in vertical joints	4080	3180	3437	welds	R	4.00	-	-	-		R	184 665.31	0.79	Assume 20 bars per joint at 2 welds each (1.5MW hybrid X factor 100m/49m=2.04)
Inject grout in horizontal joint (4 cu ft/ ring joint)	104	132	124	Cubic ft	R	30.00	3.51	m^3	R	14 344.93	R	50 369.11	0.22	Concurrent with rebar welding. Merkel's Duragrout application with labour costing.
Attach closure joint forms (1 set = (6) leaves)	26	33	31	sets	R	350.00	31.00	h	R	118.54	R	3 674.74	0.02	1 crew hour per set of 3 joints
Supply, place and vibrate closure pour concrete	104	132	124	Cubic yards	R	150.00	94.80	m^3	R	2 003.75	R	189 963.92	0.81	Av 4 cubic yards / 3 joints; Use 60MPa concrete mixed by J Babs and priced by combination of Merkel's and local suppliers with sundries markup.
Hoist, install, level and grout concrete tower top connection plate	24	24	24	Man hours	R	40.30	24.00	man hours	R	25.32	R	607.68	0.00	Connection plate hoisted with strand post tensioning anchors attached. Merkel's hour rate for semi-skilled labourer.
Install, stress and grout vertical strand tendons	30	40	37	tendons										
Supply (80) post tensioning anchors (12 strand-15.2mm)	60	80	74	each	R	193.00								Installation cost is included in precast. (Assume part of lump sum for prestressing reinforcement installation.)
For this study, supply (19) vertical post tensioning ducts (100mm diameter) between tower top and mid (51m).	10137	13864	12799	Lineal ft	R	2.50	969	m	R	3.47	R	3 364.85	0.01	Installation cost is included in precast. Assume Merkel's 100mm diameter PVC sleeve @ R 13.89 per 4m. Duct length based on tendon lengths for modelled tower.
For this study, supply (29) vertical post tensioning ducts (100mm diameter) between tower mid and bottom (49m).							1421	m	R	3.47	R	4 934.42	0.02	Installation cost is included in precast. Assume Merkel's 100mm diameter PVC sleeve @ R 13.89 per 4m. Duct length based on tendon lengths for modelled tower.
Supply and install (480) pieces of 15.2mm diameter post tensioning strand	78490	104600	97140	lbs	R	0.68					R	1 868 102.62	7.99	Calculate material price, installation and jacking costs as lump sum using free construction costing data and Merkel's.
Stress (8) tendons teminated at segment 50% and 32 at top segment	30	40	37	Operations	R	500.00		lump sum						Includes rental of P/T jacks and pumps
Transport of prestressing reinforcement							1.5	round trips	R	8 933.91	R	13 400.87	0.06	Transport cost from steel fabrication plant. Two loads: 28t truck.
Grout 40 (58 at half height for this study) post tensioning tendons	375	340	350	Cubic ft	R	20.00	12.57	m^3	R	14 344.93				For this study use calculated volume for prestressed concrete design. Merkel's Duragrout application with labour costing. (Included in lump sum for prestressing reinforcement.)
Allowance for material handling, unloading and equipment							-	-	-		R	134 316.00	0.57	Crane cost covered in item 1
											R	3 449 223.78	14.75	
Supervision, overhead, and profit for strand post tensioning sub contractor	8	8	8	%							R	275 937.90	1.18	
											R	3 725 161.68	15.93	

7	**Erect nacelle and rotor (Precast)**													
Preparation for jack-up operation			N/a											
Supply and install (3) jack-up tendons with			N/a											
Anchors top and bottom			N/a											
Fabricate (18) upper thruster assemblies			N/a											
Install (18) upper thruster assemblies			N/a											
Fabricate (24) lower thruster assemblies			N/a											
Install (24) lower thruster assemblies			N/a											
Remove special pedestal crane and prepare for reinstallation (2 days with crew of 6)			N/a											
Erect transitions section and turbine nacelle (crew of 3 for 5 days)	120	140	134	man hours	R	40.30	134.29	man hours	R	25.32	R	3 400.11	0.01	Use LTL 850 crane WindPACT Area 2 study - crane costs elsewhere (hybrid tower labour x 2) Merkel's semi-skilled.
Supply, install and torque 1.25in (31.7mm) diameter HS bolts	64	75	72	each	R	14.20	-	-	-		R	13 705.22	0.06	
Erect hub and blades to turbine nacelle (crew of 3 for 5 days)	120	144	137	man hours	R	40.30	137.14	man hours	R	25.32	R	3 472.46	0.01	Use LTL 850 crane WindPACT Area 2 study - crane costs elsewhere (hybrid tower labour x 2) Merkel's semi-skilled.
Disconnect base flange of steel tube from anchor bolts			N/a											
Jack-up steel tube with turbine and blades			N/a											
Jack-up steel tube in 12 in lifts (12 lifts per hour)(16 hour shift) 6 people x 16 =			N/a											
Jack-up equipment rental			N/a											
Monitor with control transits			N/a											
For final 24 inches inspect and adjust rotationally to assure lift frame staffing cones mate into female sockets			N/a											
Allowance for equipment and small cranes							-	-	-		R	53 726.40	0.23	
											R	**74 304.19**	**0.32**	
8	**Finishing and clean-up (Precast)**													
Remove upper and lower thruster assemblies			N/a											
Supply, install, and torque (128) - 1.5 in diameter high strength bolts			N/a											
Remove jack-up tendons and anchors			N/a											
Lower and remove tower base support frame (3 days for a crew of 4)			N/a											
Install weather protective flashing over concrete to steel joint	16	16	16	man hours	R	40.30	16.00	man hours		25.32	R	405.12	0.00	Crew of 4 for 4 hours. Merkel's semi-skilled.
Supply, hoist in and install ladders and platforms inside concrete tower	328	328	328	Lineal ft	R	100.00	99.97	m	-		R	440 556.48	1.88	
Remove exterior scaffold platforms and connecting ladders				Lump sum			-	-	-		R	124 242.30	0.53	Use LTL-600 crane (crane costs included elsewhere)
Touch up paint on steel tube exterior			N/a											Use LTL-600 crane (crane costs included elsewhere)
											R	**565 203.90**	**2.42**	
Summary of construction costs											**R**	**17 990 407.67**		
General contractor field overhead	10	10	10	%							R	1 799 040.77	7.69	
General contractor administrative overhead	10	10	10	%							R	1 799 040.77	7.69	
General contractor profit	10	10	10	%							R	1 799 040.77	7.69	
Total manufacture, construction and installation cost of one prestressed precast tower											**R**	**23 387 529.98**	**100.00**	

Detailed conceptual cost estimates of the all cast-in-place concrete tower manufacture and construction. The structure of the NREL costing model was used and local prices was inserted where possible. Original costs are for a 3.6MW turbine with a tower of 100m in height. Where necessary, quantities was linearly interpolated between values for the 1.5MW and 3.6MW towers. Construction is on a 28 month schedule. Furthermore, costs were determined and a percentage of the total, so that NREL costs can be integrated easily where local values could not be found. Inflation rate calculations were calculated using the site http://fxtop.com/en/inflation-calculator.php. The time of the NREL study is aassumed to be 31 July 2004 and for this study as August 2014.

No	Item (3.6MW description unless stated otherwise)	Quantity for 1.5MW	Quantity for 3.6MW	Quantity for 3MW	Units	NREL unit cost (2004 $)	Quantity	Units	Study cost (2014 Rand) Per unit	Per tower	% per tower	Comments
1	**Mobilization and site development for 50 towers**											
	Access road				lump sum		-	-	-	R 262 534.05	1.37	Access road allowance - after windPACT Area 4 balance of station study
	Site offices and office equipment				lump sum		-	-	-	R 53 726.40	0.28	
	Management & supervision recruitment and relocation				lump sum		-	-	-	R 26 863.20	0.14	
	Design/develop special pedestal cranes 30t capacity			N/a								
	Fabricate, assemble 2 special pedestal cranes for erecting precast elements			N/a								
	Equipment move-in and setup						-	-	-	R 26 863.20	0.14	
	other mobilization and site development cost						-	-	-	R 26 863.20	0.14	
	Mobilize/demobilize (6) LTL-600 crane to site			N/a								
	Rental for (6) Lampson LTL-600 crawler cranes for precast segment unload and erection to 100m			N/a								Crane selection from windPACT Area 2 turbine rotor and blade logistics.
	Labour cost to assemble crane per turbine			N/a								
	Labour cost to relocate crane per turbine			N/a								
	Crane cribbing cost per turbine			N/a								
	Meals and lodging for crew per turbine			N/a								
	Fuel cost per month			N/a								
	Mobilize/demobilize (1) LTL-850 crane	1	1	1	lump sum	R 484 727.00			-	R 130 213.18	0.68	
	Rental for (1) Lampson LTL-850 Crane for nacelle, hub and blade erection at 100m level	12.7	17.3	15.99	months	R 88 667.00	15.99	months	-	R 412 065.13	2.15	
	Labour cost to assemble crane per turbine	1	1	1	per turbine	R 7 332.00	1.00	per turbine	-	R 98 480.49	0.51	
	Labour cost to relocate crane per turbine	1	1	1	per turbine	R 2 730.00	1.00	per turbine	-	R 36 668.27	0.19	
	Crane cribbing cost per turbine	1	1	1	per turbine	R 808.00	1.00	per turbine	-	R 10 852.73	0.06	
	Meals and lodging for crane crew per turbine	1	1	1	per turbine	R 1 161.00	1.00	per turbine	-	R 15 594.09	0.08	
	Fuel cost per month	12.7	17.3	15.99	per month	R 4 222.00	15.99	per month	-	R 18 130.43	0.09	
	Other equipment rental	28	28	28	months	R 10 000.00	28.00	months	-	R 75 216.96	0.39	
										R 1 194 071.33	**6.23**	

2												
Foundation construction per tower (Cast-in-place)												
Survey layout and location						1	lump sum		R	8 000.00	0.04	Use data by Dr. peter day.
Geotechnical investigation (per tower location)	50	50	50	each	R 1 000.00	50	wind farm	R 500 000.00	R	10 000.00	0.05	Use data by Dr. Peter day: R500000 fixed cost for wind farm.
						1	lump sum		R	200 000.00	1.04	Use data by Dr. Peter day: R200000 WTG cost per site.
Excavation	1725	2445	2239.29	cubic yards	R 8.00	1712.05	m^3	R 134.19	R	229 739.44	1.20	With large excavator. Merkel's pricing for earthworks.
Supply and install concrete forms (19.2m by 19.2m by 3.66m deep)	2200	3024	2788.57	sq Ft	R 2.50	259.06	m^2	R 341.78	R	88 540.94	0.46	Use Merkel's rough formwork for sides of bases.
Supply, place and consolidate foundation concrete	1008	1588	1422.29	cubic yards	R 89.90	1087.41	m^3	R 1 525.09	R	1 658 395.89	8.66	Use 90% of gross foundation volume to account for central thickening of foundation. Merkel's 30MPa/19mm RC base mixing at site.
Reinforcing steel	143200	231500	206271.43	Lbs	R 0.45	93.56	t	R 16 509.95	R	1 544 721.60	8.06	Assume Merkel's R12 mild reinforcement bars
A-490 anchor bolts and couplers (reuse upper bolts)			N/a									
Precision locating template for anchor bolts and post tensioning anchors and ducts	4	4	4	each	R 12 500.00	-	-	-	R	13 431.60	0.07	
Backfill and tamp (after post tensioning)	650	650	650	cubic yards	R 6.00	497	m^3	R 47.81	R	23 759.54	0.12	Tamp 10ft around footing. Merkel's 93% Mod AASHTO compacted earth filling obtained from excavations on site.
Untamped backfill	1200	1200	1200	cubic yards	R 1.00	917	m^3	R 44.56	R	40 882.02	0.21	Merkel's uncompacted earth filling obtained from excavations on site.
									R	**3 817 471.03**	**19.93**	

3												
Shop fabrication of steel (Concrete top connection ring) (Cast-in-place)												
Tube section material												
Tube section fabrication, rolled and welded				N/a								
Base flange ring (Dim 3.96mOD x 3.45mID x 0.127m thk)				N/a								
Cut, weld, stress relieve				N/a								
Drill holes, mill after welding first tube section				N/a								
Top flange ring (Dim 3.66mOD x 2.64mID x0.127m thk)												
Cut, weld, stress relieve	11132	14684	13669.14	lbs	R 2.00	6.20	t	-	R	367 196.92	1.92	Weight include 33% waste
Drill holes, mill after welding first tube section				lump sum		-	-	-	R	40 294.80	0.21	
Concrete tower top connection ring (Dim 5.23mOD x 2.56mID x 0.152m thk)				N/a								
Cut, weld, stress relieve				N/a								Weight include 33% waste
Drill holes to match tower flange, mill to match tube flange				N/a								
Fabricate and install internal galvanized ladders				N/a								Use 30 ib per vertical ft
Surface preparation, prime and paint				N/a								
2 Coats primer on interior surfaces				N/a								
Primer and epoxy finish coats on exterior				N/a								
Truck delivery (see note 3) $27 per kW*(49m/86m)=15.38/kW for 1.5MW tower				N/a								
Truck delivery of top flange plate only				lump sum		1	load	R 4 466.96	R	4 466.96	0.02	Use transport rates for 28t truck delivery from steel fabrication plant to site.
									R	**411 958.67**	**2.15**	

4					Cast-in-place concrete operation						
Design and Fabricate (4) A forms					N/a						Divide total form costs by 50 towers
Design and Fabricate (2) B forms					N/a						Divide total form costs by 50 towers
Design and Fabricate (2) C forms					N/a						Divide total form costs by 50 towers
Design and Fabricate (2) D forms					N/a						Divide total form costs by 50 towers
Design and Fabricate (4) E forms					N/a						Divide total form costs by 50 towers
Design and Fabricate (1) F form					N/a						Divide total form costs by 50 towers
Install 16 forms and start-up at precast plant					N/a						Divide total form costs by 50 towers
					N/a						
Precast (99) A, B, C, D, E and F segments per tower					N/a						
Daily strip and set up forms					N/a						Outer form = 3.566m x 5.18m with 15 ties
Supply end plates and weld to horizontal rebar					N/a						
Supply and install rebar (nominal)					N/a						Merkel's straight R12 mild steel bars for vertical reinforcement. Use calculated mass of nominal reinforcement for modelled tower.
					N/a						Merkel's curved R12 mild steel bars for horizontal reinforcement. Use calculated mass of nominal reinforcement for modelled tower.
Supply and install embedments (7) per segment					N/a						Include male/female alignment
Supply duct for erection post tensioning bars (4) per segment					N/a						
Install strand post tensioning duct sleeves (13) average per segment					N/a						
Install bar post tensioning anchor plates and trumpets (12) per ring					N/a						33 rings
											Volume calculated from tower dimensions. 60MPa concrete mixed by J Babs and priced by combination of Merkel's and local suppliers.
Supply and place concrete - cy/segment average					N/a						Profit and sundries markup included in section 5.
Strip, handle, cure and store segments					N/a						
Total cubic yards of PC concrete					N/a						
Supervision, quality control, maintenance shop overhead					N/a						
General and administrative and profit					N/a						
	6383938	9076688	8307330.86	lump sum		778.10	m^3	1931.91	R	1 503 219.17	7.85	Concrete: Volume calculated from tower dimensions. 60MPa concrete mixed by J Babs and priced by combination of Merkel's and local suppliers. No labour cost included.
Direct material costs for cast-in-place concrete construction						7.75	t	16509.85	R	127 951.34	0.67	Reinforcing: Merkel's straight R12 mild steel bars for vertical reinforcement. Use calculated mass of nominal reinforcement for modelled tower.
						7.75	t	16613.36	R	128 753.54	0.67	Reinforcing: Merkel's curved R12 mild steel bars for horizontal reinforcement. Use calculated mass of nominal reinforcement for modelled tower.
Direct labour costs for cast-in-place concrete construction	11650123	14754556	13867575.14	lump sum		-	-	-	R	3 725 274.45	19.45	For this study it would be reasonable to assume local labour cost to be 10% of that for USA.
Equipment and site overhead for cast-in-place concrete construction	3606812	3766249	3720695.57	lump sum		-	-	-	R	999 497.89	5.22	
									R	**6 484 696.39**	**33.85**	

													Note 5. Segment weights range from 57.3 kips (57300 lbs) (26t) to 32.4 kips (32400 lbs)(14.7t) for 3.6MW tower. Calculate cost for round trip per segment between precast factory and site.
Truck delivery (99 precast segments per tower)				N/a									
													Include re-usable tie-bolt hardware. Assume Merkel's special formwork for rectangular columns.
Fabricate joint closure forms (8 sets of 3 forms)				N/a									
Erect 34 rings of 3 segments each				N/a									
Strip, clean and oil (3) top fixtures and (6) forms				N/a									Concurrent with leveling and shimming
Set shims with level and glue gaskets				N/a									0.5 crew hour per segment
Hoist and set 99 segments				N/a									0.5 crew hour per segment - hoist directly from delivery truck
Supply post tensioning bars and couplers				N/a									0.5 crew hour per 4 bars (1.5 MW hybrid X factor 100m/49m=2.04 x ration by no. of segments).
Install and stress 168 post tensioning bars with couplers				N/a									0.5 crew hour per 4 bars (1.5 MW hybrid X factor 100m/49m=2.04 x ration by no. of segments).
Install top positioning fixtures				N/a									0.5 crew hour per 3 segments
Place and weld rebar splices and ties in vertical joints				N/a									Assume 20 bars per joint at 2 welds each (1.5MW hybrid X factor 100m/49m=2.04)
Inject grout in horizontal joint (4 cu ft/ ring joint)				N/a									Concurrent with rebar welding. Merkel's Duragrout application with labour costing.
Attach closure joint forms (1 set = (6) leaves)				N/a									1 crew hour per set of 3 joints
Supply, place and vibrate closure pour concrete				N/a									Av 4 cubic yards / 3 joints; Use 60MPa concrete mixed by J Babs and priced by combination of Merkel's and local suppliers with sundries markup.
Hoist, install, level and grout concrete tower top connection plate	24	24	24	Man hours	R	40.30	24.00	man hours	25.32	R	607.68	0.00	Connection plate hoisted with strand post tensioning anchors attached. Merkel's hour rate for semi-skilled labourer.
Install, stress and grout vertical strand tendons	30	40	37	tendons									
Supply (80) post tensioning anchors (12 strand-15.2mm)	60	80	74	each	R	193.00							Installation cost is included in precast. (Assume part of lump sum for prestressing reinforcement installation.)
For this study, supply (19) vertical post tensioning ducts (100mm diameter) between tower top and mid (51m).	10137	13864	12799	Lineal ft	R	2.50	969	m	3.47	R	3 364.85	0.02	Installation cost is included in precast. Assume Merkel's 100mm diameter PVC sleeve @ R 13.89 per 4m. Duct length based on tendon lengths for modelled tower.
For this study, supply (29) vertical post tensioning ducts (100mm diameter) between tower mid and bottom (49m).							1421	m	3.47	R	4 934.42	0.03	Installation cost is included in precast. Assume Merkel's 100mm diameter PVC sleeve @ R 13.89 per 4m. Duct length based on tendon lengths for modelled tower.
Supply and install (480) pieces of 15.2mm diameter post tensioning strand	78490	104600	97140	lbs	R	0.68		lump sum		R	1 868 102.62	9.75	Calculate material price, installation and jacking costs as lump sum using free construction costing data and Merkel's.
Stress (8) tendons teminated at segment 50% and 32 at top segment	30	40	37	Operations	R	500.00							Includes rental of P/T jacks and pumps
Transport of prestressing reinforcement							1.5	round trips	R 8 933.91	R	13 400.87	0.91	Transport cost from steel fabrication plant. Two loads: 28t truck.
Grout 40 (58 at half height for this study) post tensioning tendons	375	340	350	Cubic ft	R	20.00	12.57	m^3	14344.93				For this study use calculated volume for prestressed concrete design. Merkel's Duragrout application with labour costing. (Included in lump sum for prestressing reinforcement.)
Allowance for material handling, unloading and equipment							-	-	-	R	134 316.00	0.70	Crane cost covered in item 1
										R	2 024 726.44	10.57	
Supervision, overhead, and profit for strand post tensioning sub contractor	8	8	8	%						R	161 978.12	0.85	
										R	**2 186 704.56**	**11.42**	

6					**Erect nacelle and rotor (Cast-in-place)**									
Preparation for jack-up operation				N/a										
Supply and install (3) jack-up tendons with				N/a										
Anchors top and bottom				N/a										
Fabricate (18) upper thruster assemblies				N/a										
Install (18) upper thruster assemblies				N/a										
Fabricate (24) lower thruster assemblies				N/a										
Install (24) lower thruster assemblies				N/a										
Remove special pedestal crane and prepare for reinstallation (2 days with crew of 6)				N/a										
Erect transitions section and turbine nacelle (crew of 3 for 5 days)	120	140	134	man hours	R	40.30	134.29	man hours	R	25.32	R	3 400.11	0.02	Use LTL 850 crane WindPACT Area 2 study - crane costs elsewhere (hybrid tower labour x 2) Merkel's semi-skilled labourer.
Supply, install and torque 1.25in (31.7mm) diameter HS bolts	64	75	72	each	R	14.20	-	-	-		R	13 705.22	0.07	
Erect hub and blades to turbine nacelle (crew of 3 for 5 days)	120	144	137	man hours	R	40.30	137.14	man hours	R	25.32	R	3 472.46	0.02	Use LTL 850 crane WindPACT Area 2 study - crane costs elsewhere (hybrid tower labour x 2) Merkel's semi-skilled labourer.
Disconnect base flange of steel tube from anchor bolts				N/a										
Jack-up steel tube with turbine and blades				N/a										
Jack-up steel tube in 12 in lifts (12 lifts per hour)(16 hour shift) 6 people x 16 =				N/a										
Jack-up equipment rental				N/a										
Monitor with control transits				N/a										
For final 24 inches inspect and adjust rotationally to assure lift frame staffing cones mate into female sockets				N/a										
Allowance for equipment and small cranes							-	-	-		R	53 726.40	0.28	
											R	**74 304.19**	**0.39**	
7					**Finishing and clean-up (Cast-in-place)**									
Remove upper and lower thruster assemblies				N/a										
Supply, install, and torque (128) - 1.5 in diameter high strength bolts				N/a										
Remove jack-up tendons and anchors				N/a										
Lower and remove tower base support frame (3 days for a crew of 4)				N/a										
Install weather protective flashing over concrete to steel joint	16	16	16	man hours	R	40.30	16.00	man hours	R	25.32	R	405.12	0.00	Crew of 4 for 4 hours. Merkel's semi-skilled.
Supply, hoist in and install ladders and platforms inside concrete tower	328	328	328	Lineal ft	R	100.00	99.97	m	-		R	440 556.48	2.30	
Remove exterior scaffold platforms and connecting ladders				Lump sum			-	-	-		R	124 242.30	0.65	Use LTL-600 crane (crane costs included elsewhere)
Touch up paint on steel tube exterior				N/a										Use LTL-600 crane (crane costs included elsewhere)
											R	**565 203.90**	**2.95**	
Summary of construction costs											**R**	**14 734 410.07**		
General contractor field overhead	10	10	10	%							R	1 473 441.01	7.69	
General contractor administrative overhead	10	10	10	%							R	1 473 441.01	7.69	
General contractor profit	10	10	10	%							R	1 473 441.01	7.69	
Total manufacture, construction and installation cost of one prestressed cast-in-place tower											**R**	**19 154 733.10**	**100**	

Detailed conceptual cost estimates of the all steel tower manufacture and construction. The structure of the NREL costing model was used and local prices was inserted where possible. Original costs are for a 3.6MW turbine with a tower of 100m in height. Where necessary, quantities was linearly interpolated between values for the 1.5MW and 3.6MW towers. Construction is on a 28 month schedule. Furthermore, costs were determined and a percentage of the total, so that NREL costs can be integrated easily where local values could not be found. Inflation rate calculations were calculated using the site http://fxtop.com/en/inflation-calculator.php. The time of the NREL study is aassumed to be 31 July 2004 and for this study as August 2014.

No	Item (3.6MW description unless stated otherwise)	Quantity for 1.5MW	Quantity for 3.6MW	Quantity for 3MW	Units	NREL unit cost (2004 $)	Quantity	Units	Study cost (2014 Rand) Per unit	Per tower	% per tower	Comments
1	**Mobilization and site development for 50 towers**											
	Access road				lump sum		-	-	-	R 262 534.05	1.27	Access road allowance - after windPACT Area 4 balance of station study
	Site offices and office equipment				lump sum		-	-	-	R 53 726.40	0.26	
	Management & supervision recruitment and relocation				lump sum		-	-	-	R 26 863.20	0.13	
	Design/develop special pedestal cranes 30t capacity			N/a								
	Fabricate, assemble 2 special pedestal cranes for erecting precast elements			N/a								
	Equipment move-in and setup						-	-	-	R 26 863.20	0.13	
	other mobilization and site development cost						-	-	-	R 26 863.20	0.13	
	Mobilize/demobilize (4) LTL-600 cranes to site	3	4	4	lump sum	R 415 091.00	-	-	-	R 446 026.90	2.15	
	Rental for (4) Lampson LTL-600 crawler cranes for steel tower erection, truck unload and pedestal crane installation.	60	84	77.14	months	R 78 000.00	77.14	months	-	R 1 616 397.12	7.81	Crane selection from windPACT Area 2 turbine rotor and blade logistics.
	Labour cost to assemble crane per turbine	1	1	1	per turbine	R 3 685.00	1.00	per turbine	-	R 49 495.45	0.24	
	Labour cost to relocate crane per turbine	1	1	1	per turbine	R 1 560.00	1.00	per turbine	-	R 20 953.30	0.10	
	Crane cribbing cost per turbine	1	1	1	per turbine	R 538.00	1.00	per turbine	-	R 7 226.20	0.03	
	Meals and lodging for crew per turbine	1	1	1	per turbine	R 605.00	1.00	per turbine	-	R 8 126.12	0.04	
	Fuel cost per month	60	84	77.14	per month	R 4 222.00	77.14	per month	-	R 87 492.67	0.42	
	Mobilize/demobilize (1) LTL-850 crane	1	1	1	lump sum	R 484 727.00			-	R 130 213.18	0.63	
	Rental for (1) Lampson LTL-850 Crane for nacelle, hub and blade erection at 100m level	10.4	15	13.69	months	R 88 667.00	13.69	months	-	R 357 281.90	1.73	
	Labour cost to assemble crane per turbine	1	1	1	per turbine	R 7 332.00	1.00	per turbine	-	R 98 480.49	0.48	
	Labour cost to relocate crane per turbine	1	1	1	per turbine	R 2 730.00	1.00	per turbine	-	R 36 668.27	0.18	
	Crane cribbing cost per turbine	1	1	1	per turbine	R 808.00	1.00	per turbine	-	R 10 852.73	0.05	
	Meals and lodging for crane crew per turbine	1	1	1	per turbine	R 1 161.00	1.00	per turbine	-	R 15 594.09	0.08	
	Fuel cost per month	10.4	15	13.69	per month	R 4 222.00	13.69	per month	-	R 15 521.85	0.07	
	Other equipment rental	28	28	28	months	R 10 000.00	28.00	months	-	R 75 216.96	0.36	
										R 3 372 397.29	**16.293**	
2	**Foundation construction per tower (Steel)**											
	Survey layout and location						1	lump sum		R 8 000.00	0.04	Use data by Dr. peter day.
	Geotechnical investigation (per tower location)	50	50	50	each	R 1 000.00	50	wind farm	R 500 000.00	R 10 000.00	0.05	Use data by Dr. Peter day: R500000 fixed cost for wind farm.
							1	lump sum		R 200 000.00	0.97	Use data by Dr. Peter day: R200000 WTG cost per site.
	Excavation	1500	2218	2012.86	cubic yards	R 8.00	1538.93	m^3	R 134.19	R 206 509.01	1.00	With large excavator. Merkel's pricing for earthworks.
	Supply and install concrete forms (18.3m by 18.3m by 3.66m deep)	2160	2880	2674.29	sq Ft	R 2.50	248.44	m^2	R 341.78	R 84 912.21	0.41	Use Merkel's rough formwork for sides of bases.
	Supply, place and consolidate foundation concrete	972	1440	1306.29	cubic yards	R 89.90	998.72	m^3	R 1 525.09	R 1 523 139.02	7.36	Use 90% of gross foundation volume to account for central thickening of foundation. Merkel's 30MPa/19mm RC base mixing at site.
	Reinforcing steel	51440	76200	69125.71	Lbs	R 0.45	31.35	t	R 16 509.95	R 517 667.35	2.50	Assume Merkel's R12 mild reinforcement bars
	A-490 anchor bolts and couplers (reuse upper bolts)			N/a								
	Precision locating template for anchor bolts and post tensioning anchors and ducts	4	4	4	each	R 12 500.00	-	-	-	R 13 431.60	0.06	
	Backfill and tamp (after post tensioning)	650	650	650	cubic yards	R 6.00	497	m^3	R 47.81	R 23 759.54	0.11	Tamp 10ft around footing. Merkel's 93% Mod AASHTO compacted earth filling obtained from excavations on site.
	Untamped backfill	1200	1200	1200	cubic yards	R 1.00	917	m^3	R 44.56	R 40 882.02	0.20	Merkel's uncompacted earth filling obtained from excavations on site.
										R 2 628 300.75	**12.698**	

3	**Shop fabrication of steel tower (3 Tapered tubes and heavy base flange ring, tower top flange ring)**													
Tube section material	516100	899200	789742.86	lbs	R	0.18	271.71	t			R	4 557 251.59	22.02	Used calculated mass for steel tower design for study with Macsteel plate costs.
Tube section fabrication, rolled and welded	516100	899200	789742.86	lbs	R	0.72	42.69	%			R	1 945 490.70	9.40	Allowance for NDT. Calculated cost increase for plate rolling and welding at 42.69%.
Weld quartered tube sections (for this study a different tower is used with differing section amounts)		3600	3000	$/kW	R	15.87	467.17	m	R	1 467.80	R	685 712.13	3.31	WindPACT area 2 Figure 4-13 adjusted to tower height. For this study calculate according to tower dimensions. Costing a combination of free construction data and Merkel's.
Base flange ring (Dim 8.052mOD x 7.544mID x 0.127m thk)														
Cut, weld, stress relieve	13913	18178	16959.43	lbs	R	2.50	7.69	t	-		R	569 480.65	2.75	Weight include 33% waste
Drill holes, mill after welding first tube section				lump sum			-	-	-		R	40 294.80	0.19	
Top flange ring (Dim 4.216mOD x 3.912mID x0.127m thk)														
Cut, weld, stress relieve	4192	5684	5257.71	lbs	R	2.00	2.38	t	-		R	141 239.03	0.68	Weight include 33% waste
Drill holes, mill after welding first tube section				lump sum			-	-	-		R	40 294.80	0.19	
Concrete tower top connection ring (Dim 5.23mOD x 3.556mID x 0.152m thk)				N/a										
Cut, weld, stress relieve				N/a										Weight include 33% waste
Drill holes to match tower flange, mill to match tube flange				N/a										
Fabricate and install internal galvanized ladders	9840	9840	9840.00	lbs	R	3.00	4.46	t	-		R	396 500.83	1.92	Use 30 ib per vertical ft
Surface preparation, prime and paint														
2 Coats primer on interior surfaces	12240	13320	13011.43	lump sum			2550.62	m^2	R	51.02	R	130 139.61	0.63	Use Merkel's rates and calculations for primer. Tower inside area = 1275.31m^2
Primer and epoxy finish coats on exterior	30600	33300	32528.57	lump sum			2580.66	m^2	R	51.02	R	131 672.33	0.64	Use Merkel's rates and calculations for primer. Tower outside area = 1290.33m^2. Assume epoxy cost is similar to primer.
Truck delivery (see note 3) $48 per kW*(100m/130.2m)=36.87/kW for 3.6MW tower	1500	3600	3000.00	$/kW	R	31.39	5.5	round trips	R	8 933.91	R	49 136.51	0.24	56 ft to 64 ft long per windPACT Area 2 turbine rotor and blade logistics - Transport from Shereveport, LA. Adjusted for tower height. Calculate transport for this study by scaling for 50t truck.
							407.565	man hours	R	25.32	R	10 319.55	0.05	Merkel's steel truck loading cost forsemi-skilled labourer @ 1.5 man hours per ton.
											R	**8 697 532.53**	**42.021**	
4	**Field erection of steel tube & pedestal crane (Steel)**													
Fabricate jack-up frame and base supports (4)				N/a										
Install base support system and jack-up frame				N/a										
Rig, erect and fit 17 tube sections (labour)	410	748	651.43	man hours		40.3	651	man hours	R	25.32	R	16 494.17	0.08	Max weight of tube section, 50 kips lift height 328 ft. Use LTL-600 crane. 1.5 hybrid amount x (17 sections/3 sections)
Weld (20) field joints with track-mounted welder $26.24/kW	1500	3600	3000.00	$/kW		10.71	-	-	-		R	878 541.77	4.24	Includes allowance for NDT - 20 horizontal welds to connect erected tube sections (Fig. 4-13 WindPACT technical area 2 adjusted for length of weld.)
Grout and torque tower base (labour)	40	40	40.00	man hours		40.3	40.00	man hours	R	25.32	R	1 012.80	0.00	Merkel's hour rate for semi-skilled labourer.
Grout and torque tower base (Material and equipment)				lump sum			-	-	-		R	11 416.86	0.06	
Erect special pedestal crane on top of steel tube (assume 5 days with crew of 8 to fully install)				N/a										
											R	**907 465.60**	**4.3843**	

5	**Erect nacelle and rotor (Steel)**													
Preparation for jack-up operation				N/a										
Supply and install (3) jack-up tendons with				N/a										
Anchors top and bottom				N/a										
Fabricate (18) upper thruster assemblies				N/a										
Install (18) upper thruster assemblies				N/a										
Fabricate (24) lower thruster assemblies				N/a										
Install (24) lower thruster assemblies				N/a										
Remove special pedestal crane and prepare for reinstallation (2 days with crew of 6)				N/a										
Erect transitions section and turbine nacelle (crew of 4 for 4 days)	120	140	134	man hours	R	40.30	134.29	man hours	R	25.32	R	3 400.11	0.02	Use LTL 850 crane WindPACT Area 2 study - crane costs elsewhere. Merkel's semi-skilled labourer.
Supply, install and torque 1.25in (31.7mm) diameter HS bolts	64	64	64	each	R	14.20	-	-	-		R	12 206.64	0.06	
Erect hub and blades to turbine nacelle (crew of 4 for 4 days)	120	144	137	man hours	R	40.30	137.14	man hours	R	25.32	R	3 472.46	0.02	Use LTL 850 crane WindPACT Area 2 study - crane costs elsewhere. Merkel's semi-skilled labourer.
Disconnect base flange of steel tube from anchor bolts				N/a										
Jack-up steel tube with turbine and blades				N/a										
Jack-up steel tube in 12 in lifts (12 lifts per hour)(16 hour shift) 6 people x 16 =				N/a										
Jack-up equipment rental				N/a										
Monitor with control transits				N/a										
For final 24 inches inspect and adjust rotationally to assure lift frame staffing cones mate into female sockets				N/a										
Allowance for equipment and small cranes							-	-		-	R	53 726.40	0.26	
											R	**72 805.61**	**0.3517**	
6	**Finishing and clean-up (Steel)**													
Remove upper and lower thruster assemblies				N/a										
Supply, install, and torque (128) - 1.5 in diameter high strength bolts				N/a										
Remove jack-up tendons and anchors				N/a										
Lower and remove tower base support frame (3 days for a crew of 4)				N/a										
Install weather protective flashing over concrete to steel joint				N/a										Crew of 4 for 4 hours
Supply, hoist in and install ladders and platforms inside concrete tower				N/a										
Remove exterior scaffold platforms and connecting ladders				Lump sum			-	-		-	R	137 002.32	0.66	Use LTL-600 crane (crane costs included elsewhere) 1.5 hybrid amount X 100m/49m
Touch up paint on steel tube exterior				Lump sum			1290.33	m^2	R	82.33	R	106 237.85	0.51	Use Merkel's rates and calculations for aluminium paint. Tower outside area = 1290.33m^2.
											R	**243 240.17**	**1.1752**	

Summary of construction costs					
				R	**15 921 741.94**	
General contractor field overhead	10	10	10 %	R	1 592 174.19	7.69
General contractor administrative overhead	10	10	10 %	R	1 592 174.19	7.69
General contractor profit	10	10	10 %	R	1 592 174.19	7.69
Total manufacture, construction and installation cost of one tubular steel tower				**R**	**20 698 264.52**	**100**

Mix design for 60MPa concrete supplied by James Olawuyi. Material costing from suppliers and Merkel's labour and equipment rates for 30MPa/19mm reinforced concrete column.

Cement mass per bag =	50	kg

Malmesbury sand RD =	2.65
Greywacke stone RD =	2.65
Chryso Premia RD =	1.05
Cement RD =	3.14
Silica fume RD =	2.20

Typical 60MPa Concrete mix and costing for 1 m^3

Component	Mass/m^3 (kg/m^3)	Unit	Unit cost (2014 ZAR/Unit)	Quantity/ m^3	Cost (2014 ZAR/m^3)
Cement (CEM I 52.5)	522.5	bag	R 106.24	10.450	R 1 110.21
Silica fume (Sikafume)	27.50	kg	R 9.50	27.500	R 261.25
Fine aggregate (Malmesbury sand)	770.0	m^3	R 421.80	0.2906	R 122.56
Coarse aggregate (13.2mm Graywacke stone)	940.0		R 255.60	0.3547	R 90.67
Superplasticizer (Chryso Premia 310)	9.750	m^3	R 28 500.00	0.0093	R 264.64
Semi skilled worker		hour	R 25.32	0.0880	R 2.23
Labourer		hour	R 17.88	3.1120	R 55.64
Concrete artisan		hour	R 27.76	0.4400	R 12.21
Fuel		liter	R 7.25	0.2000	R 1.45
300 liter concrete mixer		day	R 484.43	0.0550	R 26.64
Vibrator unit and poker		day	R 133.97	0.0550	R 7.37
				Subtotal	R 1 954.87
Overheads and sundries @ 2.5%		%	2.5		R 48.87
Profit @ 10%		%	10		R 200.37
Total		m^3	1		R 2 204.12

*Volume for cement is for amount of bags (i.o.w. 10.4 bags)
*PPC cement unit cost for delivery in Caledon in 50kg bags inc. vat @ 14%
*Malmesbury sand price for delivery from Somerset Sand en Klip in Somerset West to Caledon inc. vat @14%
*Chryso Premia 310 unit price @ R25 per liter inc. vat @14%.
*Sikafume price @ R285 per 30kg inc. vat @14%
*Price for 13mm gray stone for delivery from S.N. Albertyn Sandmyn in Botrivier to Caledon

Costing of steel prestressing reinforcement. Material, installation and jacking pricing and labour hours using free construction costing data. Labour rates using PPiS.

Item	Hourly rate (2014 $)	Hours/200 ft	2014 $/ft	Merkel's (August 2014 ZAR) Hourly rate	Assumption	ZAR/m
Material			$ 20.10			R 703.08
Reinforcing foreman	$ 53.73	2.77	$ 0.74	R 47.62	Foreman	R 7.10
Reinforcing labourer	$ 52.30	11.09	$ 2.90	R 34.84	Steel fixer	R 20.79
Equipment operators	$ 40.78	2.77	$ 0.57	R 34.84	Driver/machine operator	R 5.19
Semi-skilled labour	$ 34.06	5.54	$ 0.94	R 25.32	Semi-skilled worker	R 7.55
Pressure grout/MUD JACK 250 CF	$ 25.64	8.32	$ 1.07			R 37.29
100t hydraulic jacks	$ 2.58	1.39	$ 0.02			R 0.62
					Total	R 781.63
					Total cost of prestressing reinforcement	R 1 868 102.62

*Labour cost for Merkel's foreman at R9000.00/month. Assume 21 day month and 9 hour day.

Section	Length (m)	Amount	Total length (m)
Top	51	19	969
Bottom	49	29	1421
		Total	2390

Steel tower material cost estimation. Use costs from Macsteel price list (excl. vat) for Cape Town on 3 September 2014. Take costs for plates that have approximately the same size as particular section. Vat @ 14% included into price calculations.

ρ =	7850	kg/m^3
Vat	14	%

Tower tube section													Macsteel plate				Section material cost (ZAR)
Section	Top station	Thickness	Height	Middle Perimeter	Middle Dtop	Middle Dbot	Outside Rtop	Outside Rbot	Inside Rtop	Inside Rbot	Volume (m^3)	Mass (t)	Closest dimensions (mm) Length	Height	Thickness	Cost ZAR/t	
flange1+S1	97.5	0.023	2.64	11.36	3.58	3.65	1.80	1.84	1.78	1.82	0.66	5.18	10000	2400	22	R 14 525.70	R 85 749.55
S2	94.86	0.021	2.74	11.61	3.65	3.74	1.84	1.88	1.82	1.86	0.64	4.99	12000	3000	22	R 14 681.20	R 83 562.67
S3	92.12	0.019	2.73	11.86	3.74	3.81	1.88	1.92	1.86	1.90	0.62	4.83	12000	3000	20	R 14 681.20	R 80 811.14
S4-7	89.39	0.019	10.82	12.47	3.81	4.13	1.92	2.07	1.90	2.05	2.50	19.59	12000	3000	20	R 14 681.20	R 327 846.25
S8-9+flange2	78.57	0.018	5.46	13.21	4.13	4.28	2.07	2.15	2.05	2.13	1.30	10.19	12000	3000	18	R 14 681.20	R 170 520.83
	73.11	0.018			4.28		2.15		2.13								
flange3+S10	73.11	0.017	2.06	13.46	4.28		2.15		2.13		0.47	3.70	13000	2400	16	R 14 647.20	R 61 765.11
S11	71.05	0.016	2.95	13.46	4.28		2.15		2.13		0.64	4.99	12000	3000	16	R 14 681.20	R 83 459.81
S12	68.1	0.017	2.95	13.46	4.28		2.15		2.13		0.67	5.30	13000	2400	16	R 14 647.20	R 88 450.03
S13	65.15	0.018	2.95	13.45	4.28		2.15		2.13		0.71	5.61	12000	3000	18	R 14 681.20	R 93 848.45
S14	62.2	0.019	2.95	13.45	4.28		2.15		2.13		0.75	5.92	12000	3000	18	R 14 681.20	R 99 039.12
S15	59.25	0.019	2.95	13.45	4.28		2.15		2.13		0.75	5.92	12000	3000	18	R 14 681.20	R 99 039.12
S16	56.3	0.020	2.95	13.45	4.28		2.15		2.13		0.79	6.23	12000	3000	20	R 14 681.20	R 104 227.35
S17	53.35	0.021	2.95	13.44	4.28		2.15		2.13		0.83	6.54	12000	3000	20	R 14 681.20	R 109 413.15
S18	50.4	0.023	1.95	13.44	4.28		2.15		2.13		0.60	4.73	13000	2400	22	R 14 647.20	R 78 991.56
flange4	48.45	0.023	0.12	13.44	4.28		2.15		2.13		0.04	0.29					R 4 861.02
flange5	48.33	0.023	0.12	13.44	4.28		2.15		2.13		0.04	0.29	12000	2400	22	R 14 681.20	R 4 872.30
S19	48.21	0.023	2.95	13.44	4.28		2.15		2.13		0.91	7.16					R 119 777.44
S20	45.26	0.024	2.95	13.43	4.28		2.15		2.13		0.95	7.47	12000	3000	25	R 14 681.20	R 124 955.94
S21	42.31	0.025	2.95	13.43	4.28		2.15		2.13		0.99	7.78	12000	3000	25	R 14 681.20	R 130 131.99
S22	39.36	0.026	2.95	13.43	4.27		2.15		2.12		1.03	8.08	12000	3000	25	R 14 681.20	R 135 305.61
S23	36.41	0.028	2.95	13.42	4.27		2.15		2.12		1.11	8.70	13000	2400	28	R 14 775.20	R 146 578.08
S24	33.46	0.030	2.95	13.41	4.27		2.15		2.12		1.19	9.32	13000	2400	30	R 14 775.20	R 156 974.42
flange6	30.51	0.030	0.13	13.41	4.27		2.15		2.12		0.05	0.41					R 6 917.52
flange7	30.38	0.030	0.13	13.41	4.27		2.15		2.12		0.05	0.41	13000	2400	30	R 14 775.20	R 6 917.52
S25	30.25	0.030	2.45	13.41	4.27		2.15		2.12		0.99	7.74					R 130 368.59
S26	27.8	0.032	2.95	13.41	4.27		2.15		2.12		1.27	9.94	13000	2400	32	R 14 775.20	R 167 360.96
S27	24.85	0.032	2.95	13.41	4.27		2.15		2.12		1.27	9.94	13000	2400	32	R 14 775.20	R 167 360.96
S28	21.9	0.035	2.95	13.40	4.27		2.15		2.12		1.38	10.86	13000	2400	35	R 14 775.20	R 182 922.38
S29	18.95	0.038	2.45	13.39	4.26		2.15		2.11		1.25	9.79	10000	2400	40	R 14 653.70	R 163 468.77
flange8	16.5	0.038	0.15	13.39	4.26		2.15		2.11		0.08	0.60					R 10 008.29
flange9	16.35	0.038	0.15	13.39	4.26		2.15		2.11		0.08	0.60	10000	2400	40	R 14 653.70	R 10 008.29
S30	16.2	0.038	1.95	13.39	4.26		2.15		2.11		0.99	7.79					R 130 107.80
S31	14.25	0.040	2.45	13.38	4.26		2.15		2.11		1.31	10.30	10000	2400	40	R 14 653.70	R 171 991.65
S32	11.8	0.045	2.45	13.37	4.26		2.15		2.11		1.47	11.57	4000	2000	45	R 14 767.10	R 194 759.10
S33	9.35	0.050	1.95	13.35	4.25		2.15		2.10		1.30	10.22	4000	2000	50	R 14 767.10	R 172 033.55
flange10	7.4	0.050	0.175	13.35	4.25		2.15		2.10		0.12	0.92					R 15 438.91
flange11	7.225	0.050	0.175	13.35	4.25		2.15		2.10		0.12	0.92	6000	2400	50	R 14 767.10	R 15 438.91
S34	7.05	0.050	2.45	13.35	4.25		2.15		2.10		1.64	12.84					R 216 144.71
S35	4.6	0.050	2.45	13.35	4.25		2.15		2.10		1.64	12.84	6000	2400	50	R 14 767.10	R 216 144.71
S36	2.15	0.050	1.95	13.35	4.25		2.15		2.10		1.30	10.22	6000	2400	50	R 14 767.10	R 172 033.55
flange12	0.2	0.050	0.2	13.35	4.25		2.15		2.10		0.13	1.05					R 17 644.47
	0								Total		28.91	271.71				Total	R 4 557 251.59

Calculate percent increase in cost from plates to welded circular tube sections. All costs were taken from Macsteel.

1 Feb 2014 ZAR =	1.04	Aug 2014 ZAR
1 Sept 2014 ZAR =	0.998	Aug 2014 ZAR

Welded tubing							2500x1200x6mm thick S355JR Plate				
Diameter (mm)	Perimeter (m)	thickness (mm)	Steel quality	Mass (kg/m)	Feb 2014 (ZAR/m)	Aug 2014 (ZAR/m)	Mass for 1.2m width (kg/m)	Equivalent mass (kg/m)	ZAR/t	Sept 2014 ZAR/m	% Cost increase
76.20	0.239	6.0	S355	10.31	R 232.53	R 241.83	56.52	11.28	R 15 635.40	R 176.29	37.17%
88.90	0.279	6.0	S355	12.17	R 274.58	R 285.56	56.52	13.15	R 15 635.40	R 205.68	38.84%
101.6	0.319	6.0	S355	14.14	R 318.86	R 331.61	56.52	15.03	R 15 635.40	R 235.06	41.08%
114.3	0.359	6.0	S355	16.01	R 361.18	R 375.62	56.52	16.91	R 15 635.40	R 264.44	42.04%
127.0	0.399	6.0	S355	17.88	R 403.34	R 419.47	56.52	18.79	R 15 635.40	R 293.82	42.76%
139.7	0.439	6.0	S355	19.78	R 446.20	R 464.04	56.52	20.67	R 15 635.40	R 323.20	43.58%
152.4	0.479	6.0	S355	21.66	R 488.61	R 508.15	56.52	22.55	R 15 635.40	R 352.59	44.12%
165.1	0.519	6.0	S355	23.54	R 531.01	R 552.26	56.52	24.43	R 15 635.40	R 381.97	44.58%
177.8	0.559	6.0	S355	25.22	R 568.84	R 591.60	56.52	26.31	R 15 635.40	R 411.35	43.82%
193.7	0.609	6.0	S355	27.82	R 627.56	R 652.67	56.52	28.66	R 15 635.40	R 448.14	45.64%
219.1	0.688	6.0	S355	31.53	R 711.25	R 739.70	56.52	32.42	R 15 635.40	R 506.90	45.93%
										Average	42.69%

Calculation of weld cost per metre for steel tower main sections using free construction data and Merkel's costs.

Free construction data item	Labour hours/LF	Hourly rate (2014 $)	2014 $/ft	Labour hours/m	Merkel's labour (ZAR/h) Hourly rate	Assumption	Weld cost (2014 ZAR/m)
Material			$ 4.47				R 156.33
Structural steel foreman	0.8	$ 57.58	$ 46.06	5.0	R 47.62	Foreman	R 238.10
Structural steel welder	0.8	$ 56.15	$ 44.92	5.0	R 34.84	Steel fixer	R 174.20
300AMP trailer mounted welder	0.8	$ 16.87	$ 13.50	5.0			R 899.17
						Total	R 1 467.80

*Labour cost for Merkel's foreman at R9000.00/month. Assume 21 day month and 9 hour day.

*Labour hours for Merkel's over 12mm vee butt weld @ 150min/m times 2.

Calculate welding cost of steel tower main sections. Use costs from Free Construction Cost Data (www.allcostdata.info) and combine with Merkel's rates. Assume 25mm full penetration butt welds (NREL bl. 112) on outside diameter.

Section	Top station	Thickness (m)	Height (m)	Outside (m) Rtop	Outside (m) Rbot	Perimeter (Weld length)	Inside (m) Rtop	Inside (m) Rbot	Weld cost (2014 ZAR)
flange1+S1	97.5	0.023	2.64	1.800	1.838	11.548	1.777	1.817	R 16 949.80
S2	94.86	0.021	2.74	1.838	1.877	11.795	1.817	1.858	R 17 312.42
S3	92.12	0.019	2.73	1.877	1.916	12.041	1.858	1.897	R 17 673.72
S4-7	89.39	0.019	10.82	1.916	2.072	13.017	1.897	2.054	R 19 105.68
S8-9+flange2	78.57	0.018	5.46	2.072	2.150		2.054	2.132	
	73.11	0.018		2.15			2.132		
flange3+S10	73.11	0.017	2.06	2.15		13.509	2.133		R 19 828.27
S11	71.05	0.016	2.95	2.15		13.509	2.134		R 19 828.27
S12	68.1	0.017	2.95	2.15		13.509	2.133		R 19 828.27
S13	65.15	0.018	2.95	2.15		13.509	2.132		R 19 828.27
S14	62.2	0.019	2.95	2.15		13.509	2.131		R 19 828.27
S15	59.25	0.019	2.95	2.15		13.509	2.131		R 19 828.27
S16	56.3	0.020	2.95	2.15		13.509	2.13		R 19 828.27
S17	53.35	0.021	2.95	2.15		13.509	2.129		R 19 828.27
S18	50.4	0.023	1.95	2.15		13.509	2.127		R 19 828.27
flange4	48.45	0.023	0.12	2.15			2.127		
flange5	48.33	0.023	0.12	2.15		13.509	2.127		R 19 828.27
S19	48.21	0.023	2.95	2.15		13.509	2.127		R 19 828.27
S20	45.26	0.024	2.95	2.15		13.509	2.126		R 19 828.27
S21	42.31	0.025	2.95	2.15		13.509	2.125		R 19 828.27
S22	39.36	0.026	2.95	2.15		13.509	2.124		R 19 828.27
S23	36.41	0.028	2.95	2.15		13.509	2.122		R 19 828.27
S24	33.46	0.030	2.95	2.15		13.509	2.12		R 19 828.27
flange6	30.51	0.030	0.13	2.15			2.12		
flange7	30.38	0.030	0.13	2.15		13.509	2.12		R 19 828.27
S25	30.25	0.030	2.45	2.15		13.509	2.12		R 19 828.27
S26	27.8	0.032	2.95	2.15		13.509	2.118		R 19 828.27
S27	24.85	0.032	2.95	2.15		13.509	2.118		R 19 828.27
S28	21.9	0.035	2.95	2.15		13.509	2.115		R 19 828.27
S29	18.95	0.038	2.45	2.15		13.509	2.112		R 19 828.27
flange8	16.5	0.038	0.15	2.15			2.112		
flange9	16.35	0.038	0.15	2.15		13.509	2.112		R 19 828.27
S30	16.2	0.038	1.95	2.15		13.509	2.112		R 19 828.27
S31	14.25	0.040	2.45	2.15		13.509	2.11		R 19 828.27
S32	11.8	0.045	2.45	2.15		13.509	2.105		R 19 828.27
S33	9.35	0.050	1.95	2.15		13.509	2.1		R 19 828.27
flange10	7.4	0.050	0.175	2.15			2.1		
flange11	7.225	0.050	0.175	2.15		13.509	2.1		R 19 828.27
S34	7.05	0.050	2.45	2.15		13.509	2.1		R 19 828.27
S35	4.6	0.050	2.45	2.15		13.509	2.1		R 19 828.27
S36	2.15	0.050	1.95	2.15		13.509	2.1		R 19 828.27
flange12	0.2	0.050	0.2	2.15			2.1		
	0				Total	467.17			R 685 718.09

For application of one coat of metal primer to steel tower.

Description	Unit	Quantity	ZAR/unit	Total (2014 ZAR)
Metal primer 5l	ea	0.09	R 352.29	R 31.71
Artisan painter	hour	0.488	R 27.76	R 13.55
Overheads and sundries @ 2.5%	%	2.5		R 1.13
Profit @10%	%	10		R 4.64
Rate	**m^2**	**1**		**R 51.02**

For application of one coat of aluminium paint to steel tower.

Description	Unit	Quantity	ZAR/unit	Total (2014 ZAR)
Aluminium paint 5l	ea	0.09	R 660.85	R 59.48
Artisan painter	hour	0.488	R 27.76	R 13.55
Overheads and sundries @ 2.5%	%	2.5		R 1.83
Profit @10%	%	10		R 7.48
Rate	**m^2**	**1**		**R 82.33**

Precast erection crew for NREL study (bl. 119)

Type	Amount	Cost/h (2014 ZAR)	Merkel's description
Carpenter	1	R 30.62	Carpenter (Ironmongery)
Iron-worker	1	R 25.32	General worker (Ironmongery)
Welder	1	R 34.84	Same class as steel fixer and driver/machine operator
Concrete labourer	1	R 27.76	reinforcement)
	Total	**R 118.54**	

Disposal and recycling of concrete and steel wind turbine towers. Salvage % and value for the former were taken from Recycling Cement (Bron 65) and Recycling and reuse (Bron 66). For the latter salvage % was also taken from Recycling and reuse (Bron 66) and its value from scrapmetalsolutions.com. Disposal of clean builder's rubble is free as of 2013/2014 to demote illegal dumping (City of Cape Town).

Description of waste material	Total mass (t)	Salvage													
		%			Unit cost/t						Total income ZAR			Comment
		Min	Mid	Max	Min €	Mid €	Max €	Min ZAR	Mid ZAR	Max ZAR	Min	Mid	Max	
Precast and cast-in-place tower														
Concrete	1867	10	33.5	57	€ 3.00	€ 7.50	€ 12.00	R 42.63	R 106.57	R 170.51	R -7 960.28	R -66 667.35	R -181 494.39	Use salvage % of Spain as min: lowest. Use Australia as highest achievable: developed country with large open areas, like South Africa.
Reinforcing steel	15.49		98		R					2 050.00	R -31 119.41	R -31 119.41	R -31 119.41	Salvage % for rebar in concrete super structure
Prestressing tendons	31.52		98		R					2 050.00	R -63 323.68	R -63 323.68	R -63 323.68	Salvage % for rebar in concrete super structure
										Total	R -102 403.37	R -161 110.44	R -275 937.48	
Steel tower														
Structural steel	271.7		100		R					2 050.00	R -557 005.50	R -557 005.50	R -557 005.50	Salvage % for heavy structural sections/tubes

Description of waste material	Total mass (t)	Transport cost												Total cost (- values represent income)		
		Unit value (ZAR/t)			For salvage (ZAR)			For disposal (ZAR)			Total (ZAR)			Min	Most likely	Max
		Close	Mid	Far	Min	Mid	Max	Min	Mid	Max	Min	Mid	Max			
Precast and cast-in-place tower																
Concrete	1867	R 25.63	R 64.03	R 79.54	R 4 785.32	R 40 057.46	R 84 667.40	R 43 067.84	R 79 517.05	R 63 871.89	R 47 853.15	R 119 574.52	R 148 539.29	R -133 641.24	R 52 907.17	R 140 579.01
Reinforcing steel	15.49	R 25.63	R 64.03	R 79.54	R 388.99	R 972.01	R 1 207.46	R 7.94	R 19.84	R 24.64	R 396.93	R 991.84	R 1 232.10	R -30 722.48	R -30 127.57	R -29 887.31
Prestressing tendons	31.52	R 25.63	R 64.03	R 79.54	R 791.55	R 1 977.90	R 2 457.01	R 16.15	R 40.37	R 50.14	R 807.70	R 2 018.27	R 2 507.15	R -62 515.98	R -61 305.42	R -60 816.53
										Total	R 49 057.78	R 122 584.63	R 152 278.54	R -226 879.70	R -38 525.81	R 49 875.17
Steel tower																
Structural steel	271.7	R 25.63	R 64.03	R 79.54	R 6 962.57	R 17 397.93	R 21 612.27	R -	R -	R -	R 6 962.57	R 17 397.93	R 21 612.27	R -550 042.93	R -539 607.57	R -535 393.23

Transport cost based on a 28t truck. Unit rate from Teravaninthorn and Raballand (bron 63). For delivery from the fabrication plant to the site. Scale value for 50t truck for steel tower sections.

Tower type	Fabrication plant distance (km) Close	Most likely	Far	Unit rate per km 2005 $	2005 ZAR	2014 ZAR	Delivery cost ZAR Close	Most likely	Far	Round trip cost ZAR Close	Most likely	Far	Comments
Precast	41.4	84.9	106	$ 1.08	R 6.44	R 11.02	R 456.22	R 935.58	R 1 168.10	R 912.44	R 1 871.16	R 2 336.20	Distances for: Grabouw industrial, Cape Concrete Blackheath, Montague Gardens Industrial.
Steel	85.9	227	1389	$ 1.93	R 11.49	R 19.68	R 1 690.36	R 4 466.96	R 27 333.04	R 3 380.72	R 8 933.91	R 54 666.09	Distances for: CISCO Kuilsriver, AMSA Saldanha, Hall Longmore Wadeville.

Transport for disposal of recyclable tower material. Cost based on Merkel's 8 t open truck. Assume tipper.

Solid waste disposal plant	Distance from site (km)	Unit costs (ZAR) Fixed per day	Per km	Overtime/ h	Transport time per trip (h) Upload	Round trip travel	Unload	Total	Overtime (h)	Trips per day Fraction	Rounded	Mass per day (t)	Total cost per day (ZAR)	Unit costs ZAR/km	ZAR/t
Caledon	5.5	R 805.00	R 4.00	R 35.00	1.00	0.18	0.50	1.68	0.00	5.346534653	5.00	40.00	R 1 025.00	R 18.64	R 25.63
Hermanus	38		R 4.00	R 35.00	1.00	0.95	0.50	2.45	0.80	3.673469388	4.00	32.00	R 2 049.00	R 6.74	R 64.03
Kleinmond	46		R 4.00	R 35.00	1.00	1.15	0.50	2.65	0.00	3.396226415	3.00	24.00	R 1 909.00	R 6.92	R 79.54

*Assume average speed of 40 km/h for close and 80km/h for middle and far trips.

*Assume 9 working hours in a day.